University of Southampton
Faculty of Natural and Environmental Sciences
School of Ocean and Earth Science

Development of microfluidic pre-concentration system for metals in seawater

PhD THESIS

Marta Skiba

Thesis for the degree of Doctor of Philosophy

October, 2015

Graduate School of the National Oceanography Centre, Southampton

This PhD dissertation by Marta Skiba has been produced under the supervision of:

Supervisors

Prof. Peter J. Statham

Prof. Matt C. Mowlem

Chair of Advisory Panel

Dr. Douglas P. Connelly

UNIVERSITY OF SOUTHAMPTON

ABSTRACT

FACULTY OF NATURAL AND ENVIRONMENTAL SCIENCES

SCHOOL OF OCEAN AND EARTH SCIENCE

Doctor of Philosophy

DEVELOPMENT OF MICROFLUIDIC PRE-CONCENTRATION SYSTEM FOR METALS IN SEAWATER

by Marta Skiba

In-situ marine biogeochemical sensing allows measurement at high frequency to investigate short and long-term variability in processes in ocean waters. In trace analyses, not only the low concentrations of analytes but also possible interferences from the matrix and other elements must be considered, therefore a pre-concentration step prior to the determination of trace metals needs to be implemented. The way forward for improved in-situ analyses of manganese in seawater was to build on the existing technology of the Sensors Group at NOC, Southampton and develop a pre-concentration system for coupling to spectrophotometric Lab on a Chip (LOAC) technologies.

This thesis describes the development and optimisation of LOAC analyser for manganese determination in aquatic environments, integrated with pre-concentration. Optimised conditions for the extraction of manganese from seawater with a Toyopearl iminodiacetate resin column were developed using Mn-54 tracer. Conditions evaluated were optimal pH for manganese removal, optimal flow rate required for full recovery of manganese, and the concentration and the volume of the acid solution needed for quantitative elution of manganese from the resin.

The LOAC system used the colorimetric 1-(2-Pyridylazo)-2-naphthol (PAN) method for Mn determinations. The modified method was used for manganese determinations, when sodium dodecyl sulfate (SDS) was used as surfactant, with calibration curves constructed and precision (in the range 1.08 - 3.81 % RSD) and the LOD of the method assessed (3SD, typically 14 nM with 10 cm cell).

Results of the adaptation of the modified PAN method on the chip and its coupling to a resin column for collection of manganese proves the concept of on-chip preconcentration.

The design and production method of the microfluidic chips and the operation procedure of the bench-top LOAC manganese determination system with the resin column implemented on the chip are described. The LOAC system coupled with the resin column and PAN chemistry was used for manganese determination with calibration curve constructed and precision of the method determined (0.86 - 2.69 % RSD).

Declaration

Declaration of authorship

I, Marta Skiba, declare that this thesis entitled "Development of Microfluidic pre-concentration system for metals in seawater" and the work presented in it are my own, and have been generated by me as the result of my own original research.

I confirm that:

1. This work was done wholly or mainly while in candidature for a research degree at this University;

2. Where any part of this thesis has previously been submitted for a degree or any other qualification at this University or any other institution, this has been clearly stated;

3. Where I have consulted the published work of others, this is always clearly attributed;

4. Where I have quoted from the work of others, the source is always given. With the exception of such quotations, this thesis is entirely my own work;

5. I have acknowledged all main sources of help;

6. Where the thesis is based on work done by myself jointly with others, I have made clear exactly what was done by others and what I have contributed myself.

Marta Skiba

Acknowledgements

I would like to express my special appreciation and thanks to my supervisors Prof. Peter Statham and Prof. Matt Mowlem for the opportunity they gave me and for their support throughout this project.

I special thank you to Peter for all the patience and encouragement he gave me during long months I spent undertaking my lab work. Without his guidance and constant feedback this PhD would not have been achievable.

I gratefully acknowledge the funding received towards my PhD from the Natural Environment Research Council and Royal Society of Chemistry.

I greatly appreciate the support received through the collaborative work undertaken with Geosciences Advisory Unit, University of Southampton. Thank you to Dr. Pawel Gaca for sharing knowledge and help and to Dr. Phil Warwick for making this data collection possible.

Thank you to the Sensors Group, NOC, Southampton. I am very grateful to all those who were always so helpful and provided me with their assistance throughout my dissertation.

My deep appreciation goes out to all my family and friends. Special thanks go to Tomek for his encouragements, advise, enthusiasm and continuous optimism. I am grateful to my friends for their support and the warmth they extended to me during this time. I would like to say a heartfelt thank you to my Mum and Dad for always believing in me and encouraging me and for helping in whatever way they could during this challenging period.

Contributions to the work:

Contributions to the work:

Andy Harris: Design and fabrication of the electronics control boxes;

Dr Alexander Beaton and Dr Adrian Nightingale: Chip design consultation;

Gregory Slavik: Chip manufacture;

Dr Victoire Rerolle: Lab View program preparation;

Dr Jeroen Broeders: Lab View program modification.

Contents

1 Introduction **1**

1.1 Trace metal biogeochemistry in marine waters 1

1.1.1 Role of trace metals in marine biogeochemical cycles 1

1.1.2 Dissolved manganese speciation, sources, sinks and distributions in the ocean 3

1.2 Analytical methods 9

1.2.1 Pre-concentration 9

1.2.2 Laboratory based manganese determination methods 10

1.3 Measurements of manganese in natural waters. In-situ technology. 16

1.4 LOAC technology and an in-situ manganese analyser 17

1.5 Manganese LOAC analyser overview 18

1.6 Thesis objectives and outline 18

2 Methods **21**

2.1 Contamination control 21

2.2 Manganese determination using PAN methods 22

2.2.1 Spectrophotometric methods 22

2.2.2 The PAN method 24

2.2.3 Manganese standards 26

2.3 Pre-concentration 26

2.4 Pre-concentration systems using chelating resins 27

2.5 A bench-top iron analyser 29

2.5.1 Use of NTA resin for pre-concentration 29

2.5.2 Use of 8-HQ resin for pre-concentration 34
2.6 Choice of resin for a combined spectrophotometric LOAC pre-concentration system 38
2.7 Use of Mn-54 radiotracer 39
2.7.1 Introduction 39
2.7.2 Background and instrumentation 40
2.7.3 Use of Mn-54 in the present study 41
2.8 Microfluidic chip 42
2.9 Summary 42

3 Optimisation of the pre-concentration procedure using Mn-54 radio tracer 45
3.1 Pre-concentration using Mn-54 46
3.1.1 Reagents, solutions and equipment 46
3.1.2 Analytical procedure 47
3.1.3 Results from column optimisation experiments 47
3.2 Summary and conclusions of pre-concentration optimisation experiments . 67

4 Development of the microfluidic chip and a aplication of the PAN technique 71
4.1 Introduction 72
4.2 Development of the Microfluidic chip 72
4.2.1 Microfluidic test-chips - design and production 72
4.2.2 Microfluidic chip with pre-concentration column 74
4.3 Determination of Manganese with PAN 77
4.4 Using the PAN reagent prepared with Triton X-100 78
4.4.1 Application of the PAN method on chip - Triton X-100 78
4.4.2 Observation of the PAN reagent using a microscope 81
4.4.3 PAN - Triton X-100 - spectrophotometric measurements 84
4.5 Choice of alternative surfactant 86
4.6 PAN reagent prepared with SDS 88
4.6.1 PAN - SDS - off chip measurements 88

4.6.2 PAN - SDS - method performance 93
4.6.3 Application of PAN method on chip - PAN - SDS 99
4.7 Summary and conclusions 103

5 On-bench Lab on a Chip spectrophotometric manganese analyser with pre-concentration 105
5.1 Introduction 105
5.2 System parts and materials 106
5.2.1 Microfluidic chip - optical cell optimisation 107
5.2.2 System design 110
5.3 System performance 117
5.4 Pump system tests 126
5.5 Optimisation of elution 136
5.6 System tests and calibration 145
5.7 Summary and conclusions 155

6 Conclusions and future directions 157
6.1 Summary of achievements 157
6.2 Recommendations for future work 159

A Data for Chapter 4 161

B Data for Chapter 5 169

List of Tables

1.1 Manganese determination. Analytical techniques. Table 1/3. 13

1.2 Manganese determination. Analytical techniques. Table 2/3. 14

1.3 Manganese determination. Analytical techniques. Table 3/3. 15

2.1 Ligand groups used in some chelating resins 28

3.1 0.05 M HCl 53

3.2 0.04 M HCl 55

3.3 0.03M HCl 57

3.4 Elution profile. Eluting acid 0.001M HCl 59

3.5 Elution profile. Eluting acid 0.5 M HCl. 63

3.6 Elution profile. Eluting acid 0.5 M HCl. 64

3.7 Elution profile. Eluting acid 0.5 M HCl. 65

3.8 Elution profile. Eluting acid 0.5 M HCl. 66

3.9 Elution profile. Eluting acid 0.5 M HCl. 67

3.10 Conditions tested for manganese uptake and elution from the Toyopearl resin 69

4.1 On chip experiments. PAN - Triton X-100. Sample premixed with reagent. 79

4.2 Iron measurements on the chip. 81

4.3 Spectrophotometric measurements. PAN SDS. Sample in 0.02 M HCl. Sample buffer 0.04 M NaOH. 94

4.4 Off chip (560 nm) spectrophotometric calibration data. 95

4.5 The spectrophotometric measurements data used to construct the calibration curves. 98

4.6 Summary of off chip and on chip spectrophotometric calibration data (10 cm cell). 99

4.7 Spectrophotometric calibration data. On and off chip measurements (572 nm). 101

5.1 The response from the MQ water diffused with MQ-red dye solution on chip with the measurements cell 600 μm and 500 μm wide 110

5.2 Internal volumes of the channels 115

5.3 Sequence of operation for the system, with final volumes used 116

5.4 Mn standards measurements PAN-SDS. Solutions diffused in the measurement cell of the the chip. 500 nM. Figure 5.14. 121

5.5 Mn standards measurements PAN-SDS. Solutions diffused in the measurement cell of the the chip. 1000 nM. Figure 5.15. 122

5.6 On chip experiments. No pre-concentration. 123

5.7 Relation between the volume of the sample and the pre-concentration factor and the resulting theoretical LOD 124

5.8 Pump tests using dye solution. Pump number and the solutions pumped in the system for manganese determination are listed for information: pump 1 – MQ, standatd, sample; pump 2 – acid solution; pump 3 – reagent; pump 4 – buffer. 126

5.9 Pump test. Pump 2 used at flow rate 600 $\mu L/min$ for 60 seconds. 127

5.10 Pump test. Pump 3 used at flow rate 60 $\mu L/min$ for 200 seconds. 127

5.11 Pump test. Pump 4 used at flow rate 60 $\mu L/min$ for 200 seconds. 128

5.12 Pump test. Pump 2, flow 600 $\mu L/min$, pump 3, flow 60 $\mu L/min$ used simultaneously for 60 seconds. 128

5.13 Pump test. Pump 2, flow 600 $\mu L/min$, pump 4, flow 60 $\mu L/min$ used simultaneously for 60 seconds. 129

5.14 Pump test. Pump 2, flow 600 $\mu L/min$, pump 3 and 4, flow 60 $\mu L/min$ used simultaneously for 60 seconds. 130

5.15 Pump test. Pump 2, 3 and 4 used simultaneously at flow rate 60 $\mu L/min$ for 200 seconds. 131

5.16 Boric acid buffer volume error and its impact on pH change. Boric acid dissolved in 0.4 M NaOH. 132

5.17 Boric acid buffer volume error and its impact on pH change. Boric acid dissolved in 0.5 M NaOH 132

5.18 The results for 1500 nM and 2500 nM manganese standard measurements eluted with 900 μL acid volume. 139

5.19 The results for 2500 nM manganese standard measurements eluted with 900 μL and 400 μL acid volume. 141

5.20 The results for 250 nM and 500 nM manganese standard measurements eluted with 300 μL acid volume. 143

5.21 pH measurements. 10 steps, each step 30 μL 144

5.22 pH measurements. 10 steps, each step 60 μL 144

5.23 On chip measurements with pre-concentration and 10 step elution. 90 μL eluting acid 145

5.24 On-chip measurements with pre-concentration 149

5.25 On chip measurements with and withouth pre-concentration. 151

5.26 On chip measurements. 10 step elution. (a) 1 mL manganese standard solution was loaded on the column equal to 1.5 nanomoles of manganese (one mL of 1500nM = 1.5 nmoles). (b) Eluted with 90 μL volume of acid in each step so for each step manganese concentration was calculated taking into account the 90 μL volume of eluting acid. The volume of the measurement cell was 15 μL. 152

5.27 Results from test on developed system. SLEW-2. 154

A.1 Spectrophotometric measurements. PAN Triton X-100. Sample in 0.01 M HCl, sample buffer boric acid in 0.15 M NaOH. 162

A.2 Spectrophotometric measurements. PAN Triton X-100. Sample in seawater pH 8.0. 163

A.3 Spectrophotometric measurements. PAN Triton X-100. Sample in MQ. . . 164

A.4 Spectrophotometric off chip measurements. PAN SDS. Sample in seawater pH 8.0 165

A.5 Spectrophotometric off chip measurements. PAN SDS. Sample in 0.02 M HCl. Sample buffer boric acid in 0.4 M NaOH. Part 1/2 166

A.6 Spectrophotometric off chip measurements. PAN SDS. Sample in 0.02 M HCl. Sample buffer boric acid in 0.4 M NaOH. Part 2/2 167

B.1 Data - Figure 5.8 170

B.2 Data - Figure 5.10 170

B.3 Data - Figure 5.12 171

B.4 Data - Figure 5.13 171

B.5 Data - Figure 5.17 172
B.6 MQ-Dye experiment data 172
B.7 MQ-Dye experiment data 173
B.8 MQ-Dye experiment data 173
B.9 MQ-Dye experiment data 173
B.10 Data - Figure 5.18 174
B.11 Data - Figure 5.19 174
B.12 Data - Figure 5.20 175
B.13 Data - Figure 5.21 175
B.14 Data - Figure 5.22 176
B.15 Data - Figure 5.23 176
B.16 Data - Figure 5.24 176
B.17 Data - Figure 5.25 177
B.18 Data - Figure 5.26 177
B.19 Data - Figure 5.27 178
B.20 Data - Figure 5.28 178

List of Figures

1.1 Following an episode of enhanced Saharan dust input over the North East Atlantic Ocean, surface concentrations were elevated up to around 3 nM [1]. 7

1.2 Typical profile of dissolved manganese in the open ocean with higher surface concentrations rapidly dropping to low deep water concentrations [1]. 8

1.3 Concentrations of dissolved manganese in the western Indian Ocean [2]. . 8

2.1 Change in form of PAN with pH [3]. 24

2.2 Reactions of PAN A. 25

2.3 Reactions of PAN B. 25

2.4 Schematic diagram of continuous flow system for pre-concentration (NTA resin) and determination of Fe(III) in sea water. 30

2.5 Elution profile of dissolved iron. 1.5 M HCl injected as a sample (1,2); MQ pH 1.9 (3); sea water pH 1.9 (4); 10 nM standard solution pH 1.9 (5). 32

2.6 Elution profile. 1.5 M HCl injected as a sample; pre-concentration 20 seconds. 33

2.7 Elution profile. MQ sample; pH 1.9; pre-concentration 120 seconds. 33

2.8 Schematic diagram of continuous flow system for pre-concentration (8-HQ resin) and determination of Fe(III) in sea water. 35

2.9 Calibration curve for Fe(III) standards prepared in seawater. 36

2.10 A vertical profile of dissolved iron (dFe) at the Rothera Antarctic Time Series Station. 37

2.11 Toyopearl AF – chelate - 650M resin. 39

2.12 A metal complex with the iminodiacetate anion. 39

2.13 Sodium Iodide detector [4]. 41

3.1 Column design. 46

3.2 Effect of sample pH on manganese uptake on the resin. 48

3.3 Effect of sample flow rate on manganese uptake on the resin. 48

3.4 Manganese recovery. Flow rate of 0.2 mL/min and eluting acid strengths ranged from 0.05 M to 0.02 M HCl. 49

3.5 Manganese recovery. Flow rate of 0.2 mL/min and eluting acid strengths ranged from 0.005 M to 0.001 M HCl. 50

3.6 Manganese recovery. Flow rate of 0.2 mL/min and eluting acid strengths ranged from 0.5 M to 0.02 M HCl. 80 μL resin volume. 51

3.7 Manganese recovery. Elution rate of 0.2 mL/min and eluting acid strength 0.05 M HCl. 80 μL resin volume. 52

3.8 Manganese recovery. Flow rate of 0.2 mL/min and eluting acid strength 0.04M HCl. 80 μL resin volume. 54

3.9 Manganese recovery. Flow rate of 0.2 mL/min and eluting acid strength 0.03 M HCl. 80 μL resin volume. 56

3.10 Manganese recovery. Flow rate of 0.2 mL/min and eluting acid strength 0.001 M HCl. 20 μL resin volume. 58

3.11 Manganese recovery. Flow rate of 0.2 mL/min and eluting acid strength 0.5 M HCl. 20 μL resin volume. Sample 1. 60

3.12 Manganese recovery. Flow rate of 0.2 mL/min and eluting acid strength 0.5 M HCl. 20 μL resin volume. Sample 2. 60

3.13 Manganese recovery. Flow rate of 0.2 mL/min and eluting acid strength 0.5 M HCl. 20 μL resin volume. Sample 3. 61

3.14 Manganese recovery. Flow rate of 0.2 mL/min and eluting acid strength 0.5 M HCl. 20 μL resin volume. Sample 4. 61

3.15 Manganese recovery. Flow rate of 0.2 mL/min and eluting acid strength 0.5 M HCl. 20 μL resin volume. Sample 5. 62

4.1 Schematic diagram of the microfluidic chip used to introduce solutions, the reagent and sample (or standard or blank) simultaneously into the optofluidic cell and diffuse. 73

4.2 Test chip design. 73

4.3 Chip with four measurement cells, LEDs (large rectangles) and photodiodes (small rectangles). 74

4.4 Chip with measurement cell and channels and connections designed to attach the column to the chip. LED (large rectangle) and photodiode (small rectangle). 75

4.5 Test chip with Perspex pre-concentration column. 76
4.6 Test chip with flexible teflon pre-concentration column with teflon connectors with frits are shown. 76
4.7 On chip measurements. PAN-Triton-X. Diffusion. 300 nM Mn(II) Replicates 1-3. 79
4.8 On chip measurements. PAN-Triton-X. Preformed Mn-PAN complex. 900 nM Mn(II) Replicates 1-3. 80
4.9 Observation under microscope. PAN Triton X-100, 8 hours mixing time, 48 hours after preparation. Bottom of flask shown. 82
4.10 Observation under microscope. PAN Triton X-100, 17 hours mixing time, 48 hours after preparation, picture 1. 82
4.11 Observation under microscope. PAN Triton X-100, 8 hours mixing time, 112 hours after preparation. 83
4.12 Observation under microscope. PAN Triton X-100, 23 hours mixing time, just after preparation. 83
4.13 Spectrophotometric measurements of Mn-PAN with Triton X-100. Manganese standards were in 0.01 M HCl, and buffered to pH 9.7 with boric acid in 0.15 M NaOH. 85
4.14 Spectrophotometric measurements of Mn-PAN with Triton X-100. Manganese sample is seawater with pH adjusted to 8.0 using ammonia solution. 85
4.15 Spectrophotometric measurements of Mn-PAN with Triton X-100. Manganese sample is prepared in MQ (no buffer). 86
4.16 Structure of the anionic detergent sodium dodecyl sulfate (SDS), showing the hydrophilic and hydrophobic regions. 87
4.17 Simple illustration of a sodium dodecyl sulfate micelle, with the hydrophobic tail attracted to the metal complex. 87
4.18 Observations under a microscope. PAN - SDS, 2 hours mixing time, after 1 day. 89
4.19 Observation under microscope. PAN - SDS, 2 hours mixing time, after 7 days. 89
4.20 Spectrophotometric measurements. PAN-SDS. Sample in MQ. Blank, 300 nM, 400 nM and 600 nM. 90
4.21 Spectrophotometric measurements. PAN-SDS. Sample in sea water. Blank, 300 nM, 500 nM and 1000 nM. 90
4.22 Spectrophotometric measurements. PAN-SDS. Sample in 0.02 M HCl. Blank, 300 nM, 500 nM, 1000 nM and 2000 nM. 91

4.23 Spectrophotometric measurements. PAN-SDS. Sample in 0.02 M HCl. 300 nM Replicate 1 and Replicate 2. 91

4.24 Spectrophotometric measurements. PAN-SDS. Sample in 0.02 M HCl. 500 nM Replicate 1 and Replicate 2. 92

4.25 Spectrophotometric measurements. PAN-SDS. Sample in 0.02 M HCl. 1000 nM Replicate 1 and Replicate 2. 92

4.26 Spectrophotometric measurements. PAN-SDS. Sample in 0.02 M HCl. 2000 nM Replicate 1 and Replicate 2. 93

4.27 Spectrophotometric measurements. PAN SDS. 300 nM, 400 nM, 600 nM. Calibration. Samples in MQ. 95

4.28 Spectrophotometric measurements. PAN SDS. 300 nM, 500 nM, 1000 nM and 2000 nM.Calibration. Samples in 0.01 M HCl. 96

4.29 Spectrophotometric measurements. PAN SDS. 200 nM, 400 nM, 500 nM and 1000 nM. Calibration. Samples in 0.02 M HCl. 96

4.30 Spectrophotometric off chip measurements. PAN SDS. 200 nM, 400 nM, 500 nM and 1000 nM. Calibration. Samples in 0.02 M HCl. 572 nm. Off chip. 99

4.31 Spectrophotometric on chip measurements. PAN SDS. 200 nM, 400 nM, 500 nM and 1000 nM. Calibration. Samples in 0.02 M HCl. On chip. . . . 100

4.32 Spectrophotometric on and off chip measurements. PAN SDS. 100

4.33 On chip measurements. PAN SDS. Blank, 500 nM, 1000 nM. 101

4.34 On chip measurements. PAN SDS. 500 nM. 102

4.35 On chip measurements. PAN SDS. 500 nM. Voltage values converted to Mn(II) concentrations. 103

5.1 Diagram showing the solutions directed into the chip with Hamilton Syringe Pumps used to control the flows. 107

5.2 Test chip design with measurement cell 500 μm wide. 108

5.3 Test chip - measurement cell 500 μm wide. MQ water diffused with MQ-red dye solution. 109

5.4 Test chip - measurement cell 600 μm wide. MQ water diffused with MQ-red dye solution. 109

5.5 Diagram showing the flow of solutions in the system with Sensor group piston pumps and valves. 111

5.6 The first design for on bench chip with the custom designed pump implemented on the chip. 112

5.7 Final design for on bench chip for use with syringe pumps. 113

5.8 Mn standard measurements (500 nM and 1000 nM) with PAN-SDS. Solutions premixed before injecting in to the chip. 117

5.9 Mn standard measurements (500 nM and 1000 nM) with PAN-SDS. Solutions premixed before injecting in to the chip. Voltage values converted to nM concentrations. 118

5.10 Mn standards measurements PAN-SDS. Solutions diffused in the measurement cell of the the chip. Blank and 1000 nM. 118

5.11 MQ-dye measurement. Response recorded when valves turn on/off. 119

5.12 Manganese standard measurements PAN-SDS. Solutions diffused in the measurement cell of the the chip. Blank and 500 nM. 120

5.13 Blank measurements PAN-SDS. Solutions diffused in the measurement cell of the chip. 120

5.14 Mn standards measurements PAN-SDS. Solutions diffused in the measurement cell of the the chip. 500 nM Replicates 1-7. 121

5.15 Mn standard measurements PAN-SDS. Solutions diffused in the measurement cell of the the chip. 1000 nM Replicates 1-8. 122

5.16 Calibration curve. No pre-concentration 123

5.17 Dye-MQ measurements. Rep 1-11. Enlarged. 125

5.18 Blank measurements. Solutions diffused in the measurement cell of the chip. Boric acid buffer in 0.5 M NaOH. Replicates 1-5. 133

5.19 Manganese standards measurements. 2000 nM. Solutions diffused in the measurement cell of the chip. Boric acid buffer in 0.5 M NaOH. Replicates 1-6. 133

5.20 Manganese standards measurements. 2000 nM. Solutions diffused in the measurement cell of the chip. Boric acid buffer in 0.5 M NaOH. Replicates 1-7. 134

5.21 Manganese standards measurements. 2000 nM. Solutions diffused in the measurement cell of the chip. Boric acid buffer in 0.5 M NaOH. Replicates 1-5. 134

5.22 Manganese standards measurements. 2000 nM. Solutions diffused in the measurement cell of the chip. Boric acid buffer in 0.5 M NaOH. Replicates 1-4. 135

5.23 Manganese standards measurements. 2000 nM. Withdrawn manually. Solutions diffused in the measurement cell of the chip. Boric acid buffer in 0.5 M NaOH. Replicates 1-5. 136

5.24 Eluted manganese standard measurements. 1500 nM. Solutions diffused in the measurement cell of the chip. Boric acid buffer in 0.5 M NaOH. 10 steps. 900 μL acid volume. 137

5.25 Eluted manganese standard measurements. 2500 nM. Solutions diffused in the measurement cell of the chip. Boric acid buffer in 0.5 M NaOH. 10 steps. 900 μL acid volume. 138

5.26 Eluted manganese standard measurements. 2500 nM. Solutions diffused in the measurement cell of the chip. Boric acid buffer in 0.5 M NaOH. 10 steps. 400 μL acid volume. 140

5.27 Eluted manganese standard measurements. 500 nM. Solutions diffused in the measurement cell of the chip. Boric acid buffer in 0.5 M NaOH. 10 steps. 300 μL acid volume. 142

5.28 Eluted manganese standard measurements. 250 nM. Solutions diffused in the measurement cell of the chip. Boric acid buffer in 0.5 M NaOH. 10 steps. 300 μL acid volume. 142

5.29 Blank measurements. Solutions diffused in the measurement cell of the chip. Replicates 1-5. Sample buffer in 0.5 M NaOH. 1 step. 300 μL acid volume. 147

5.30 1000 nM measurements. Solutions diffused in the measurement cell of the chip. Replicates 1-5. Boric acid buffer in 0.5 M NaOH. 1 step. 300 μL acid volume. 147

5.31 300 nM measurements. Solutions diffused in the measurement cell of the chip. Replicates 1-8. Boric acid buffer in 0.5 M NaOH. 1 step. 300 μL acid volume. 148

5.32 Calibration. On-chip measurements with pre-concentration. 148

5.33 SLEW-2 measurements. Solutions diffused in the measurement cell of the chip. Rep 1-5. Boric acid buffer in 0.5 M NaOH. 1 step. 300 μL acid volume. 153

Chapter 1

Introduction

Contents

1.1 Trace metal biogeochemistry in marine waters 1
1.1.1 Role of trace metals in marine biogeochemical cycles 1
1.1.2 Dissolved manganese speciation, sources, sinks and distributions in the ocean 3
1.2 Analytical methods 9
1.2.1 Pre-concentration 9
1.2.2 Laboratory based manganese determination methods 10
1.3 Measurements of manganese in natural waters. In-situ technology. 16
1.4 LOAC technology and an in-situ manganese analyser 17
1.5 Manganese LOAC analyser overview 18
1.6 Thesis objectives and outline 18

1.1 Trace metal biogeochemistry in marine waters

1.1.1 Role of trace metals in marine biogeochemical cycles

Macronutrients and micronutrients are important in the process of characterisation of ocean biogeochemistry. Macronutrients such as nitrate, ammonia, silicic acid or phosphate are required in large proportion for the normal growth and development of a plant, and are required for the synthesis of macromolecules such as lipids, proteins and carbohydrates. Marine phytoplankton therefore need to consume significant quantities of seawater macronutrients they require for growth. Micronutrients, mostly trace metal

elements (present in ocean waters at less than 0.1 μM) [5] e.g. iron, manganese, zinc, copper, nickel, cobalt and cadmium are required in small quantities but they are essential for some critical biological processes. A lack of availability of the trace metal micronutrients required by the planktonic organisms, will control the rate of some important enzymatic reactions and on a global scale the productivity of the oceans and the biogeochemical cycles of elements such as carbon and nitrogen [5].

An example of a cellular process where trace metals are essential is photosynthesis, where light energy is converted into chemical energy in plants. This chemical energy is stored in carbohydrate molecules synthesized from carbon dioxide and water. Solar energy is used to power the thermodynamically demanding reaction of water splitting. At the heart of a photosystem lies the reaction center (RC), where light energy is converted to electrochemical potential energy and the water-splitting reaction occurs. Water-splitting involves a cluster of four manganese (Mn) ions, which is the oxygen evolving centre (OEC) and the site of water oxidation. Photosystem II (PSII), one of the protein complexes located in the thylakoid membranes of all types of plants, algae, and cyanobacteria, absorbs light and excites electrons in the reaction-center to a higher energy level which are trapped by the primary electron acceptors. The by-product of the water-splitting reaction is molecular oxygen. In this process OEC of photosystem II generates dioxygen from water using the manganese center [6, 7]. Thus if manganese is not available, photosynthesis and growth are inhibited with very low concentrations of manganese, e.g. less than 100 pM in Southern Ocean waters [8, 9, 10, 5, 11, 12].

A further example of the importance of manganese in biogeochemical cycles is the removal of nitrogen (ammonia, nitrate, organic nitrogen) from the ocean which is due to the reduction of nitrate to dinitrogen (N_2). From the classical nitrogen cycle ammonia in marine sediments is oxidised to nitrate by nitrifying bacteria and nitrate is reduced to N_2 by denitrifying bacteria. However, it is suggested that manganese may also take part in the formation of N_2. The production of N_2 can be a result of reduction of nitrate by Mn^{2+} or the oxidation of NH_4 and organic-N by Mn_2O in the presence of O_2. The Mn^{2+} formed is re-oxidised to MnO_2 by O_2 in a catalytic cycle that is affecting nitrogen speciation and the marine nitrogene cycle. Luther et al. [13] reported that a manganese cycle can provide more force for oxidation of organic matter than O_2 and that manganese catalysed oxidation of NH_4 and organic-N to N_2 is likely a process that is important on a global scale. In ecosystems with lower pH, like lakes, a similar cycle may involve iron. Fe^{2+} can react with NO_3 to form N_2 [13].

Doi et al. reports that manganese plays an important role in geochemical cycles of

trace metals in the ocean and is an essential micronutrient for phytoplankton growth, like iron, zink and cobalt. The vertical profiles of manganese in the open ocean generally show the scavenging type, indicating that manganese is not depleted for phytoplankton growth, unlike iron and zinc [14]. However Martin et al. reported a possibility that manganese deficiency may be a factor controlling phytoplankton growth in the Southern Ocean, with the surface manganese concentration in the Drake Passage reported at 0.08 nmol, and the nutrient like vertical profile [15]. Middag et al. suggested that manganese is a factor of importance partly explaining the HNCL conditions in the Southern Ocean, next to significant controls by the combination of Fe limitation and light limitation. Extremely low concentrations of dissolved manganese in the surface layer, correlate with the nutrients PO_4 and NO_3, and moderately well with Si, indicating intense involvement of manganese in the plankton biological cycle. Middag et al. also suggested that the increased manganese demand under lower concentrations of Fe would explain the trend of higher manganese nutrient ratios where ambient concentrations of Fe tended to be lower. This is indicative of co-limitation by manganese and Fe of phytoplankton growth in the Southern Ocean. Dissolved Mn has been shown to be potentially (co-)limiting in lab experiments and to some extent in the field. However a response to manganese addition is not always observed, indicating that in some parts of the Southern Ocean an ambient concentrations of dissolved manganese are in adequate supply , i.e not limited [12].

In addition to its importance in biological processes, manganese in its solid oxide form, can be an important carrier phase for other elements. For example the oxidation products of manganese and iron discharged with hydrothermal effluents lead to scavenging of rare earth elements (REE). In natural waters precipitation of manganese and iron oxides is widespread and therefore REE patterns of seawater may be affected by the fractionation during the scavenging process [16]. Inorganic adsorption reactions with the surface of MnO_2 particles may cause cerium scavenging from seawater [17]. Manganese nodules cover part of the sea floor and the sediments underlying the nodules are greatly enriched in this element [18].

1.1.2 Dissolved manganese speciation, sources, sinks and distributions in the ocean

Manganese is the most abundant transition metal in nature after iron. It exists in the oxidation states Mn(II), Mn(III) and Mn(IV), in natural waters as soluble Mn^{2+} ions

and insoluble Mn^{3+} and Mn^{4+} oxides. [19, 20]. No information on organic forms of manganese in seawater could be found, and generally inorganic forms predominate.

The solubility of manganese in seawater is controlled by the oxidation of Mn^{2+} and the reduction of manganese oxides. Dissolved Mn^{2+} ions in oxic seawater are unstable and will precipitate as manganese oxides, which are removed throughout the water column by scavenging and sinking [21, 12]. However, particulate manganese may be regenerated under sub-oxic conditions [22] and manganese oxides can be reduced to soluble manganese ions [12].

The distribution of manganese in the ocean is determined by external inputs including atmospheric and river sources [22, 23, 2, 12], sediment [22, 12] or hydrothermal vents [2].

Atmospheric inputs are the main sources of manganese and many other trace metal elements (particulate and dissolved forms) to the open ocean by rain (wet) or by dust (dry) deposition, and the most important source for dust inputs into the oceans are deserts. The effect of the atmospheric inputs can be clearly seen in central ocean gyres (Atlantic and Pacific Oceans), which has led to the suggestion that these kind of inputs may influence the primary production of the oceans. The Sahara and Sahel desert regions in Africa are the largest sources of dust in the Atlantic Ocean. The Asian deserts are the main dust source in the North Pacific Ocean and the Australian deserts are the main dust input to the South Pacific Ocean. The Arabian deserts provide dust to the Northwestern Indian Ocean. Dusts can travel hundreds of miles away from their origins by strong winds, and so deposition patterns depend on meteorological conditions and emission patterns. Thus, the effect of atmospheric inputs on surface ocean biogeochemistry can be seen even in remote oceanic areas (Figure 1.1) [1].

Rivers transport manganese rich sediments to coastal waters, and can indirectly supply manganese in dissolved and particulate forms to the ocean systems. We can observe high manganese concentrations (up to around 5 nM/L) in the coastal waters due to the fluvial discharges. Furthermore, manganese is known to have a benthic source on continental shelves from reducing sediments, which further increases its concentration in shelf waters, although on a seasonal basis [24]. The shelf is an important source of manganese for the open ocean as demonstrated in several continental margins for example the western South Pacific Ocean, New Zealand, the eastern North Atlantic Ocean, and the European shelf. Manganese enrichments have also been reported in water masses over the shelf regions of oceanic islands e.g. the Kerguelen Plateau of the Southern Ocean,

and the Galapagos Archipelago of the Equatorial of the Pacific Ocean [25].

Hydrothermal inputs are a crucial source of manganese to the deep-seas especially along the mid-ocean ridges [26]. The most enriched metals in hydrothermal vent fluids are iron and manganese, and these elements are involved in redox reactions that change between reduced dissolved forms Fe(II) and Mn(II) and the oxidized forms of Fe(III) and Mn(IV), which are stable. In the open ocean manganese is enriched in the hydrothermal vent fluids, total dissolved and particulate manganese concentrations are even 100 times greater than the normal water column values. Therefore manganese can be used as a sensitive tracer of the hydrothermal activity [16, 12] and may be used to discover new vent systems. Conditions suitable for microbial manganese oxidation are created at hydrothermal vents where reducing hydrothermal fluids reach in Mn(II) mix with the oxygenated ambient seawater. For example in Galapagos, where vents reach warm temperature of 10-20 deg C, the manganese concentrations are around 10-40 μM [26]. Hydrothermal manganese input has been also shown in the Bransfield Strait near the Antarctic Peninsula. Close to the Antarctic continent and the Antarctic Peninsula, reductive dissolution from (anoxic) sediments or land run off (i.e. ice melt) can also be a source for the dissolved manganese [12].

Manganese once it enters the ocean is under the influence of various processes. Direct sunlight influences manganese concentrations [27]. Manganese oxides Mn(IV) or colloidal particles from deep water are believed to be transported back to surface waters by upwelling or vertical mixing, and then photo-reduced to soluble Mn(II), resulting in an increase of the concentration of dissolved manganese Mn(II) at the surface [28]. Manganese can also be scavenged by a wide range of living and dead organisms and particles, e.g. particulate minerals, phytoplankton, and skeletal materials, sinking to the deep water of the ocean [5]. In the productive shelf seas export of particulate matter to the sea floor and subsequent microbial breakdown can lead to anoxic sediments and conditions like these allow for the manganese to be mobilised from the sediments into the pore water and subsequently flux out into the overlying water column [12]. Indeed Mn(II) oxidation in the marine environment is largely microbially catalyzed and this results in elevated Mn(II) concentrations in reducing environments such as near oxic-anoxic interfaces within sediments and in anoxic basins. At hydrothermal vents conditions are suitable for microbial manganese oxidation when fluids rich in Mn(II) mix with oxygenated ambient seawater. Thus enhanced manganese scavenging is caused by manganese-coated bacteria that settled out from the vent plume and accumulate in the underlying sediments [26]. In environments such us near oxic-anoxic interfaces within sediments and in anoxic basins,

dissolved manganese concentrations are elevated and microbially mediated manganese oxidation is especially evident [26]. Loch Etive (Scotland) has two main basins with classic fjordic features. Statham et al. 2005 reports the use of AUV Autosub in Loch Etive, showing substantial variability in concentrations of dissolved manganese, between less than 25 nM in surface waters and above 600 nM in the deepest basin. The upper basin of Loch Etive is isolated from the lower basin by a sill, which isolates the waters in the deepest part for periods of, on average, 16 months. Due to primarily benthic respiration in the isolated deep waters behind the sill, oxygen decreases and manganese increases to nearly micromolar concentrations. A sedimentary source of manganese is driven by the redox conditions present. These conditions depend on the bacterially driven oxidation of organic carbon within the sediments. After oxygen and nitrate are exhausted then oxidised manganese will be reduced and dissolved manganese will be released. Other factors like bioturbation can enhance the release of dissolved manganese, however the major factor influencing the release of dissolved manganese will be the amount of labile carbon in the sediment [29].

Middag et al. 2011 reports the examples of regions where (nearly) anoxic sediments are observed, listing semi-enclosed deep basins like the Black Sea or Cariaco Trench [12]. High levels of dissolved iron and manganese are reported by Saager et al. for the Black Sea, the Cariaco Trench, Framvaren Fjord and hypersaline Tyro and Bannock basins [9]. The Baltic Sea consists of several deep basins. A transition zone with strong vertical redox gradients (pelagic redoxcline) can be observed in the Black Sea, in the Baltic Sea and in many fjords. It is formed as the result of strong stratification of the deep water column.

The typical oceanic distribution of manganese is now well known [22, 10, 23, 2, 30, 12]. Vertical distributions of manganese show highest concentrations in surface waters (between around 1 and 3 nM), mainly due to dust inputs [23] and are also the result of the reduction of manganese oxides [27, 19, 12]. Concentrations decrease over the top few hundred meters to around 0.5 - 0.2 nM and to around 0.2 – 0.1 nM in deep waters (Figure 1.2) [1].

Overall, the concentrations of dissolved manganese are above 40 pM. The lowest reported surface concentration is in the Atlantic Sector of the Southern Ocean with 40 pM [12] and the highest surface concentration is in the Lapter Sea of the Arctic Ocean with 20 nM [12]. The deep-water concentrations of dissolved manganese are in a range between 50 pM in the deep Makarov Basin of the Arctic Ocean [12] and 12 nM in the Eastern Tropical Pacific Ocean [31]. However, Kerguelen Islands in the Southern Ocean,

showed an exceptionally high concentrations of dissolved manganese even in the offshore deep water (up to 8.6 nM). It is believed that the main source of the manganese in this region is the island system itself [32].

In line with those general trends Morley et al. reported maximum manganese concentrations in South Indian Ocean in the upper water column to be about or below 1 nM and very low deep water manganese concentrations (Figure 1.3) [2].

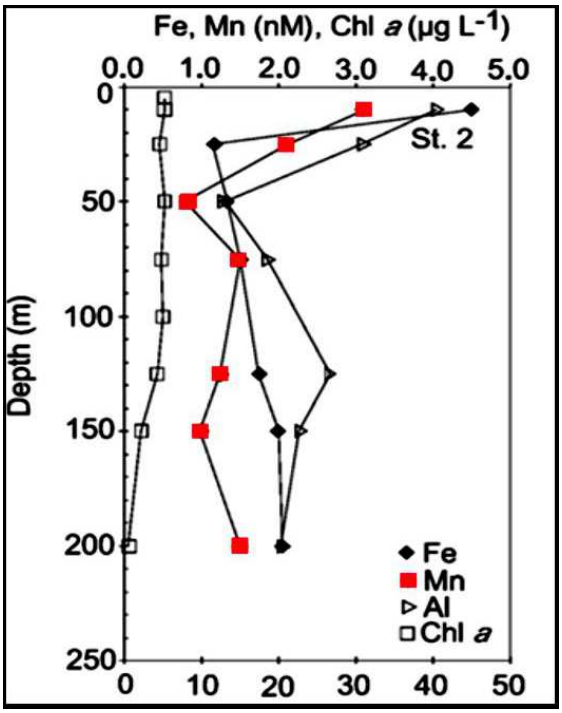

Figure 1.1: Following an episode of enhanced Saharan dust input over the North East Atlantic Ocean, surface concentrations were elevated up to around 3 nM [1].

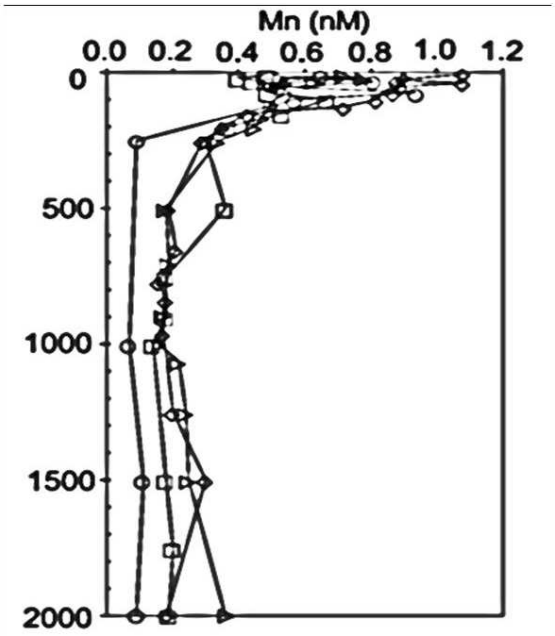

Figure 1.2: Typical profile of dissolved manganese in the open ocean with higher surface concentrations rapidly dropping to low deep water concentrations[1].

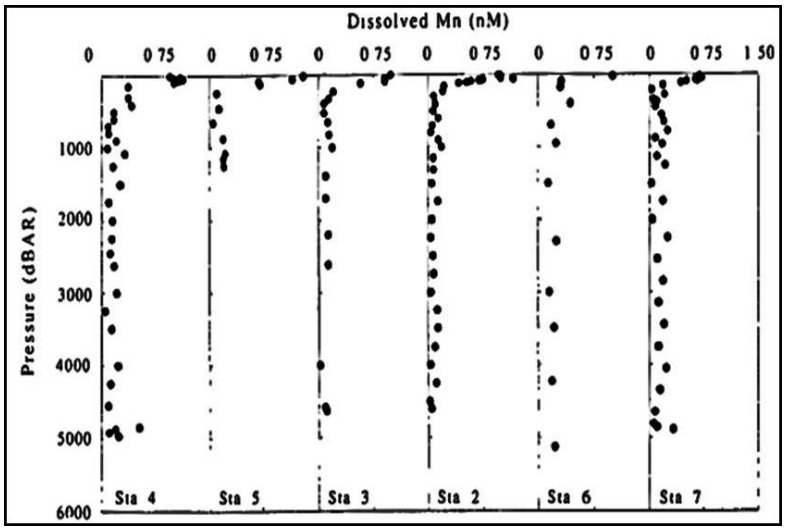

Figure 1.3: Concentrations of dissolved manganese in the western Indian Ocean [2].

To better understand this important trace element new tools are needed and in particular methods for in-situ analysis.

1.2 Analytical methods

1.2.1 Pre-concentration

Direct determination of manganese ions at very low concentrations typical of ocean systems is difficult due to the lack of sensitivity of the measurement techniques. In trace analyses, not only the low concentration of the analytes but also possible interferences from the matrix and other elements must be considered. The extremely low concentrations of metal ions in seawater and the sample salt matrix make direct analysis difficult or impossible. Therefore a pre-concentration step prior to the determination of trace metals is necessary and most of the methods use a pre-concentration step [33] when applied to ocean waters. On-line pre-concentration techniques where the pre-concentration occurs immediately before the introduction into the instrument, and is part of a continuous analytical process developed during recent years combine both pre-concentration and determination steps.

To explain the pre-concentration principle, we can use a simple example. If the detection limit of the analytical method without pre-concentration is 1000 nM, and we need to determine the metal in a sample containing only a few nM of analyte, we might first pass 1000 mL of the sample through the column containing the resin absorbing the analyte with 100 % retention efficiency. The analyte of interest would then be eluted from the column with say 5 mL of an appropriate reagent, achieving a pre-concentration of 1000 / 5 = 200 and the detection limit would be reduced to approximately 5 nM [33]. With very low detection limits care needs to be taken to avoid contributions of impurities from reagents, therefore pre-purifying some of the reagents before the analysis as part of the analytical procedure, often using a resin column, may be necessary.

There are many pre-concentration techniques that can be used for trace metal determination, including: solid phase extraction, solvent extraction and electrochemical methods [34, 35].

Solid phase extraction (SPE) is a separation process in which a liquid sample (mobile phase) is passed through a stationary phase to separate the analyte from the mixture. The analytes of interest are retained on the stationary phase, and can be removed by rinsing with an appropriate eluent. Solid phase extraction can be categorised into: normal phase, reversed phase and ion exchange. Ion exchange resins can be divided into three groups: cation, anion and chelating exchangers. Cation or anion collection by the resin is based on exchange of the counter ion for another ion. Cation exchangers exchange positively

charged ions (cations), and anion exchangers exchange negatively charged ions (anions). In chelating resins, the SPE method most often applied to trace metals in seawater, counter ions are bound to the resin by coordinate covalent bonds or by electrostatic interactions. The interaction of functional groups (ligand) of the chelating resin and metal (in the form of cation or oxy-anion) allows selective removal of the target metals via suitable functional groups in the chelating resins [34]. Chelating solid phase materials have been widely used for pre-concentration and separation of trace metal ions [36], and appear most readily interfaced with Lab on a Chip (LOAC) technology (see below). The efficiency of adsorption of the analyte on to the column is influenced by several factors such as the flow rate of the water through the column and the sample pH [33].

During the determination of trace amounts of metals not all the metal of interest may be adsorbed on the resin. Part of the metal may be present in bound form and may be inaccessible to the resin. This may be when the metal is in the form of strong complexes that are not dissociated, in colloidal form or insoluble in acid. Only labile and free metals can be extracted or adsorbed on the resin and measured. Water samples may contain naturally occurring or man-made chelating agents, which may form strong complexes with metals in the sample or weaker complexes. When these complexes are stronger than the complexes formed with the chelating agent used in the method of pre-concentration, very low metal recoveries may be obtained. The metal chelating efficiency of the resin may also be lower in sea water than in fresh water due to the complicated speciation of metals in sea water. Destruction of the complexes by ultraviolet light or acid before the sample goes through the column allows for complete recovery of metals [33]. The type of pre-concentration resin and conditions used are important in the overall performance of a system. Whilst iron, for example, is known to have strong bonds with ligands in seawater, dissolved manganese appears to be predominantly present as ionic form of Mn^{2+}. This simplicity of speciation led to the choice of manganese as the focus of the system to be developed.

1.2.2 Laboratory based manganese determination methods

Several techniques have been used for manganese determination in collected water samples, including catalytic [37, 38, 39], chemiluminescence [14, 12], UV spectrophotometry [40, 39, 37], inductively coupled plasma-mass spectrometry (ICP-MS) [41, 42, 43], inductively coupled plasma optical emission spectrometry (ICP-OES) [44] and X-ray fluorescence spectrometry [45].

Colorimetric spectrophotometric methods

The most suitable colorimetric methods for the determination of manganese are based on formation of coloured manganese reagent complexes. A spectrophotometric method using 1-(2-pyridylazo)-2naphthol (PAN) was developed by Chin et al. [40], for determination of dissolved manganese in seawater. This used the iron specific chelating agent desferrioxamine B, to mask iron interferences [40]. This method was tested by measuring dissolved manganese concentrations in-situ using the SCANNER system [46, 40], as described in section 1.3.

Catalytic spectrophotometric methods

A highly sensitive catalytic spectrophotometric detection method for manganese determination is described by Resing et al. [37]. The method, modified after Olaffson et al. [38], is based on flow injection analysis with on-line pre-concentration on a 8-hydroxyquinoline (8-HQ) column (immobilised on a vinyl polymer gel). Mn(II) acts as catalyst in the reaction between leucomalachite green and potassium periodate. Mn(II) concentration is determined by detection of the product of the reaction, malachite green. The limit of detection reported is 36 pM [37]. This method was further modified by Aguilar-Islas et al. [39] with: Toyopearl AF-Chelate 650M (Toyopearl) resin used instead of 8-HQ; addition of nitrilotriacetic acid as an activator ligand which increased sensitivity and decreased the LOD; on-line buffering of acidified samples before column loading; use of more soluble sodium periodate in place of potassium periodate; pH of samples adjusted to 8.5 (vs. 7.8); higher acid concentration to elute the manganese from the IDA resin; and a stronger reaction buffer to neutralize the acid.

There are many other catalytic methods for the determination of manganese [47], most of them, however, have strong temperature dependencies and long reaction times, which is not desirable for in-situ analysis [40]. The lack of their use in environmental studies indicates their lack of suitability for routine measurements.

ICP-MS and ICP-OES methods

A method was used by Warnken et al. [41] for manganese measurements with pre-concentration on commercially available iminodiacetate resin Toyopearl AF-Chelate 650M and determination by ICP-MS. In the method ammonium chloride buffer with a pH of 8.8 was mixed with the sample on-line prior to loading on the resin and 1 M HNO_3 acid

was used for column elution. Milne et al. used high resolution inductively coupled mass spectrometry (HR-ICP-MS) for manganese determination along with a range of other trace metals [43]. In the reported method samples were irradiated using a low power UV system to destroy any organic ligands before pre-concentration and extraction. For the pre-concentration Toyopearl resin was used, nitrilotriacetic acid (NTA) resin and 8-HQ resin were also tested. Elements were eluted from the resin with 1 mL of 1 M $Q - HNO_3$ solution.

Chemiluminescence detection

Doi et al. [14] analysed picomolar levels of manganese in seawater by chelating resin concentration and chemiluminescence detection. In this method, manganese in the sample solution is collected on iminodiacetate-immobilized chelating resin, and then eluted with acidic solution containing hydrogen peroxide. The resulting eluent is mixed with luminol solution and aqueous ammonia after removal of otherwise interfering iron ions by a chelating resin column. The detection limit (3SD) reported for manganese is 5 pM from 9 mL of seawater sample.

Middag et al. [12] used the chemiluminescence method developed by Doi et al. [14], modified to buffer the samples in-line with ammonium borate buffer after the method of Aquilar-Islas et al. [39]. Samples were acidified to pH 1.8 (with 12 M HCl) and buffered in-line to a pH of 8.5 $\pm$ 0.2 with 0.5 M ammonium borate sample buffer. In this method the buffered sample was pre-concentrated for 200 seconds on Toyopearl AF-Chelate 650M column.

Luminol-hydrogen peroxide Chemiluminescence detection was earlier used by Okamura et al. [48] for manganese determination. In this work 8-quinolinol resin immobilized on the partially fluorinated silicon alkoxide glass column 8-hydroxynoquinoline was used for removing of interfering metals in the sample and carrier solution.

Fluorescence spectrometry

Yamini et al. [45] measured manganese in natural water with X-ray fluorescence spectrometry after pre-concentration with powdered silica gel. In the method PAN was used as a chelating agent with quantitative extraction at pH 9.5 – 10.5.

LOD values reported for the methods described and method information are shown in Tables 1.1, 1.2 and 1.3.

Table 1.1: Manganese determination. Analytical techniques. Table 1/3.

Analytical techniques. Determination of manganese in seawater at low concentrations.			
Analytical technique: Spectrophotometry			
Pre-concentration	LOD	Method information	Reference
-	22 nM	In-situ analyser Scanner - Hydrothermal plumes; - Complexing reagent PAN; color formation $<$ 1 s; - Desferrioxamine B - High viscosity of Triton X-100, 50 cm glass bead column used to promote mixing	CS Chin et al., 1992
Toyopearl	0.03 nM	Method after Resing and Mottl 1992; - Toyopearl instead of 8-HQ; - Nitrilotriacetic acid as an activator ligand which increased sensitivity and decreased LOD; - Sample 1.6 mL; pH 8.5-9.0 (vs.7.8); - 1cm column (85 μL); 2 min loading; - Precision 3.2 % - 6.9 % (n=4).	AM Aguilar-Islas et al., 2006
8-HQ	0.036 nM	Method after Olafsson 1986; - Reaction of leucomalachite green and potassium periodate with Mn(II); - 15 mL of sweater; pH 7.8; 3.7 mL/min; - Precision between 1.5 % and 5.4 % (n=6).	J A Resing et al., 1992

Table 1.2: Manganese determination. Analytical techniques. Table 2/3.

Analytical techniques. Determination of manganese in seawater at low concentrations.			
Analytical technique: ICP-MS			
Pre-concentration	LOD	Method information	Reference
Toyopearl	0.02 nM	- 1M HNO3 acid for column elution; - Column loading pH 8.8; - Precision better than 5 %; 1 mL sample; - 3 min column rinse period with deionised water to avoid interference.	KW Warnken et al., 2000
Nobias-chelate PA1	-	- Samples (40 mL) were loaded onto the column at a pH of 6.2; - 0.6 mL/min 3 min; - Eluted with 3-4 mL of 1 M Q-HNO3 (7-8 min).	DV Biller et al., 2012
Toyopearl (NTA and, 8-HQ also tested)	0.007 nM	- Samples irradiated using UV system to destroy organic ligands - 12 mL sub samples (off-line); - pH 6.4 prior to loading onto the resin (manganese recovery about 60 %); - Eluted with 1 mL of 1M Q-HNO3 for 30 seconds; - The sensitivity of manganese was variable and strongly correlated with pH; the highest sensitivity was at pH 8.1, though full recovery was not achieved (about 90 %) - Precision 4.6 % (n=3)	A Milne et al., 2010

Table 1.3: Manganese determination. Analytical techniques. Table 3/3.

Analytical techniques. Determination of manganese in seawater at low concentrations.			
Analytical technique: AAS			
Pre-concentration	LOD	Method information	Reference
Amberlite XAD-4	-	-PAN dissolved in water/ethanol (25/75 v/v), -10 mL buffer and 5 mL PAN were added to 50-60 mL of sample solution; Loading pH 9.0.	M Tuzen et al., 2007
Analytical technique: ICP-OES			
Pre-concentration	LOD	Method information	Reference
PAN modified magnetic nanoparticles	0.002 nM	PAN modified magnetic nanoparticles used for separation and pre-concentration of Mn(II). Mn ions were adsorbed from solution at pH 9.5 and desorbed from nanoparticles with 10 mL of DMSO : HNO_3 (1:1 v/v).	M Khajeh et al., 2012
Analytical technique: Fluorescence			
Pre-concentration	LOD	Method information	Reference
Powdered silica gel	-	PAN used as chelating agent with quantitative extraction at pH 9.5 - 10.5.	Y Yamini et al., 2009

1.3 Measurements of manganese in natural waters. In-situ technology.

The vast majority of data on dissolved manganese and other important metals such as iron in marine waters have been obtained by collection of samples from research ships and then the analysis of this water on shore using a wide variety of techniques. However these approaches are slow, may have associated artifacts once the sample is removed from the water column, and give only very limited spatial and temporal coverage.

To be able to better understand biogeochemical processes in the ocean we need to be able to perform in-situ marine biogeochemical sensing [49] and make measurements at high frequency, to investigate spatial, short and long term variability in processes in ocean waters [50]. The marine environment is characterised by a large range of temperature and pressure and is biologically active with complex chemical compounds and biological species. Many of these variable parameters interfere with measurement techniques. Additionally many of the parameters of interest, like nutrients, are present in very small concentrations. Therefore high sensitivity and precision are required [49]. Oceans are very dynamic environments and to be able to understand them, long term biogeochemical sensing is required, as well as measurements at high frequency and over extended space scales [50]. Lab on a chip technology can help provide these data [51].

Several in-situ systems have been developed and used in marine systems to collect dissolved manganese and iron data from samples in real time. Examples are:

1. The submersible chemical analyser SCANNER developed in 1986 was used for the determination of iron and manganese in-situ. Total dissolved iron was analysed with colorimetric detection, using ferrozine, and reducing Fe(III) to Fe(II) with ascorbic acid, whilst dissolved manganese was analysed using 1-(2-pyridylazo)-2-napthol [52, 46, 53], with detection limits of 22 nM for manganese and 25 nM for iron [53].

2. SUAVE (Submersible System Used to Assess Vented Emissions) was another system used for colorimetric determination of total iron and Mn(II) [54], with detection limit given as 5 nM for iron and 10 nM for manganese [37].

3. The ZAPS method (Zero Angle Photon Spectrometer) is based on fluorescence detection, and was developed and used for the determination of manganese in seawater, with a quoted detection limit of less than 0.1 nM [55].

4. The Fe-Osmo analyser, was an osmotically pumped analyser for the determination

of iron, with the colorimetric detection of iron, based on reduction of Fe(III) to Fe(II) with ascorbic acid and complexation with ferrozine [56] [57].

5. Statham et al. developed an in-situ metal analyser, based on spectrophotometric detection, using 1-(2-pyridylazo)-2-naphtol for the determination of manganese. The analyser was designed for use with an autonomous underwater vehicle (AUV). The analyser had a limit of detection of 25 nM [29].

6. Another analyser used for in-situ determination of iron using colorimetric detection, was the submersible chemical analyser ALCHEMIST [58] and CHEMINI (Chemical Miniaturized Analyser) [59].

Despite many advantages, there are still limitations to the in-situ systems, such as limited operational life, caused by reagents ageing and power supply and in particular the lack of sensitivity to measure low oceanic concentrations [51, 60, 61, 62].

1.4 LOAC technology and an in-situ manganese analyser

The techniques described above summarise chemical methods used for manganese detection in seawater. However the most obvious way forward for improved in situ analyses was to build on an existing technology in the Sensors Group at Southampton, and develop a pre-concentration system for coupling to spectrophotometric LOAC technologies in the laboratory.

Lab on a chip technology integrates standard laboratory processes with chemical and biochemical analysis, on a micro scale chip device [63]. LOAC, also called a micro total analysis system, integrates multiple steps of analysis, such as: sampling, sample treatment, reaction and detection, on a single device [64, 65]. LOAC technologies have the significant advantages of small size, portability, limited reagent and power requirements, faster analysis and response times [51, 66, 63, 65, 67] and reduced risk of sample loss and contamination [61] of the sample and of the measuring system, especially important for trace analytes [68]. Smaller volumes of reagents are less hazardous to use [69, 70], the risk involved with transportation and storage of toxic and hazardous chemicals is also reduced [71] and the analysis process is more environmentally friendly [70] with small volumes of waste produced [71]. All this allows for continuous processing of samples [67] and simple safer operation on a smaller device.

Sensors should be easy to place in different locations, require minimum intervention

of direct operation and to be disposable if necessary [68], and must be resistant to fouling, corrosion [60] and interfering compounds (with concentrations often higher than the analyte measured) [66]. Sensors could provide real-time information.

The associated system requirements for LOAC technology need to be carefully thought through, including the fabrication material, the method of providing liquid flow through the micro-channels and the need for a sensitive detection technique.

1.5 Manganese LOAC analyser overview

In a LOAC system for manganese, the typically low concentration of the analyte in seawater and possible interferences must be considered. The pre-concentration approach has the potential to address both issues and thus substantially improve the abilities of existing direct LOAC colorimetric systems. Therefore a manganese analyser with an incorporated pre-concentration step is needed. The production and building of the pre-concentration chip for an on bench manganese analyser as described here is based on the same materials as the main chemical analyser reported by Floquet et al. [72]. The extensive and detailed development and optimisation of the system is described in this thesis.

1.6 Thesis objectives and outline

The main aim of the work reported here is therefore the development of a new LOAC system capable of later deployment in marine waters for determination of manganese at natural concentrations and incorporating a pre-concentration step onto a chip based spectrophotometric system. We therefore developed a new and innovative approach to enhance sensitivity through use of on chip chelating resin pre-concentration. Initially, the pre-concentration and analytical techniques are considered, and the selected resin is tested for capacity, uptake and elution characteristics. The chosen analytical method is optimised for use on bench-top flow injection analysis system for analysing manganese in the laboratory. The main objectives are:

a) Evaluate uptake and elution characteristics of manganese in seawater with a chelating resin (Chapter 3)

b) Optimise and investigate the chemistry of the PAN reaction with manganese in

order to make it suitable for use with a LOAC system (Chapter 4)

c) Design and make a spectrophotometric LOAC microfluidic system to allow coupling of the resin column and PAN chemistry (Chapter 5)

d) Carry out initial tests on the combined LOAC system (Chapter 5)

The generic challenges associated with interfacing existing colorimetric systems with pre-concentration methods are characterised. The new micro-fluidic chip is designed and produced and the analytical method incorporating the pre-concentration step is optimised following laboratory testing with certified reference materials.

The structure of the thesis largely follows those objectives after the introduction in Chapter 1 and review of the methods used in Chapter 2. The final chapter provides an overview of the work, and suggests future research directions.

Chapter 2

Methods

Contents

2.1 Contamination control 21
2.2 Manganese determination using PAN methods 22
2.2.1 Spectrophotometric methods 22
2.2.2 The PAN method 24
2.2.3 Manganese standards 26
2.3 Pre-concentration 26
2.4 Pre-concentration systems using chelating resins 27
2.5 A bench-top iron analyser 29
2.5.1 Use of NTA resin for pre-concentration 29
2.5.2 Use of 8-HQ resin for pre-concentration 34
2.6 Choice of resin for a combined spectrophotometric LOAC pre-concentration system 38
2.7 Use of Mn-54 radiotracer 39
2.7.1 Introduction 39
2.7.2 Background and instrumentation 40
2.7.3 Use of Mn-54 in the present study 41
2.8 Microfluidic chip 42
2.9 Summary 42

2.1 Contamination control

A good working practice is based on selection of appropriate high purity reagents, appropriate equipment and the relevant for in-situ analysis environment for work. There are

many steps which occur from the collection of the sample to the final determination where the possibility of contamination may occur, therefore a critical approach to the analysis, including storage and all handling stages is crucial as each additional stage in analysis can introduce contamination. Contamination control methods need to be rigorously applied. There is a high possibility of introducing contamination with the buffer solution. To avoid contributions of impurities from reagents, pre-purifying some of the reagents before the analysis as part of the analytical procedure, often using a pre-concentration column, may be necessary [34].

Good laboratory practice can lead to the reduction of measurement error to an acceptable level. Errors which are consistent and lead to bias in the data are systematic errors. Random errors may vary in size and magnitude but will tend to zero if enough measurements are made. Every analytical measurement has some degree of uncertainty. Instrumental errors, errors of method and operative errors can be classified and avoided. Random errors are difficult to determine and the analyst has no control over them, however they can be minimised. Random errors can be introduced during sampling, sample handling and preparation, chemical pre-treatments and detection. One of the possible random problems occurring may be that the reproducibility of the measurement is not of the desired quality. Outliers are analytical results far from average with low probability that they are correct and therefore it is important to identify them. All data should be reported and the outliers clearly flagged. Possible problems with the analytical procedure may be diagnosed by replicate analysis of a single sample and regular replicate analysis of a single control standard allows monitoring of the instrument reproducibility [34].

Outliers were identified were possible by using the Z score (negative or positive) for a series of replicates. The Z score is the difference between the mean and the data point value divided by the standard deviation of the population. Where Z is above plus or minus 1, the point is considered suspect.

2.2 Manganese determination using PAN methods

2.2.1 Spectrophotometric methods

Spectrophotometry is the quantitative measurement of the reflection or transmission properties of a material as a function of wavelength. The amount of light passing through the sample is measured by the photometer, which delivers a voltage signal. The signal

changes as the amount of light absorbed by the liquid changes. The development of colour is linked to the concentration of a substance in solution and the concentration can be measured by determining the extent of absorption of light at the appropriate wavelength.

A spectrophotometer makes it possible to measure the fraction of light of different wavelengths transmitted by a sample. The signal is amplified and is routed to the final step of analogue-to-digital conversion and display absorbance in quantifiable units.

When a chemical species absorbs visible light, electrons in the normal ground state are raised to a higher energy excited state. The difference in energy between the two states of the absorbing species is equal to the energy of the light absorbed. As a beam of a single wavelength, passes through an absorbing solution, the intensity of the light decreases as photons are removed from the beam and the more light-absorbing entities there are in the light path, the greater is the amount of light that will be absorbed.

Absorbance readings are collected over a range of concentrations to form calibration curves - from which, unknown analyte concentrations may be determined. Beer's Law tells us that if a sample absorbs light of a particular wavelength, the absorbance is directly proportional to the concentration of substance in solution. Lamberts law states that the intensity of the transmitted light decreases exponentially as the path length increases.

Concentration and absorbance are thus directly related via the Beer-Lambert Law, equation (1).

$\log \frac{I_o}{I} = \varepsilon cb$ (1)

where A is the absorbance, ε (M^{-1} cm^{-1}) is the absorptivity coefficient of the solution, b (cm) is the length of the optical path and c (M) is the concentration of the absorbing compound.

The molar absorptivity ε is a constant which is characteristic of the substance absorbing the light and of the wave-length. The quantity I/I_o represents the fraction of the incident light which passes through unabsorbed, is called the transmittance, T, and is often expressed as a percentage. The quantity $\log I_o/I$, which is termed absorbance is proportional to the concentration of the absorbing species. Absorption depends on molar absorptivity (ε), cell length (b) and concentration of the absorbing compound (c).

Often the substance by itself does not absorb light and very sensitive and selective reagents are added which react with only one component in solution to form an intense colour, even if the substance is in very low concentration. The amount of light absorbed

by the sample is related to the colour change caused by the chemical reaction. The amount of the absorption is then used to determine the concentration of the analyte.

2.2.2 The PAN method

1-(2-Pyridylazo)-2-naphthol is widely used as colorimetric reagent for metal ions in spectrophotometric determinations [73].

1-(2-Pyridylazo)-2-naphthol can exist in solutions in three forms, which strongly depend on the pH. Acid solutions ($pH \leqslant 2$) contain the water soluble yellow-green protonated H_2L^+ (L is PAN ligand) ion and in an acidic medium PAN can easily attract a proton to its pyridine nitrogen atom. Between pH 3 and 11 PAN occurs as the neutral HL molecule, giving a yellow color when dissolved in organic solvents or with the use of surfactants. In alkaline solutions (pH $\geqslant$ 11) it exists as the water-soluble L^- anion and its o-hydroxy group can easily dissociate (Figure 2.1) [3, 74].

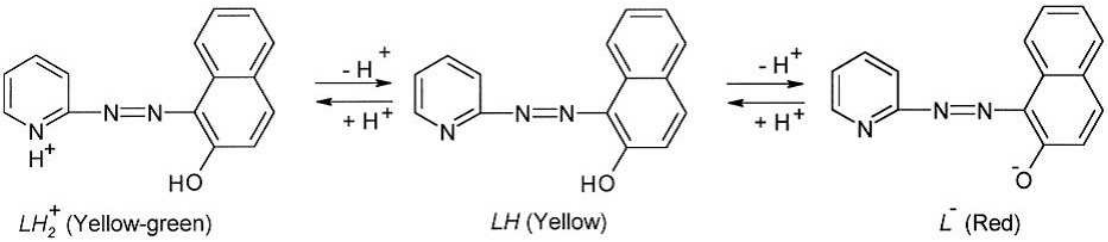

Figure 2.1: Change in form of PAN with pH [3].

PAN reagent forms highly coloured complexes with a variety of metal ions [74, 75, 73]. The divalent metal-PAN complex has tetrahedral geometry at the metal ion and exists in two tautomer form, thus acting as a tetradentate ligand. It complexes with a metal ion through the hydroxyl oxygen atom, pyridine nitrogen atom, and one of the azo group nitrogen atoms as shown in Figures 2.2 and 2.3 [74, 75].

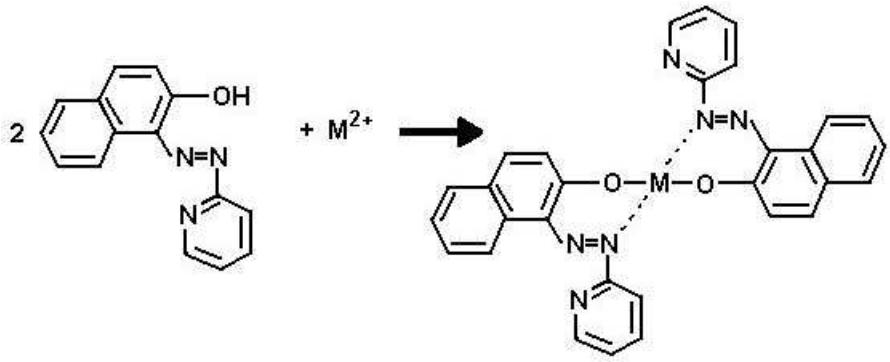

Figure 2.2: Reaction of PAN with a divalent metal ion (A).

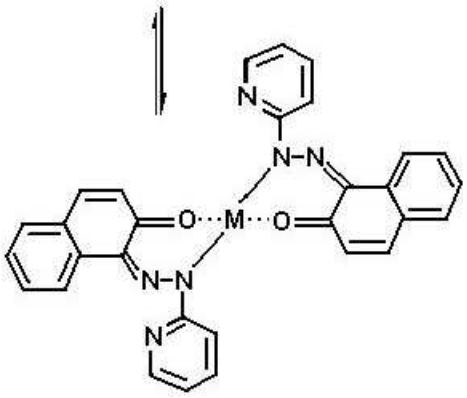

Figure 2.3: Reaction of PAN with a divalent metal ion (B).

The choice of pH for the formation of the metal-ligand complex is dependent on the type of metal. The selectivity of the PAN method is enhanced by selection of pH. For example, iron, cobalt and nickel react with PAN at pH = 4 and PAN reagent does not form complexes with manganese at such a low pH [74].

The PAN reagent in its molecular form (LH) is practically insoluble in water [3, 75] and studies of manganese determinations using PAN have generally been limited to non-aqueous systems. Watanabe [76] used PAN solubilized by the surfactant Triton X-100 as an effective colorimetric reagent in aqueous systems, demonstrating that PAN is a good candidate for manganese determinations in natural waters with the use of surfactants [40]. The method developed here for manganese determination follows the procedure described by Chin et al. [40], who applied this technique to hydrothermal vent fluids.

The PAN reagent (0.8 mM PAN solution) is prepared by adding 0.05 g of PAN

(PAN for spectrophotometric determination of metal ions, $\geqslant$ 97.0% Sigma Aldrich) to 100 mL of Triton X-100 solution (Triton X-100, laboratory grade, Sigma Aldrich) and stirring for about 8 hours until PAN is dissolved. 100 mL of boric acid buffer solution is added and made up to 250 mL volume with MQ-water. The PAN reagent has a pH of 9.0. The buffer reagent is prepared by taking 0.618 g of boric acid (boric acid 99.999 % trace metal basic, Sigma Aldrich) and dissolving in 100 mL of 0.1 N NaOH solution (sodium hydroxide 99.995 % trace metal basis, Sigma Aldrich). An iron masking agent 400 μL of Deferoxamine B (Desferal deferoxamine mesylate) is also added.

2.2.3 Manganese standards

Standard solutions were prepared with 1000 mg/L AAS Mn standard (TraceCERT, Fluka). The 1000 ppm manganese stock solution concentration is 18.2 mM. To prepare an 18.2 μM solution take 0.1 mL of the stock solution and make up to 100 mL. Working standard solutions were prepared by diluting the 18.2 μM solution. For spectrophotometric measurements the standard solution was prepared in 0.02 M HCl, MQ or sea water. When the sample was prepared in 0.02 M HCl a buffer was required. The standards are mixed with buffer and reagent directly before the measurement.

In the colorimetric measurements the blank was buffered acid solution and PAN reagent mixture, buffered seawater and PAN reagent mixture or MQ water and PAN reagent mixture, where the main source of the blank was the reagent solution.

2.3 Pre-concentration

As mentioned in the introduction pre-concentration of trace metals from seawater prior to determination is frequently needed. This is also true for the determination of manganese in LOAC devices as the current systems [62] do not have adequate sensitivity for ocean waters. Whilst there are many pre-concentration techniques that can be used for trace metal determinations, most are very difficult to incorporate into a LOAC system. Solid phase extraction is a separation process in which a liquid sample (mobile phase) is passed through a stationary phase (usually a resin) to separate the analytes from the mixture. A resin is much easier to use than e.g. solvent extraction as no non aqueous phase is needed. The analytes of interest are retained on the stationary phase, and can be removed by an appropriate eluent.

In chelating resins metal fuctional groups are chemically bound to the resin structure, and can collect the ion of interest by coordinate covalent bonds and/or by their electrostatic interactions. The interaction of functional groups (ligand) of chelating resins and metals (in form of cation or oxyanion) allows selective removal of the target metals [34]. Chelating solid phase materials have been widely used for pre-concentration and separation of trace metal ions [36], and do appear to be most readily interfaced with LOAC technology to provide the sensitivity needed to determine metals in ocean waters.

2.4 Pre-concentration systems using chelating resins

Chelating resins may be used in a variety of ways. Some techniques add an aliquot of resin to the sample and mix the solution to allow collection of the metals. The resin beads are collected, and then stored in a small volume of acid to allow diffusion of the metals into solution; the mass action effect of high concentration of protons in the acid leads to release of the metal. The vast majority of techniques use a chelating resin held in a small plastic column, through which the sample is passed.

The efficiency of adsorption of the analyte on to the column is influenced by several factors such as the flow rate of the water through the column and the sample pH. Recovery is also affected by the concentration of the chelating agent and corresponding molar concentration of metal present in the sample. The effectiveness of the column can be estimated by the number of theoretical plates 'N' and when the N is known the elution curve can be predicted. According to the plate theory, the column consists of 'N' number of theoretical plates (sections) and in each section the average concentration of solution is in equilibrium with the average amount of solute absorbed by the resin. When the amount of the analyte of interest loaded on the column is not too big, the sorption of the analyte is expected to be linear with concentration, and can be characterised by a distribution coefficient K, defined: K = concentration of ion in resin (mol/g) / concentration of ion in solution (mol/mL). The effective number of theoretical plates in the column depends on the flow rate and can be determined using the elution curve of the concentration of the analyte in the eluent eluted from the column as the function of the volume of the eluting solvent used. N is proportional to the length of the column and separation can be improved by increasing the length of the column [33]. Different types of chelating group can be bonded to the resin backbone (Table 2.1).

Table 2.1: Ligand groups used in some chelating resins

Chelating agent	Metal ions seperated	Reference
8-hydroxyquinoline (8-HQ)	Mn^{2+}, Fe^{3+}, Ni^{2+}, Co^{2+}, Cd^{2+}, Pb^{2+}, Zn^{2+}, Cu^{2+}	Sturgeon et al. 1981 [77]
	Mn^{2+}, Fe^{3+}, Ni^{2+}, Co^{2+}, Cd^{2+}, Pb^{2+}, Zn^{2+}, Cu^{2+}, Hg^{2+}	Luhrmann et al. 1985 [78]
	Mn^{2+}	Resing et al. 1992 [37]
	Cu^{2+}, Ni^{2+}, Cd^{2+}	Lan et al. 1994 [79]
	Fe^{3+}	Measures et al. 1995 [80]
	Fe^{3+}	Laes et al. 2005 [81]
nitriloacetic acid (NTA)	Fe^{3+}	Lohan et al 2006 [82]
	Fe^{3+}	Pascoa et al. 2009 [83]
iminodiacetic acid (Toyopearl)	Mn^{2+}, Cu^{2+}, Cd^{2+}, Pb^{2+}, Ni^{2+}	Warnken et al. 2000 [41]
	Mn^{2+}, Cd^{2+}, Cu^{2+}, Ni^{2+}, Zn^{2+}	Beck et al. 2002 [84]
iminodiacetic acid (Chelex 100)	Fe^{3+}	Pascoa et al. 2009 [83]
Iminosalicyl group	Cd^{2+}, Zn^{2+}, Cu^{2+}, Ni^{2+}, Fe^{3+}, Co^{2+}	Kubota et al. 1989 [85]
Formysalicylic acid	Fe^{3+}	Mahmoud et al. 1997 [86]
2-Pyridinecarboxaldehyde phenylhydrazone	Fe^{2+}, Co^{2+}, Ni^{2+}, Cu^{2+}	Watanesk et al. 1986 [87]
	Mn^{2+}, Fe^{2+}, Cd^{2+}, Zn^{2+}, Co^{2+}, Pb^{2+}, Cu^{2+}	Simonzadeh et al. 1988 [88]

The most popular and well characterised chelating resins currently used are those containing 8-hydroxyquinoline (8-HQ), nitrilotriacetic acid (NTA), and imminodiacetate (Toyopearl AF 650M) groups, and all of these have been used in different parts of the work described in the thesis.

2.5 A bench-top iron analyser

To become familiar with the column pre-concentration mechanism and possible positive and negative factors that need to be taken into consideration during method development, a bench-top continuous flow analytical system with pre-concentration step was implemented and used for the determination of dissolved iron in marine waters [80, 89, 82]. The method is based on the spectrophotometric detection of iron eluted from the column and the catalytic oxidation of N,N-dimethyl-p-phenylenediamine dihydrochloride (DPD) by hydrogen peroxide was examined using different resin material. In the method used Fe(III) reacts with DPD. The products are two reddish semiquinone derivatives (DPDQ), for which absorption spectra can be monitored at 514 and 550 nm. The reduced Fe(II) produced is oxidised to Fe(III) by hydrogen peroxide, and Fe(III) can react with DPD again [90]. The pre-concentration resin was used to improve the sensitivity of the method. Seawater samples were acidified to pH 2.0 $\pm$ 0.1, and two different pre-concentration resins were used for the pre-concentration step, commercially available NTA Superflow resin and laboratory made 8-HQ resin. The objectives of the study were therefore to assess the efficiency and reliability of the resin and the analytical method, identify possible problems and if necessary implement strategies to overcome them.

2.5.1 Use of NTA resin for pre-concentration

Instrumentation and analytical procedure

The flow injection system consisted of an in-line pre-concentration column attached to a 6 port injection valve and manifold. The peristaltic pump was continuously delivering acidified sample, sample buffer, acid carrier and reagents. The 8-channel Gilson peristaltic pump with PVC tubing gave the various flow rates used for the analysis. The transmission signal was generated by a simple laboratory-built detector with a green LED as a light source and a TAOS TL257 sensor. The manifold set-up is shown in

Figure 2.4.

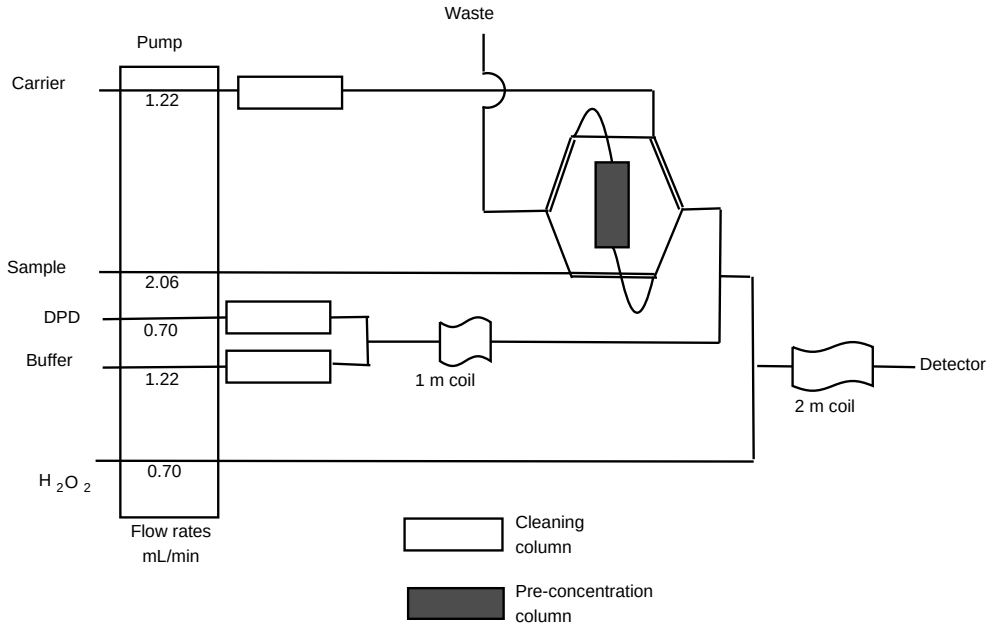

Figure 2.4: Schematic diagram of continuous flow system for pre-concentration (NTA resin) and determination of Fe(III) in sea water

The NTA Superflow resin was packed into a mini-column with an internal volume of 80 μL and polypropylene frits were used to immobilize the resin in the column. Before each experiment the entire system was cleaned with 1.5 M HCl for a minimum of 30 minutes, followed by rinsing with MQ water. Each pre-concentration-elution cycle was initiated by the programmed timing sequence of the LabVIEW programme used to run the system and collect data. During a loading time of 15 seconds the sample passed through the column. The injection valve then switched to the elute position and the acid carrier passed through the column in the opposite direction, releasing the analyte into the reagent stream, it was then mixed with other solutions in the coils and transferred to the detector. The elution time for the column was set to 335 seconds and one cycle was about 6 minutes. The sampling flow rate was 2.0 mL/min and the elution flow rate 1.22 mL/min. With the valve in the elution position sample and sample buffer were pumped through the other pump tubes and valve to waste in order to wash out the previous sample. After the elution of the column, when the peak came back to baseline and the baseline was stable, the valve was switched back to the sampling (loading) position to start the next sampling sequence. At the end of the analysis the system was washed with

distilled water, as the chelating resin could be damaged if left in too strong acid.

Reagents and solutions

Ultra-pure MQ water was used for the preparation of all reagents and standard solutions. Fe(III) stock standard solutions were prepared by diluting 1000 mg/L atomic absorption standard (Sigma-Aldrich) in MQ water and seawater and sample pH was adjusted to 1.8 - 2.0 with HCl (Romil Ultra purity acid). Several working standard solutions from 1 nM to 30 nM were prepared from the stock solution and compared with NASS and CASS certified reference materials. The DPD solution was prepared daily by dissolving 1.1 g of DPD (Fluka HPLC grade) reagent in 100 mL MQ water and acidified with 150 μL 12 M HCl (Romil Ultra purity acid). The ammonium acetate buffer solution was prepared by bubbling ammonia gas into acetic acid (Romil Super purity acid) forming ammonium acetate crystals. MQ water was then added and a saturated ammonium acetate 19.2 M solution was created. A 3.5 M reaction buffer solution was prepared by mixing 27 mL 19.2 M ammonium acetate and 123 mL MQ water. The pH of the sample buffer solution was adjusted to 9.8 with ammonia. The 1.5 M (later changed to 0.75 M) eluting acid solution was prepared by diluting 12 M HCl (Romil Super purity acid). A 5 % hydrogen peroxide solution was prepared by diluting 167 mL 30 % hydrogen peroxide (Fisher scientific, trace analysis grade) in 1 L MQ water. Reagents for this study were made in Teflon and LPDE (low density polyethylene) bottles, which had been acid soaked for a few days in 10 % HCl (Romil Super purity acid) solution and then MQ rinsed.

Pre-concentration - NTA resin

In the NTA resin nitriloacetic acid is used as a chelating agent, which forms coordination compounds with metal ions (chelates). In this study it was used to seperate iron from seawater as previously described by Lohan et al. [89, 82].

At natural pH in surface seawater iron is chelated with organic ligands, therefore to release Fe(III) and Fe(II) from complexes, samples need to be acidified. The NTA resin is able to bind trace metals like iron at pH 1.7 – 1.8 which is low enough to release the metals from organic ligands [89, 82]. However experiments showed that a strong eluting acid, minimum 0.75 M HCl, was required for a quantitative elution process.

Results

Whilst signals for high standards of iron (10 nM) were evident, high and variable peaks even with blanks made detecting low concentrations difficult. It appeared differences between the eluted sample and the buffer pH led to the baseline perturbation, even when rinsing buffer (1.5 M ammonium acetate, pH adjusted to 3.5 with acetic acid) was used to condition the resin before the acidified sample was pushed through the column [82]. Additionally, after a few weeks of experiments, the compression of the column and leakage of the solution passing through the column was observed, as a result of the increased pressure in the system. Every few weeks the resin was replaced and flow reversed before the elution stage of the experiment was applied.

The perturbation in the baseline appears when MQ water (blank) solution is analysed. Comparison to standard solutions indicated the peak height of the perturbation (the blank solution) corresponds to a few nM iron (Figure 2.5).

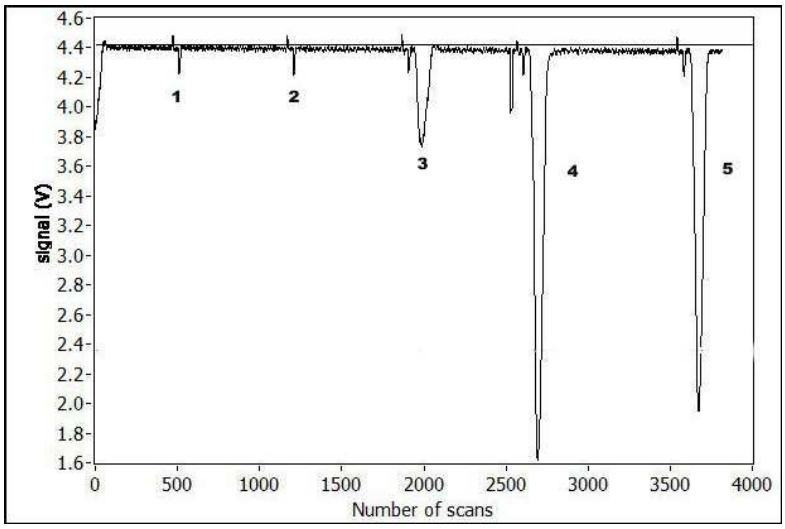

Figure 2.5: Elution profile of dissolved iron. 1.5 M HCl injected as a sample (1,2); MQ pH 1.9 (3); sea water pH 1.9 (4); 10 nM standard solution pH 1.9 (5)

Two small peaks appearing before the main peak are due to valve switching (electrical effect). The distance between the injection peaks increases with the pre-concentration time. These peaks are visible as well when only acid sample is injected instead of a water sample (Figure 2.6).

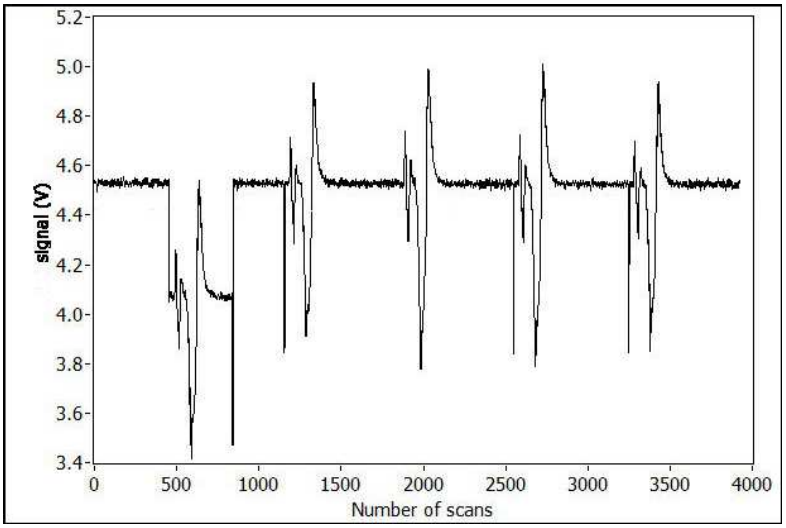

Figure 2.6: Elution profile. 1.5 M HCl injected as a sample; preconcentration 20 seconds.

Tests were performed to exclude possible contamination. MQ water samples were analysed with increasing pre-concentration time, from 20 to 120 seconds pre-concentration time (Figure 2.7). The results showed no change in peaks with longer pre-concentration time, which proves that the observed peaks are not due to MQ water contamination.

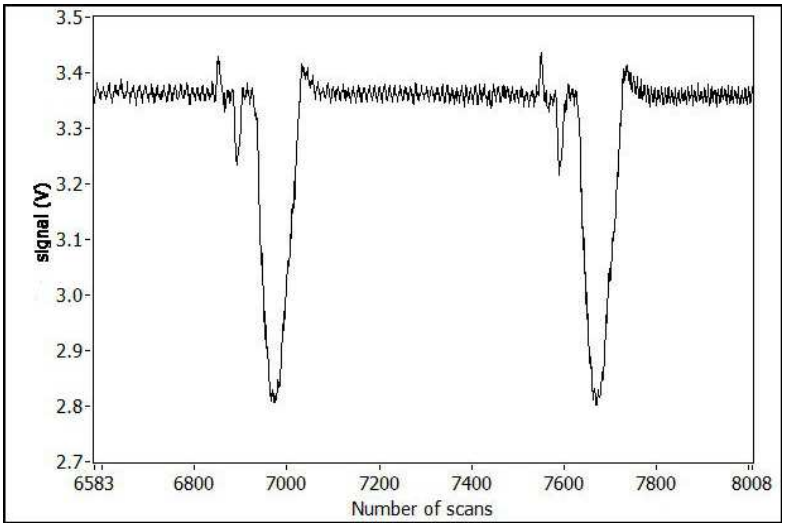

Figure 2.7: Elution profile. MQ sample; pH 1.9; pre-concentration 120 seconds.

Further experiments examined the eluent and buffer solution concentration and the pH. The HCl eluent concentration in the range of 0.1 – 2 M HCL was tested and 0.75

M HCl was chosen as it gives the same sensitivity as higher acid concentrations. The change in ammonium acetate buffer concentration affects the baseline in the same way as the changes in eluting acid strength. The most stable baseline, while using 0.75 M HCl eluting acid, was obtained for 3.5 M buffer solution. Using a rinse buffer solution (rather than MQ) still created 'blank' peaks, and this variable background signal significantly limited the application of the method.

Conclusions

The method employing the NTA Superflow resin with DPD colorimetric reagent provided a detection limit of few nM with a sample throughput rate of 10 per hour. However, the observed perturbation in the baseline when the blank solution (MQ water) was analysed, (which may correspond to approximately 5 nM iron) severely limited the application of the technique and therefore this method was not suitable for analysing iron concentrations at a few nM and lower. Also the system is very sensitive to pH change, eluting acid strength and reaction buffer solution strength. Additionally, after a few weeks of experiments, the compression of the column and leaking of the solution passing through the column was observed, as a result of the increased pressure in the system. More experiments need to be done to establish analysis conditions that would give a stable baseline and would allow for analysis of samples at sub nM concentration as has been described in the literature [89, 82]. Therefore an alternative resin was tested.

2.5.2 Use of 8-HQ resin for pre-concentration

The most important change introduced was use of a 8-hydroxynoquinoline resin (8-HQ). The method is based on Measures et al. [80]. The general instrument set-up was very similar to that used with the NTA resin.

Reagents

DPD solution and ammonium acetate buffer solutions were prepared. The pH of the sample buffer was adjusted to 6.3 $\pm$ 0.05 with acetic acid. The reaction buffer solution was prepared by taking 1 L of sample buffer solution and adding 3 mL of 15 % Brij-35 solution and 100 μL of 10 % triethylenetetramine. The 0.15 M eluting acid solution was prepared by diluting 12 M HCl (Romil Super Purity Acid). The 8-HQ resin removes iron from sea water in the pH range 3 and 6 [80]. The sample pH was adjusted in-line

with buffer prior to adsorption on the 8-HQ column to pH 5.8 ± 0.5 using sample buffer. In-line buffering prior to introduction of the acidified seawater sample into the column reduces the time of the analysis and gives better recoveries. Another very important change introduced in the method was the strength of the eluting acid. The 8-HQ resin allows the use 0.15 M HCl eluting acid, which is not as strong as 0.75 M HCl eluting acid used with the NTA resin.

Analytical procedure

The manifold was made from 0.5 mm internal diameter Teflon tubing in order to reduce the carry-over, peak tailing and analysis time. Smaller diameter tubing was used for the eluting acid and reaction buffer (0.80 mL/min), DPD and hydrogen peroxide (0.40 mL/min). The sample and sample buffer flow rates were 2.0 mL/min and 0.55 mL/min respectively. The manifold set-up, with two short mixing coils, one long reaction coil and three clean-up columns, is shown in Figure 2.8. This set-up is based on that of Dr Peter Sedwick (C. Marsay, pers. comm.).

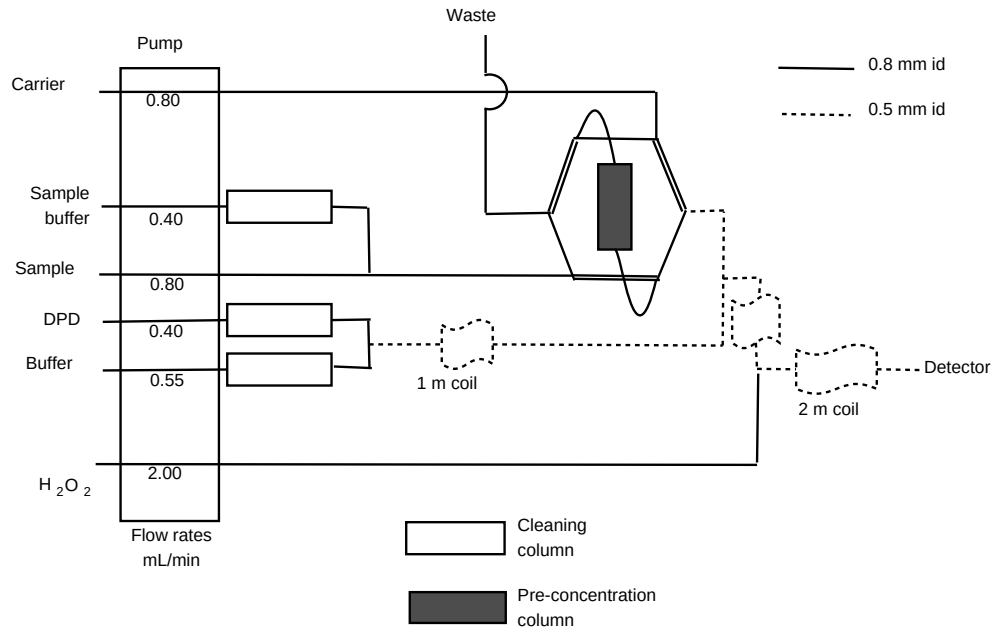

Figure 2.8: Schematic diagram of continuous flow system for pre-concentration (8-HQ resin) and determination of Fe(III) in sea water.

The same detector and LabView software as described earlier were used.

Pre-concentration - 8-HQ resin

The advantages of the 8-HQ resin are a large binding capacity that allows pre-concentration of elements from low concentration samples, it is stable, does not swell and can be exposed to acid and bases regularly. However extraction onto 8-HQ columns is pH dependent, for example Fe(III) is extracted effectively at pH values above 2.5 and Fe(II) only at pH values above 3.5 [91]. A very positive property of the 8-HQ resin is that metals can be eluted with a low concentration acid solution. In this study 0.15 M HCl solution was used to elute iron from the column, however even lower concentration have been used in the past as reported by Ussher at al. [92] where 0.05 M HCl was used for the iron elution.

Results

All the above changes resulted in a very good performance of the system and good calibration curves were obtained. The NASS-6 sample with certified iron concentration of 8.86 $\pm$ 0.82 nM was analysed and the result obtained was 9.31 $\pm$ 0.65 nM. The CASS-5 sample with certified iron concentration of 25.78 $\pm$ 1.97 nM was analysed and the result obtained was 25.81 $\pm$ 1.00 nM. The sensitivity of the system was evaluated using the slopes of calibration curves prepared in seawater; standard additions of 10.0, 20.0 and 30.0 nM Fe(III) were made (Figure 2.9.).

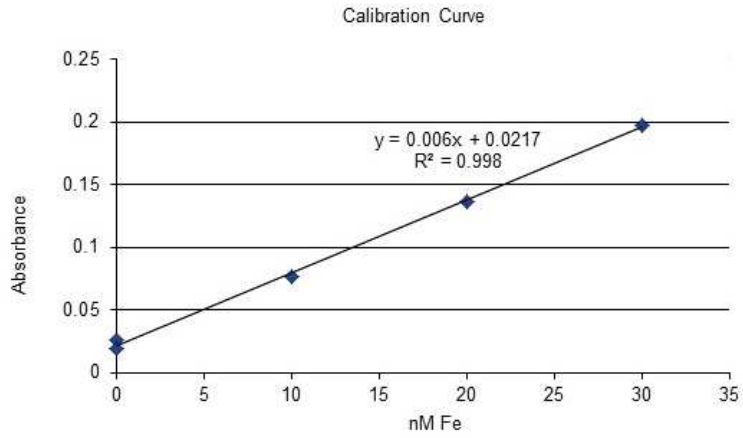

Figure 2.9: Calibration curve for Fe(III) standards prepared in seawater.

The detection limit and precision of the method depend on the amount of sample

pre-concentrated onto the column. By pre-concentrating 0.5 mL of sample (15 seconds pre-concentration, 2.0 mL/min), the Fe(III) blank was typically 460 pM $L^{-1} \pm 30$ pM L^{-1} (n=3) resulting in the limit of detection of 90 pM (defined as three times the standard deviation of the blank). The precision for the standard addition solutions was in the range 2.1-4.0 % RSD (n=4). The technique was used to analyse samples collected by Amber Annett (PhD student at Edinburgh University) from Ryder Bay, Antarctic Peninsula. Figure 2.10. shows a vertical profile of dissolved iron at the Rothera Antarctic Time Series Station.

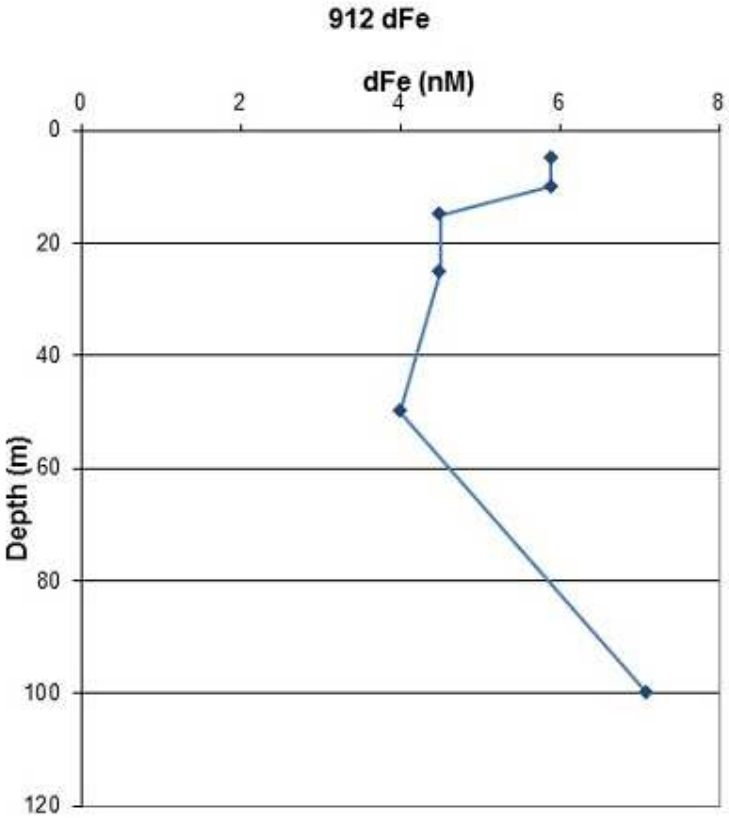

Figure 2.10: A vertical profile of dissolved iron (dFe) at the Rothera Antarctic Time Series Station.

The Figure shows around 6 nM concentration of dFe at 15 m with decrease to around 3.8 nM at 50 m and increase to around 7 nM at 100 m.

Concentration of dFe in surface waters may be a result of sea-ice melt, glacial melt, atmospheric inputs and shallow sediments, with melt water being the most probable

source of fresh water as a result of warming during summer months. Amber et al. [93] reports that dFe concentrations at 15 m are the result of melt water input as well as the mixing with underlying waters, when iron is transported from deep waters to shallower waters by upwelling, mixing and diffusion processes. The possible source of elevated iron concentrations in deeper waters is input from underlying sediments. The anoxic conditions within sediments are present when sediments are depleted in oxygen by microbial respiration. In these conditions oxidation of particulate organic carbon may take place via the reduction of Fe 3+ and as a result production of Fe 2+ which than can be redistributed into overlaying water [93].

Conclusions

Changing to the 8-HQ resin resulted in a very good performance of the system and good calibration curves were obtained. The 8-HQ resin would also allow the pre-concentration of both elements, iron and manganese. The main drawback when using the 8-HQ resin is that it is not commercially available and therefore not readily applicable to coupling with an LOAC. Ideally a suitable commercially available resin should be used.

The results from the experiments performed using the bench-top iron analyser with pre-concentration were reported in the research article by Amber L. Annett. The 'Comparative roles of upwelling and glacial iron sources in Ryder Bay, coastal western Antarctic Peninsula' [93].

2.6 Choice of resin for a combined spectrophotometric LOAC pre-concentration system

In many reported techniques Toyopearl iminodiacetate resin, Toyopearl AF –Chelate - 650M (Figure 2.11 and 2.12), was used for pre-concentration of metals in water samples. Milne et al. used the Toyopearl AF – Chelate - 650M resin for the manganese determination, however the procedure was separated into two stages, off-line extraction and pre-concentration of the elements followed by analysis of the collected eluent [43]. Beck et al. reported a ICP-MS method for manganese analysis with an on-line pre-concentration step using a Toyopearl AF-Chelate 650M resin. In this study samples for manganese analysis were adjusted to pH 9.0 $\pm$ 0.2 prior to concentration [84]. Warnken et al. [41] focused on on-line pre-concentration performance characteristics of the Toyopearl AF –

Chelate - 650M resin and showed that using 1M HNO_3 acid for column elution improves the ICP-MS intensity for manganese analysis with the sample pH adjusted to 8.8 prior to the pre-concentration stage [41].

The iminodiacetate resin is advantageous due to its ability to bind multiple trace metals with high efficiency and recovery. Toyopearl resin can be used for separation of both iron and manganese, but at different pH.

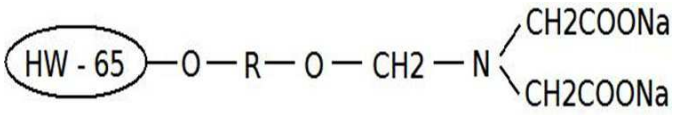

Figure 2.11: Toyopearl AF – chelate - 650M resin.(AF - Activated/Functionalized Matrices; matrix active group - iminodiacetic acid; Toyopearl HW-65 resin is a hydroxylated methacrylic polymer; R denotes a side chain)

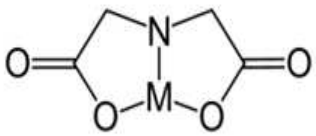

Figure 2.12: A metal complex with the iminodiacetate anion.

This chelating resin with iminodiacetate iminodiacetate (IDA) functional groups has pH stability over the range 2-12. Additionally, the Toyopearl AF – chelate - 650M (Tosh) resin is commercially available and therefore it was used in this study in the manganese separation experiments.

2.7 Use of Mn-54 radiotracer

2.7.1 Introduction

Radioactive isotopes of chemical elements are extremely useful in chemical science disciplines, because radioactive atoms can be substituted for their non radioactive counterparts, being easily detectable but still chemically identical to the original material [94]. Detection systems for radionuclides (and especially gamma emittors) are:

1) much simpler and quicker than conventional spectrophotometric or ICP-MS or ICP-OES techniques,

2) require only small volumes if activities are high, and

3) are not subject to interferences or losses often associated with other conventional analytical approaches.

Mn-54 as a gamma emitter (half life 313 days, energy 0.835MeV) can be readily obtained, and is appropriate to the present study.

2.7.2 Background and instrumentation

Radioactive decay occurs when particles or electromagnetic radiation are emitted from an atom due to the change within its nucleus. Forms of radioactive emission include alpha particles (α), beta particles (β) and gamma rays (γ). Alpha and beta particles directly ionize the atoms with which they interact, adding or removing electrons. Gamma-rays cause secondary electron emissions, which then ionize other atoms. However, some irradiated atoms are not fully ionized by collision with emitted particles, but instead have electrons promoted to an excited state. Excited atoms can return to their ground state by releasing energy as a photon of light known as scintillation photons. The intensity of light in the scintillation is proportional to the initial energy deposited in the scintillator by ionizing radiation. This light emitted corresponds to the amount of radioactivity in the sample [94].

There are two different systems of detection and counting of radiolabeled compounds based on the scintillation technique: Solid Scintillation Counting (SSC) and Liquid Scintillation Counting (LSC) depending on the scintillator material used. In SSC, the transparent inorganic crystal, called a scintillator, fluoresces when is irradiated by the sample. The most commonly used is Thallium-doped sodium iodide (NaI(Tl)) [95].

A scintillation counter measures ionizing radiation. A scintillation counter apparatus consists of a scintillator, a photo-multiplier tube (PMT), an amplifier, and a multichannel analyser (Figure 2.13). A solid scintillation counter is a radiation detector which includes a scintillation crystal [94].

Sodium Iodide detection is based on a solid crystal of sodium iodide which creates a pulse of light when radiation interacts with it. This pulse of light is converted to an electrical signal by a photomultiplier tube, which gives a reading on the instrument. The pulse of light is proportional to the amount of light and the energy deposited in the crystal. The results are obtained in counts per minute (CPM).

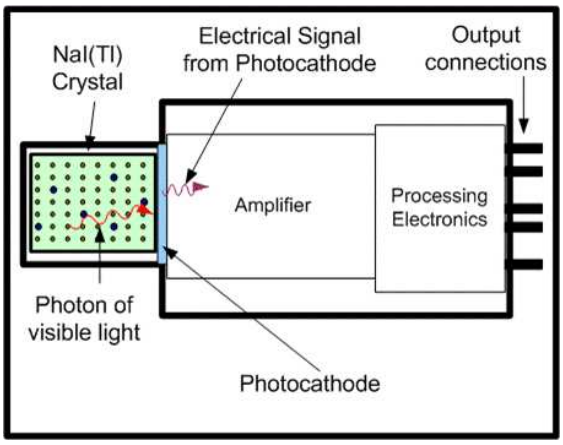

Figure 2.13: Sodium Iodide detector
[4]

To make a measurement the sample containing radioactivity is placed into a container called scintillation vial and the radioactivity level is counted in a scintillation counter called a Gamma counter. The intensity of radiation is proportional to the amount of isotope in the sample, and the spectrum indicates the identity of the isotope.

The scintillation detector with a sodium iodide crystal doped with thallium as activation impurities is one of the best instruments for counting gamma rays. The most prominent property of NaI(Tl) is its excellent light yield. The high atomic number of iodine in NaI results in high efficiency for gamma ray detection [95]. In the present study a automated gamma counter was used in collaboration with the Geosciences Advisory Unit, University of Southampton.

2.7.3 Use of Mn-54 in the present study

Up to the present, no studies have used radioactive tracers to optimise the Toyopearl AF-Chelate-650M resin column performance, except for Resing et al. [37], who used on-line concentration of manganese onto 8-HQ resin.

The objectives of this study were to optimise the extraction of manganese from seawater and assess the recovery and elution efficiency of the Toyopearl resin. The uptake of manganese on the resin, the recovery and elution efficiency of the resin is examined and the optimal conditions are obtained to enable the integration of the pre-concentration unit into a microfluidic system.

Samples were prepared by taking filtered acidified seawater (from around 2000 m in the north-east Atlantic) and adjusting its pH with NH_3 solution or HAc solution. Sea water samples were spiked with the Mn-54 tracer solution. The eluting acid solution was prepared by diluting concentrated hydrochloric acid with MQ water.

Sea water samples spiked with Mn-54 were pumped through the resin column at a given flow rate and eluted using diluted acid solution. Effluent and the elute fractions were collected and the distribution of the Mn-54 determined by gamma-counting in an automated sodium iodide gamma-counter.

2.8 Microfluidic chip

The production and building of the chip is based on the materials as reported by Floquet at al. [72]. For the purpose of this project I designed and produced test microfluidic chips following the above procedure. The specific procedure applied for microfluidic chip production follows the steps listed below: design, milling the PMMA material (polymethyl methacrylate), bonding lid and body parts of the chip, mounting the valves, LED, photodiode and tubing connectors to the chip. The microfluidic chips are designed using Autodesk Inventor Professional software. The chip is made using tinted PMMA block. The chip body is produced using grey tint PMMA ($PLEXIGLAS, Grey, 7C14GS$, *Röhm*, Darmstadt, Germany) and the lid using dark tint PMMA ($PLEXIGLASDark, 7C83GS$). The opto-fluidic cell, micro-channels, optics and detector recesses, valve inlets and mount holes are micro-milled into the PMMA. Body and lid are bonded together by exposure to chloroform vapour and aligned together using the method reported by Ogilvie et al. [96]. A green (572-nm) light-emitting diode (LED) (B5b-433-20, Roithner Laser Technik, Austria) and a TAOS photodiode (TSL257, TAOS Inc., USA) are fixed directly to the chip using Norland Optical Adhesive (NOA 68, USA).

The produced microfluidic platform with integrated pre-concentration column was tested for manganese determinations (see Chapter 5).

2.9 Summary

A bench top continuous flow analytical system for the determination of dissolved iron in marine waters was implemented and used with pre-concentration step. The system

was used to become familiar with the column pre-concentration mechanism and factors important during method development. The type of the resin and the conditions used are important in the performance of the system. Iron is known to have strong bonds with ligands in seawater. Manganese does not appear to be significantly present in complexed forms such as iron, therefore manganese was chosen as the focus of the system to be developed.

The methods described above summarise chemical techniques for manganese detection. The spectrophotometric colorimetric method has been chosen for manganese determination in this project as it is the most suitable for use on LOAC systems, and builds on previous experience in the group [51, 49, 96, 97, 98, 99, 62].

Chelating solid phase materials have the potential to be readily interfaced with LOAC technology and are widely used for the pre-concentration and separation of trace metals. Therefore here the resin pre-concentration step is combined with a manganese chemical analytical method on the microfluidic chip system for the determination of manganese in ocean waters.

The fabrication methods and components of the microfluidic device used for manganese determination and use of the radiotrace Mn-54, are explained.

Chapter 3

Optimisation of the pre-concentration procedure using Mn-54 radio tracer

Contents

3.1 Pre-concentration using Mn-54 46
3.1.1 Reagents, solutions and equipment 46
3.1.2 Analytical procedure 47
3.1.3 Results from column optimisation experiments 47
3.2 Summary and conclusions of pre-concentration optimisation experiments 67

The objectives of this study were to optimise the extraction of manganese from seawater and assess the recovery and elution efficiency of the Toyopearl resin. In a final LOAC system for deployment in natural waters, as high sampling rate as possible is desirable, and as the pre-concentration step is to be coupled to a colorimetric analysis (using the PAN) for determination of manganese, the concentration of eluate should be as compatible as possible with this method. Either strong acids or bases are difficult to manage in engineered sensor systems due to their corrosive effects on materials. As acid is used for elution of manganese, and the PAN technique needs basic conditions, as weak acid as possible for elution is required so that less base needs adding for the optimum pH for the PAN method.

Experiments were performed using a Mn-54 radio tracer to optimise the efficiency

of the Toyopearl AF-Chelate-650M resin, the effectiveness of different eluents and the time necessary for the elution process. The effect of column size and the flow rate on the recovery of the metal (chelating efficiency) at various pH values were also examined.

Studies were done using seawater spiked with Mn-54 and counting with a high efficiency gamma-counter (Thallium-Activated Sodium Iodide Crystals); see Chapter 2.

3.1 Pre-concentration using Mn-54

3.1.1 Reagents, solutions and equipment

Samples were prepared by taking filtered acidified seawater (from around 2000 m in the north-east Atlantic) and adjusting its pH with NH_3 solution or HAc solution (blank solution). Sea water samples were spiked with the Mn-54 tracer solution. The eluting acid solution was prepared by diluting concentrated hydrochloric acid with MilliQ water.

Solutions were passed through the column using a single channel peristaltic pump with appropriate tubing; speed of flow was controlled by adjusting the voltage to the DC motor of the peristaltic pump, or changing to a different internal diameter tube. Flow rates were checked either volumetrically or gravimetrically.

The resin is packed into a micro-column with an internal volume of around 80 μL and immobilized in the column with polypropylene frits. The column design is shown in Figure 3.1.

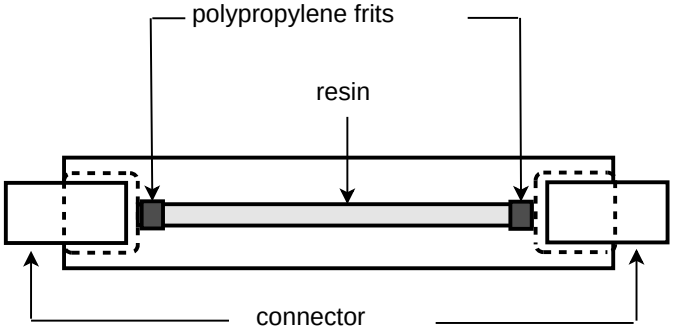

Figure 3.1: Column design.

3.1.2 Analytical procedure

Sea water samples spiked with Mn-54 were pumped through the resin column at a given flow rate and eluted using dilute acid. Effluent and the elute fractions were collected and the distribution of the Mn-54 determined by gamma-counting in an automated sodium iodide gamma-counter. The results are obtained in counts per minute. See Chapter 2 for more details.

3.1.3 Results from column optimisation experiments

Sample pH

The extraction efficiency is pH dependent and therefore to optimise the pH conditions for pre-concentration, the relationship between pH and extraction of manganese was examined. In agreement with other studies [39] results show that manganese is not recovered well when taken up on the column at low pH. A sample pH range of 2-9 was examined and results indicate that the pH should be kept above 8 for highest recovery of manganese (Figure 3.2). There is a large decrease in recovery of manganese at pH values below 6, for quantitative recovery of manganese the sample pH should be kept in the pH range 8-9.

This pH range is very convenient for seawater (typical open ocean value 8.2) and means no buffering or pretreatment of seawater (other than in the filtration) is needed prior to collection of manganese on the resin.

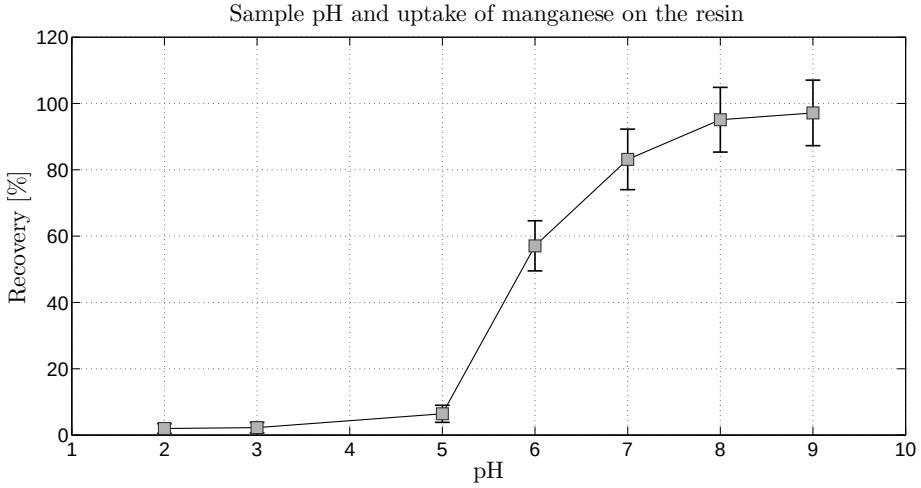

Figure 3.2: Effect of sample pH on manganese uptake on the resin.

Flow rate

The effect of the flow rate on the extraction efficiency of manganese was examined. The results of this study indicate that decreasing the flow rate improves the retention of manganese on the column. Changing the flow will therefore improve the recovery of the metal ion on the column used during experiments (Figure 3.3).

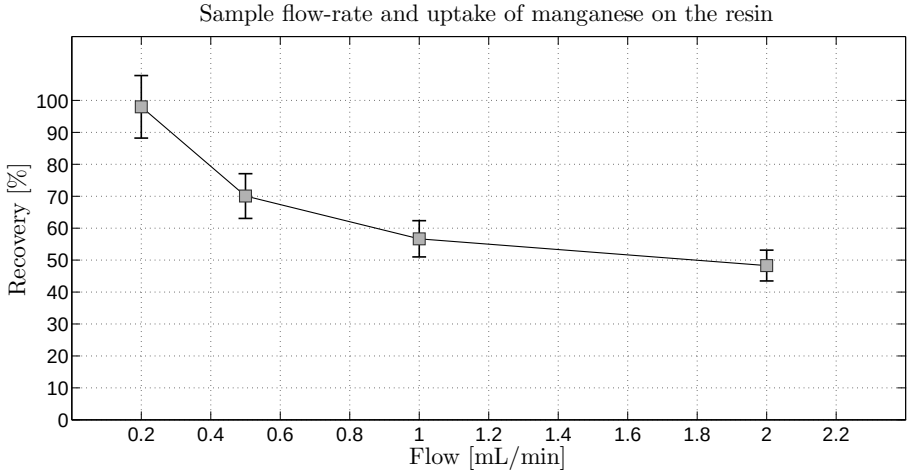

Figure 3.3: Effect of sample flow rate on manganese uptake on the resin.

Experiments examining the effect of the flow rate on the extraction efficiency performed at low flow rate of 0.2 mL/min gave full recovery of manganese. During the stage of the analysis when the sample is taken up on the resin, a flow rate of 0.2 mL/min was therefore applied, to allow full recovery of manganese.

Eluting acid strength

The strength of the eluting acid plays an important role in the use of resins. The concentration of the eluting acid must be as weak as possible as parts of the sensor system are built from sensitive materials and in the colorimetric step the pH needs to be changed to a high value. At the same time the eluting acid solution needs to be strong enough to effectively remove the analyte from the column.

Experiments where performed where Mn-54 was taken up on the resin and then removed with different strengths of the eluting acid (HCl-MQ). Uptake was done at a flow rate of 0.2 mL/min and elution at 0.8 mL/min. Eluting acid strengths ranged from 0.05 M to 0.02 M HCl (see Figure 3.4). Subsequent experiments were performed and eluting acid strengths ranged from 0.005 M to 0.001 M HCl (see Figure 3.5). All gave very similar results showing full recovery of manganese. Therefore concentration of the acid as low as 0.001 M can be used in the elution process. See subsection 'Elution profile' for elution efficiency with different strengths of the eluting acid (HCl-MQ).

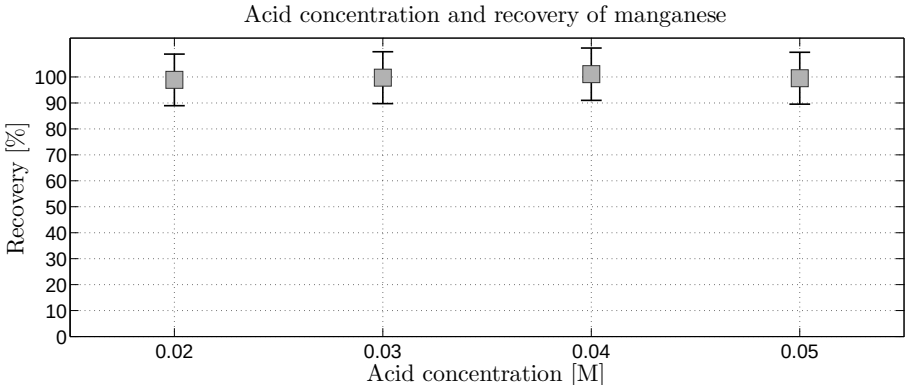

Figure 3.4: Manganese recovery. Flow rate of 0.2 mL/min and eluting acid strengths ranged from 0.05 M to 0.02 M HCl.

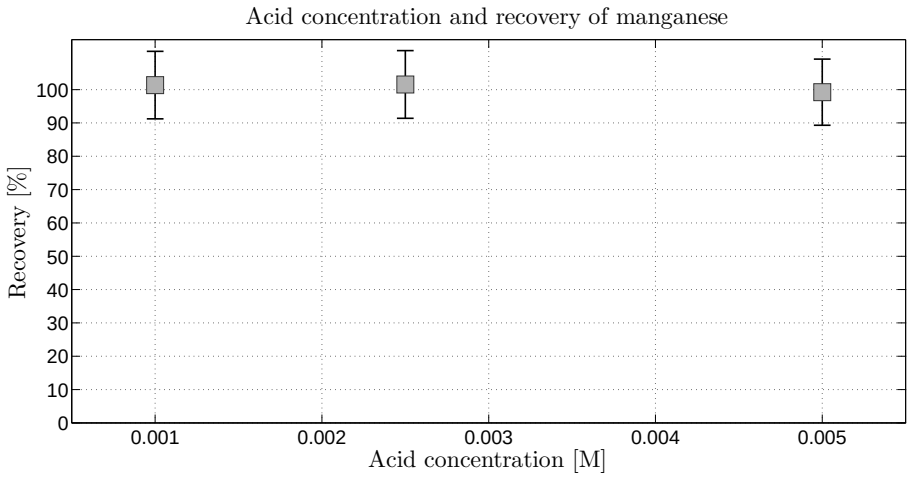

Figure 3.5: Manganese recovery. Flow rate of 0.2 mL/min and eluting acid strengths ranged from 0.005 M to 0.001 M HCl.

Elution profile

After the uptake of manganese on the resin and total elution were optimised (flow rate of 0.2 mL/min), experiments were carried out to assess the elution efficiency from the resin with acid volume passed through the column. Initial experiments used a short column (2 mm x 25 mm) able to accommodate 80 μL resin, and a eluting flow rate of 0.8 mL/min.

During the elution process (flow rate of 0.8 mL/min) each drop of the eluent (around 35 μL, measured by weight) was collected separately and the Mn-54 determined by gamma-counting. All of the manganese was eluted off the column within about 450 μL of eluting acid solution passing through the column, with most being eluted within the first 150 μL when using 0.05 M HCl eluting acid (see Figure 3.6).

The time of the elution of first fraction of analyte depends on the eluting acid strength. The lower the concentration of the acid the later the manganese is eluted from the resin (Figure 3.6) (uptake flow 0.2 mL/min, elution at 0.8 mL/min).

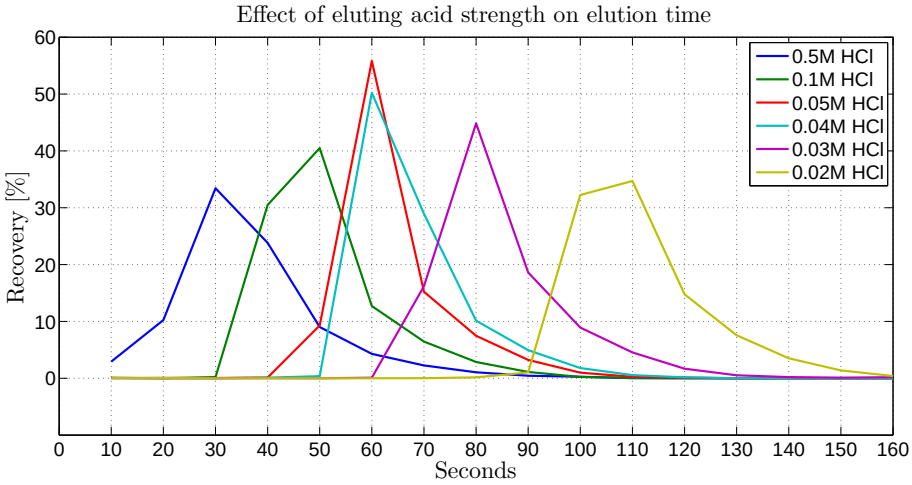

Figure 3.6: Manganese recovery. Flow rate of 0.2 mL/min and eluting acid strengths ranged from 0.5 M to 0.02 M HCl. 80 μL resin volume.

Subsequent experiments included elution with HCl in the range 0.05 to 0.001 M (Figure 3.7 to 3.10, Table 3.1 to 3.4). The % recovery was calculated by comparing the CPM value recorded for each eluted fraction to the CPM value recorded for the standard, standard assumed to be 100 %.

For pre-concentration procedure the samples were prepared using seawater (pH adjusted with NH3 or HAc). This was a blank solution used to prepare the samples spiked with Mn-54. Original solution used for standard preparation (specific activity 178.88 mCi/mg; concentration 19.41 mCi/mL) was diluted 8000 times. The blank solutions were measured using the gamma counter as about 0.2 Mn-54 standard concentration was about 250 nM. When the CPM value reported for the standard was 9500 CPM, the blank value was measured at about 20 CPM and calculated as about 0.5 nM.

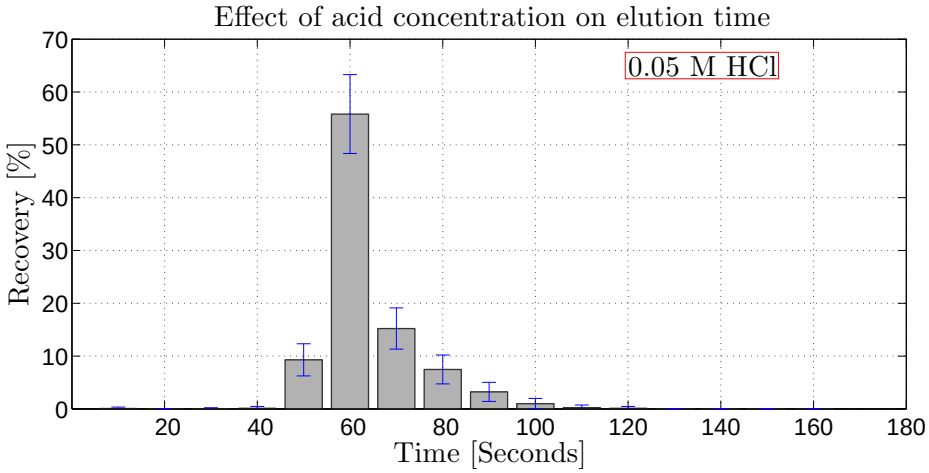

Figure 3.7: Manganese recovery. Elution flow rate of 0.2 mL/min and eluting acid strength 0.05 M HCl. 80 μL resin volume.

Table 3.1: 0.05 M HCl

Effect of acid concentration on elution time Eluting acid 0.05M HCl			
Name	CPM	% Recovery	Sum % Recovery
Blank 1	20	-	-
Blank 2	23	-	-
F1	28	0.30	
F2	2	0.02	
F3	16	0.16	
F4	74	0.79	
F5	183	1.94	
F6	89	0.94	
E1	3	0.03	
E2	9	0.09	
E3	8	0.09	
E4	15	0.15	
E5	2505	26.48	
E6	4504	47.60	99.9
E7	1095	11.57	
E8	566	5.99	
E9	235	2.49	
E10	87	0.92	
E11	16	0.17	
E12	6	0.06	
E13	0	0.00	
E14	0	0.00	
E15	6	0.06	
E16	0	0.00	
TC	2	0.02	
Standard 1	9297		
Standard 2	9506	Avarage CPM	9461
Standard 3	9582		

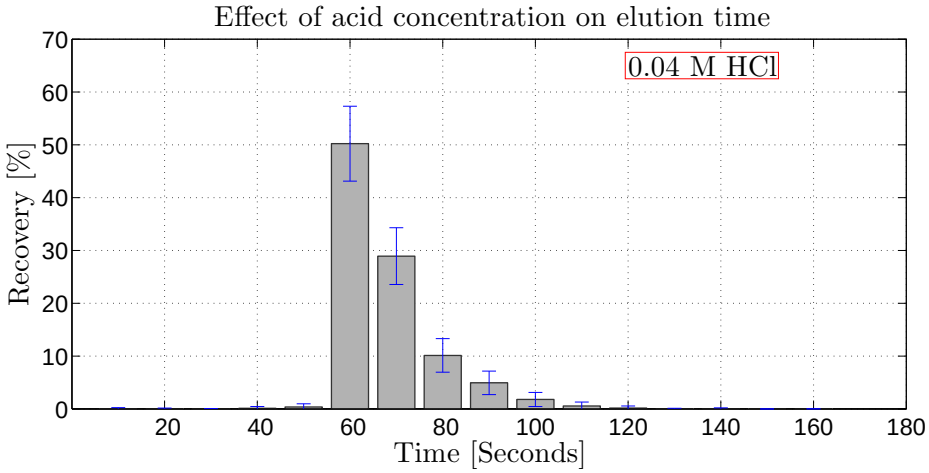

Figure 3.8: Manganese recovery. Flow rate of 0.2 mL/min and eluting acid strength 0.04 M HCl. 80 μL resin volume.

Table 3.2: 0.04 M HCl

Effect of acid concentration on elution time Eluting acid 0.04M HCl			
Name	CPM	% Recovery	Sum % Recovery
Blank 1	21	-	-
Blank 2	22	-	-
F1	18	0.19	
F2	4	0.04	
F3	12	0.13	
F4	92	0.97	
F5	200	2.12	
F6	49	0.52	
E1	4	0.04	
E2	2	0.02	
E3	0	0.00	
E4	10	0.11	
E5	34	0.36	
E6	4751	50.21	101.4
E7	2736	28.92	
E8	957	10.12	
E9	467	4.93	
E10	169	1.78	
E11	52	0.55	
E12	14	0.15	
E13	1	0.01	
E14	3	0.03	
E15	0	0.00	
E16	0	0.00	
TC	17	0.18	
Standard 1	9297		
Standard 2	9506	Avarage CPM	9461
Standard 3	9582		

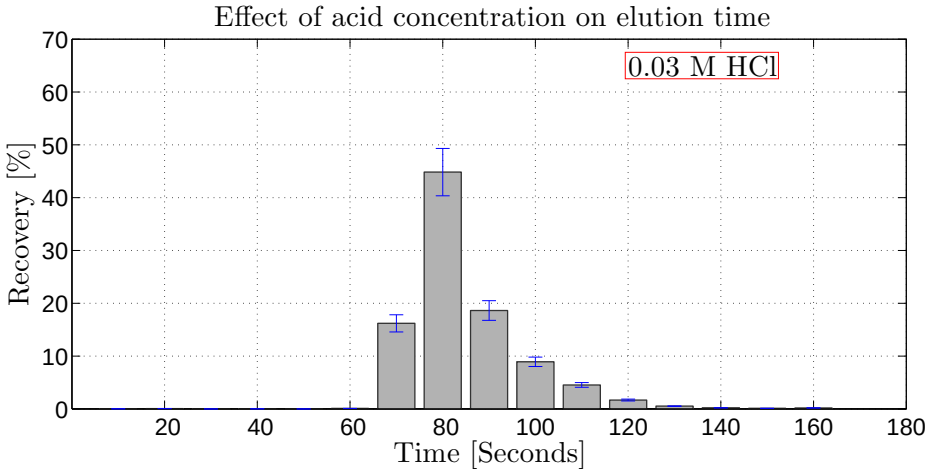

Figure 3.9: Manganese recovery. Flow rate of 0.2 mL/min and eluting acid strength 0.03 M HCl. 80 μL resin volume.

Table 3.3: 0.03M HCl

Effect of acid concentration on elution time Eluting acid 0.03M HCl			
Name	CPM	% Recovery	Sum % Recovery
Blank 1	20	-	-
Blank 2	19	-	-
F1	35	0.37	
F2	3	0.03	
F3	13	0.14	
F4	88	0.93	
F5	214	2.27	
F6	48	0.50	
E1	0	0.00	
E2	5	0.05	
E3	0	0.00	
E4	1	0.01	
E5	0	0.00	
E6	8	0.09	100.5
E7	1532	16.19	
E8	4241	44.83	
E9	1761	18.62	
E10	843	8.91	
E11	429	4.53	
E12	159	1.68	
E13	49	0.52	
E14	19	0.20	
E15	10	0.11	
E16	17	0.18	
TC	33	0.35	
Standard 1	9297		
Standard 2	9506	Avarage CPM	9461
Standard 3	9582		

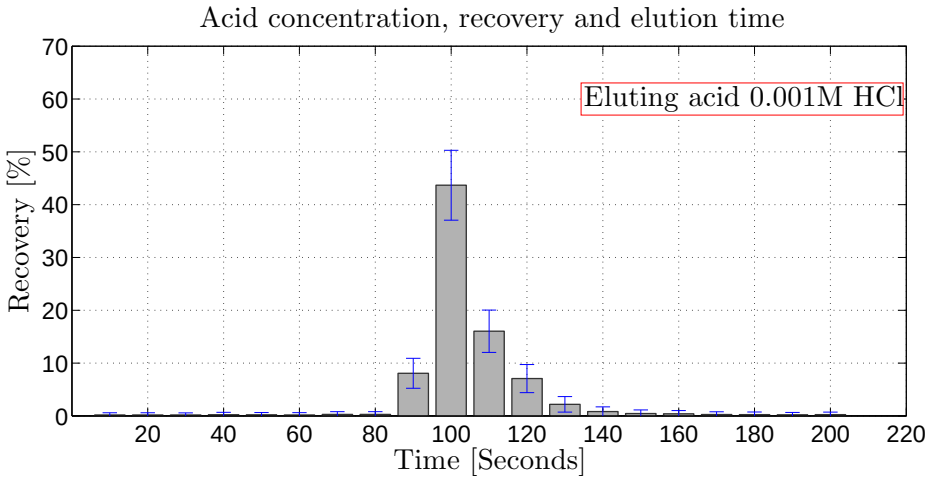

Figure 3.10: Manganese recovery. Flow rate of 0.2 mL/min and eluting acid strength 0.001 M HCl. 20 μL resin volume.

Table 3.4: Elution profile. Eluting acid 0.001M HCl

Elution profile Eluting acid 0.001M HCl			
Name	CPM	% Recovery	Sum % Recovery
E1	59	0.21	
E2	61	0.22	
E3	58	0.21	
E4	73	0.26	
E5	68	0.25	
E6	63	0.23	
E7	96	0.35	
E8	96	0.35	
E9	2815	10.15	
E10	15237	54.94	102.2
E11	5593	20.17	
E12	2466	8.89	
E13	762	2.75	
E14	283	1.02	
E15	159	0.57	
E16	133	0.48	
E17	93	0.33	
E18	84	0.30	
E19	70	0.25	
E20	81	0.29	
TC	115	-	
Standard	27733	-	

Results for analysed samples showing consistency of the elution profile, including time, and recovery of manganese, are presented below (Figure 3.11 to 3.15, Table 3.5 to 3.9).

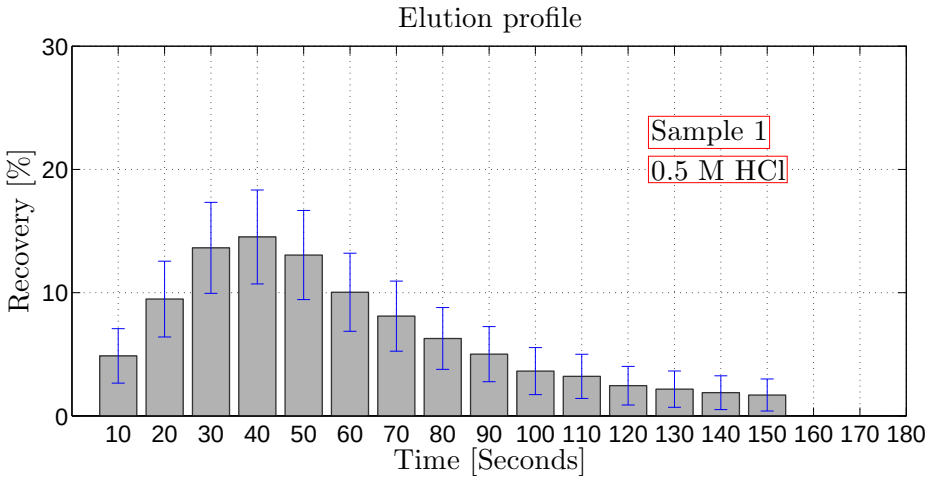

Figure 3.11: Manganese recovery. Flow rate of 0.2 mL/min and eluting acid strength 0.5 M HCl. 20 μL resin volume. Sample 1.

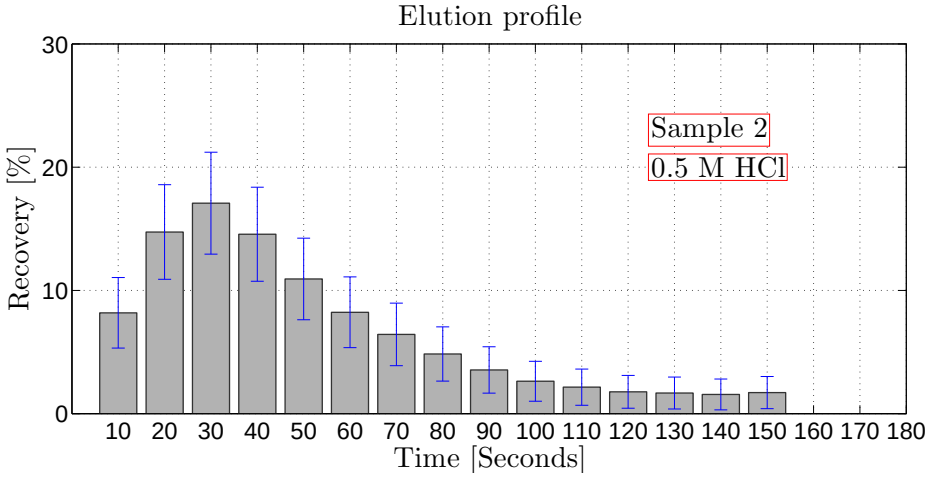

Figure 3.12: Manganese recovery. Flow rate of 0.2 mL/min and eluting acid strength 0.5 M HCl. 20 μL resin volume. Sample 2.

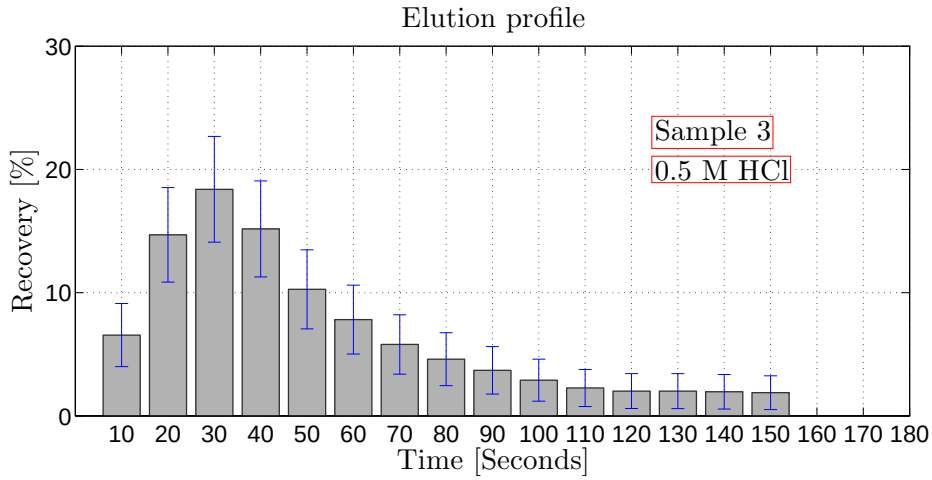

Figure 3.13: Manganese recovery. Flow rate of 0.2 mL/min and eluting acid strength 0.5 M HCl. 20 μL resin volume. Sample 3.

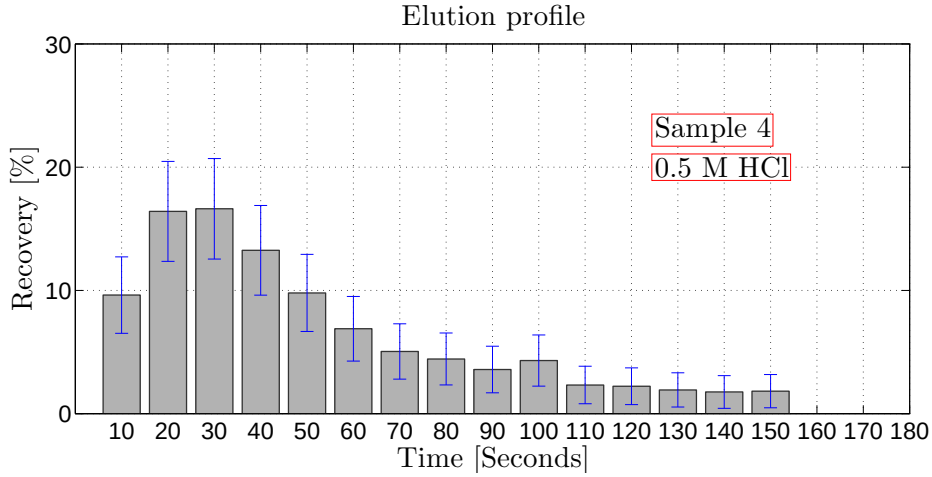

Figure 3.14: Manganese recovery. Flow rate of 0.2 mL/min and eluting acid strength 0.5 M HCl. 20 μL resin volume. Sample 4.

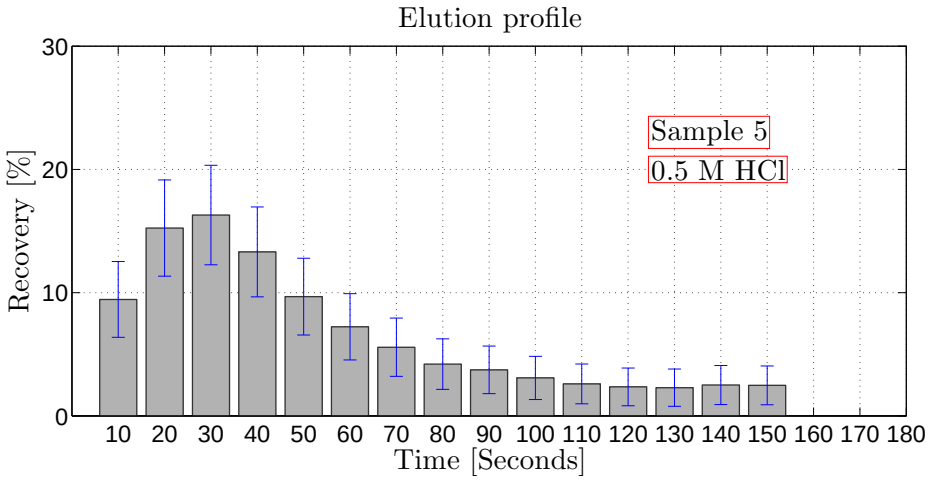

Figure 3.15: Manganese recovery. Flow rate of 0.2 mL/min and eluting acid strength 0.5 M HCl. 20 μL resin volume. Sample 5.

Table 3.5: Elution profile. Eluting acid 0.5 M HCl.

Elution profile Eluting acid 0.05 M HCl sample 1			
Name	CPM	% Recovery	Sum % Recovery
E1	991	4.73	
E2	1931	9.21	
E3	2777	13.24	
E4	2957	14.11	
E5	2659	12.68	
E6	2044	9.75	
E7	1649	7.86	
E8	1280	6.10	97.2
E9	1021	4.87	
E10	741	3.53	
E11	654	3.12	
E12	500	2.38	
E13	442	2.11	
E14	384	1.83	
E15	345	1.64	
TC	830	-	
Standard	20966	-	

Table 3.6: Elution profile. Eluting acid 0.5 M HCl.

Elution profile Eluting acid 0.05 M HCl sample 2			
Name	CPM	% Recovery	Sum % Recovery
E1	2080	8.32	
E2	3747	15.00	
E3	4342	17.38	
E4	3701	14.81	
E5	2779	11.12	
E6	2091	8.37	
E7	1635	6.54	
E8	1231	4.93	101.8
E9	901	3.61	
E10	668	2.67	
E11	546	2.19	
E12	450	1.80	
E13	426	1.70	
E14	396	1.59	
E15	434	1.74	
TC	297	-	
Standard	24989	-	

Table 3.7: Elution profile. Eluting acid 0.5 M HCl.

Elution profile Eluting acid 0.05 M HCl sample 3			
Name	CPM	% Recovery	Sum % Recovery
E1	1810	6.77	
E2	4056	15.17	
E3	5076	18.98	
E4	4189	15.66	
E5	2835	10.60	
E6	2157	8.07	
E7	1600	5.98	
E8	1270	4.75	103.2
E9	1020	3.81	
E10	801	2.99	
E11	625	2.34	
E12	556	2.08	
E13	555	2.07	
E14	540	2.02	
E15	520	1.94	
TC	249	-	
Standard	26745	-	

Table 3.8: Elution profile. Eluting acid 0.5 M HCl.

Elution profile Eluting acid 0.05 M HCl sample 4			
Name	CPM	% Recovery	Sum % Recovery
E1	2172	9.09	
E2	3705	15.51	
E3	3753	15.71	
E4	2991	12.52	
E5	2212	9.26	
E6	1555	6.51	
E7	1138	4.77	
E8	1002	4.19	94.5
E9	808	3.38	
E10	972	4.07	
E11	525	2.20	
E12	502	2.10	
E13	434	1.82	
E14	397	1.66	
E15	411	1.72	
TC	234	-	
Standard	23887	-	

Table 3.9: Elution profile. Eluting acid 0.5 M HCl.

Elution profile			
Eluting acid 0.05 M HCl sample 5			
Name	CPM	% Recovery	Sum % Recovery
E1	1829	8.76	
E2	2951	14.12	
E3	3155	15.10	
E4	2576	12.33	
E5	1873	8.97	
E6	1399	6.70	
E7	1079	5.16	
E8	814	3.90	92.7
E9	723	3.46	
E10	596	2.86	
E11	503	2.41	
E12	455	2.18	
E13	443	2.12	
E14	485	2.32	
E15	480	2.30	
TC	441	-	
Standard	20890	-	

The results show consistent elution profiles (Figure 3.11 - 3.15) and possibility to use eluting acid solution as low as 0.001 M HCl (Figure 3.10). 0.001 M HCl enables full recovery of manganese, however there is more time required to allow for the recovery of manganese and at the same time a larger volume of eluting acid solution.

3.2 Summary and conclusions of pre-concentration optimisation experiments

For the Toyopearl resin the efficient uptake of manganese requires a slow flow rate, so a compromise needs to be made between the overall time of the analysis and the efficiency of the column. When the Toyopearl resin is used for the separation and pre-concentration of manganese from sea water, optimal manganese removal occurs in the pH range 8-9.

In this pH range efficient column operation was observed when flow rates of 0.2 mL/min were used to pump the sample through the column. However, all the other solutions including the eluting acid could flow through the column at 0.8 mL/min flow rate, with full elution of manganese. All of the manganese was eluted off the column within about 385 μL of eluting acid solution, with most of the analyte being eluted within about 175 μL when a 0.8 mL/min flow rate was applied with 0.05 M HCl eluting acid solution.

The lowest concentration of hydrochloric acid tested that gave quantitative elution of the analyte of interest was 0.001 M HCl. However, the lower the concentration of the acid the later the manganese was eluted from the column, and therefore a higher concentration of eluting acid (0.5 M HCl) is preferable if one wants the sample to be eluted rapidly from the column.

The extraction of manganese from water samples and the elution efficiency of the Toyopearl resin have been examined. The best tested conditions are summarised in Table 3.10. Slower flow rates and column dimensions (width, length) could be investigated in the future.

This information can now be used to help couple the pre-concentration system to the spectrophotometric LOAC system for manganese. Before such a system can be used it proved necessary to carefully re-evaluate the PAN colorimetric technique, and this is described in Chapter 4.

Table 3.10: Conditions tested for manganese uptake and elution from the Toyopearl resin

Parameter	Optimal value	Comment
Sample flow rate	Uptake 0.2 mL/min	To allow for full recovery
Volume of the resin	20 μL	Resin capacity per 20 μL resin volume is up to about 5000 nM
Sample pH	Uptake 8-9 pH	For quantitative recovery of manganese sample pH should be kept in the pH range 8-9 (i.e. within the range of sea water pH)
Eluting acid strength	0.001 M HCl	The lowest concentration of the eluting acid tested, giving full recovery of manganese. The final concentration of the eluting acid will be chosen depending on chemical method requirements.

Chapter 4

Development of the microfluidic chip and a aplication of the PAN technique

Contents

4.1 Introduction 72
4.2 Development of the Microfluidic chip 72
4.2.1 Microfluidic test-chips - design and production 72
4.2.2 Microfluidic chip with pre-concentration column 74
4.3 Determination of Manganese with PAN 77
4.4 Using the PAN reagent prepared with Triton X-100 78
4.4.1 Application of the PAN method on chip - Triton X-100 78
4.4.2 Observation of the PAN reagent using a microscope 81
4.4.3 PAN - Triton X-100 - spectrophotometric measurements 84
4.5 Choice of alternative surfactant 86
4.6 PAN reagent prepared with SDS 88
4.6.1 PAN - SDS - off chip measurements 88
4.6.2 PAN - SDS - method performance 93
4.6.3 Application of PAN method on chip - PAN - SDS 99
4.7 Summary and conclusions 103

4.1 Introduction

With the optimisation of the resin uptake and elution completed, as described in Chapter 3, the next stages were the design and production of suitable microfluidic chips and testing of the PAN colorimetric determination step described in Chapter 2 with these chips.

4.2 Development of the Microfluidic chip

4.2.1 Microfluidic test-chips - design and production

In order to make manganese measurements on the microfluidic chip the test units were produced as described in Chapter 2.1.

The new microfluidic chips were based on an earlier design by Milani et al. [62], and Floquet et al. [72]. A key feature of this system is the diffusive mixing of reagents and sample in the narrow colorimetric channel under stopped flow conditions. Initial designs focused on introduction of reagents and sample into the colorimetric channel, and subsequent work investigated the coupling of a resin column to the chip. First, the designs of chips used are given, and their use with the PAN technique is then covered.

The system was prepared with two bench top Harvard syringe pumps to introduce solutions; the reagent and sample (or standard or blank) were pumped simultaneously into the optofluidic cell. Because of the low Reynolds number the flow is laminar and mixing (and reaction) between the streams in the microfluidic channel with stopped flow is by diffusion. The sample and reagent were introduced to the chip through the pumps through teflon plastic tubing (0.8 mm id) and then to the measurement cell in the microfluidic chip.

Figure 4.1 shows a schematic diagram of the test chip used to allow the sample and reagent to combine in the chip and diffuse in the optofluidic channel.

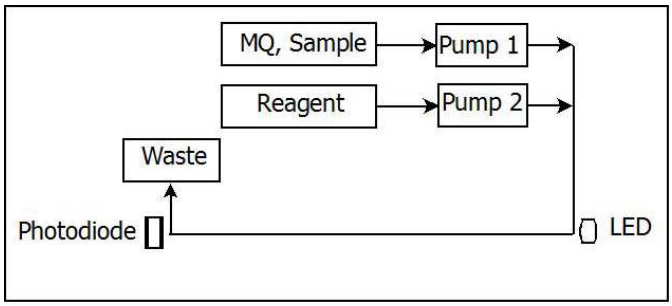

Figure 4.1: Schematic diagram of the microfluidic chip used to introduce solutions, the reagent and sample (or standard or blank) simultaneously into the optofluidic cell and diffuse.

The chip (Figure 4.2) consisted of fluid inlets, channels to carry the solutions (300 μm wide and 300 μm deep), measurement cell (600 μm wide and 300 μm deep), LED light source and photodiode detection. The spectrophotometric channel was 100 mm long.

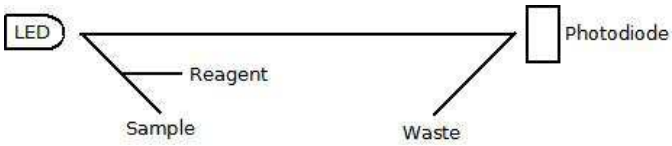

Figure 4.2: Test chip design.

A chip with four measurement cells, LEDs and photodiodes was produced (Figure 4.3), following the design of Milani [62]. This chip was used to perform experiments using the PAN reagent.

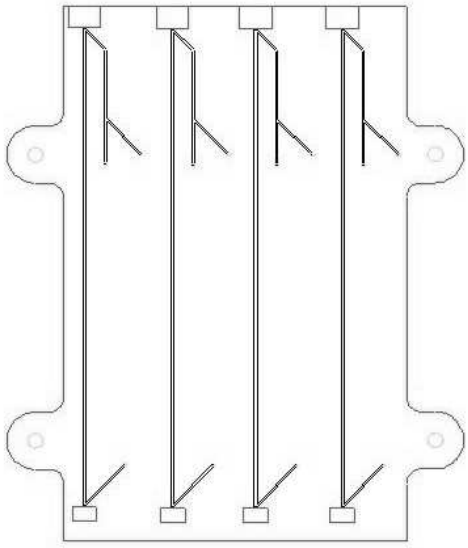

Figure 4.3: Chip with four measurement cells, LEDs (large rectangles) and photodiodes (small rectangles).

In the test systems the green LED (see section 2.8 for details) was driven by a separate mains stabilised power supply unit (PSU) that provided a constant current (up to 30 mA) at the appropriate voltage. The light from the LED passing through the optical channel in the system was measured using a TAOS TSL257 device that contains a light detector and integrated amplifier. This device delivers voltage that is directly proportional to the incoming radiation from the LED. This voltage was the analogue input to a USB-6009 DAQ device (National Instruments). The output of the TAOS device was monitored using a custom built LabVIEW programme.

Signal produced by analytical instrument is associated with noise. Noise (the random variations in voltage seen in the average signal) is typically derived from instabilities in the electronics used.

4.2.2 Microfluidic chip with pre-concentration column

In the final version of the analyser, the system contains the pre-concentration column attached to the chip, where sample is pumped through and taken up on the resin and then eluted with acid solution. After the sample is concentrated and eluent is combined with the reagent and directed into the measurement channel for manganese detection the intensity of the colour developed is measured by the detector.

The pre-concentration stage of the analysis method uses the pre-concentration resin, packed in to a mini-column. The column is filled with resin material and attached to the chip with plastic tubing. The test chip with the column is produced in order to examine the flow of solution through the microfluidic chip and through the column.

Figure 4.4 shows the design of the chip with measurement cell and channels and connections designed to attach the column to the chip. To test possible pressure and leakage issues MQ water was pumped through the device at 800 $\mu L/min$ flow rate. Tubes were connected at the end of each line by a minstack screw fitting (The Lee Company).

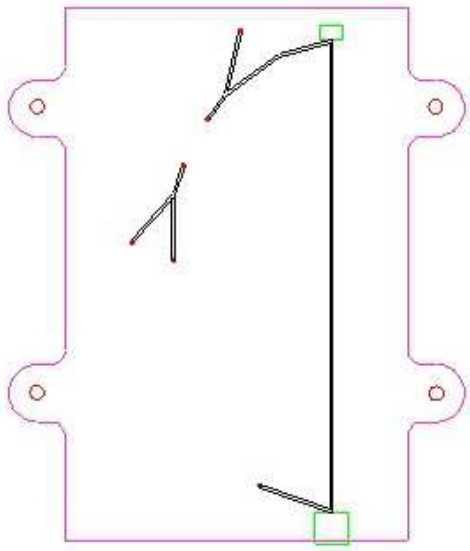

Figure 4.4: Chip with measurement cell and channels and connections designed to attach the column to the chip. LED (large rectangle) and photodiode (small rectangle).

Two kinds of pre-concentration columns were used for test experiments. One column was prepared by injecting the resin material into custom made Perspex cylinder tube Figure 4.5. The other column was prepared by injecting the material into soft teflon tube 0.8 mm id, Figure 4.6. The latter approach allows for more flexible change of the volume of the resin. With this solution there is no need to prepare a new cylinder tube to hold the resin if different resin volume is required.

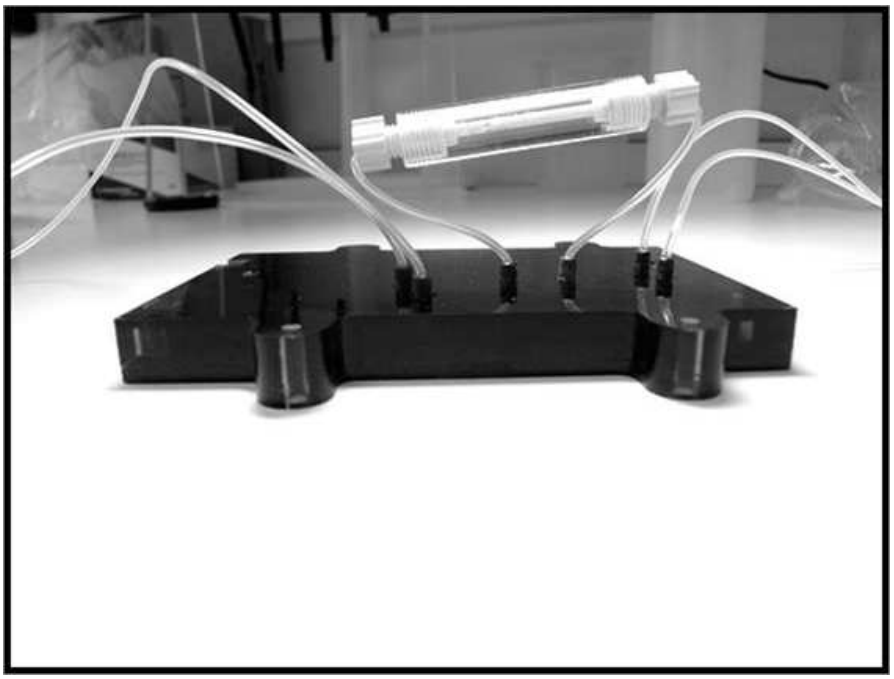

Figure 4.5: Test chip with Perspex pre-concentration column.

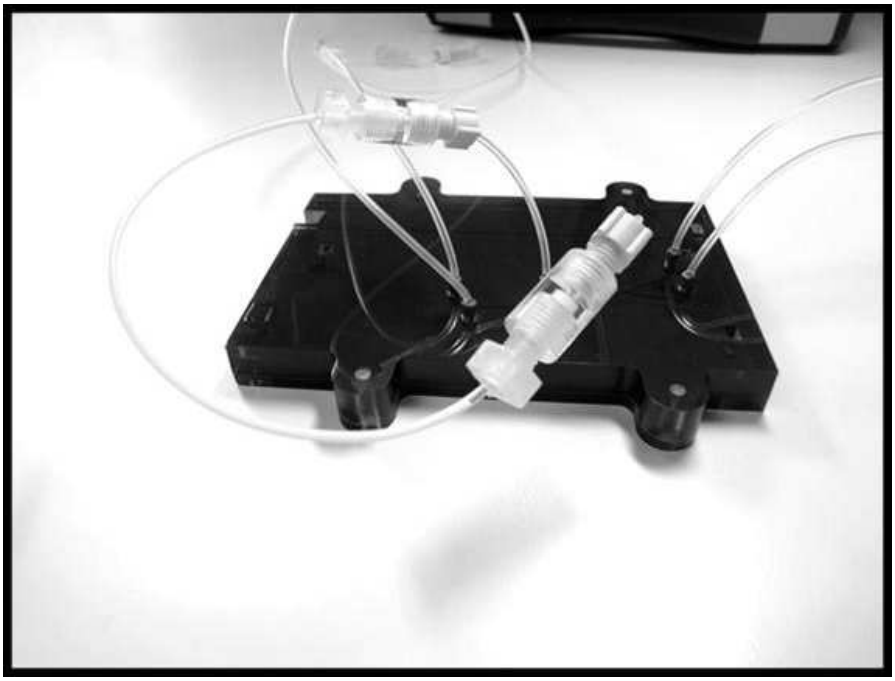

Figure 4.6: Test chip with teflon pre-concentration column with connectors with frits.

There were no pressure issues and no leakage at 800 $\mu L/min$ flow rate for both column designs used. The chip system was therefore ready to be interfaced with the colorimetric step and the resin column (Chapter 3).

4.3 Determination of Manganese with PAN

The reagent 1-(2-pyridylazo)-2-naphtol (PAN) reacts with a wide variety of metal ions, including manganese, to form coloured water-insoluble chelates. Due to the insolubility of PAN chelates in aqueous medium, the PAN reagent is prepared by dissolving it with a surfactant solution [100].

The determination of manganese based on the measurement of absorbance of manganese PAN chelate solubilised with non-ionic surfactant Triton X-100 is described by Goto et al. [101]. In a non-ionic surfactant system, the chelate is extracted in the micelle phase. The maximum absorbance of the Mn-PAN chelate occurs at 562 nm and the molar absorptivity of the manganese-PAN chelate at this wavelength found is $4.4 * 10^4$ $mole\ cm^{-1}$ [101]. The formation of the chelate is complete at pH values higher than 8.8. Goto et al. reported optimum pH at 9.2.

Goto et al. reports that it is very likely that the Mn-PAN chelate is decolorized when the dye is catalitically oxidized in the presence of manganese, since atmospheric oxidation of Mn(II) takes place in alkaline media. Oxidation can be avoided by addition of a reductant such as hydroxylamine hydrochloride or ascorbic acid. In the study reported by Goto et al. sodium ascorbate was used to avoid oxidation. The time required for full colour development varies with the temperature and it is reported to be 10 min at room temperature (15 to 30 $^{\circ}C$) and 20 min at 10 $^{\circ}C$, and Beer's law is obeyed up to 2 ppm of manganese [101].

Srijaranai et al. [100] used PAN for determination of manganese and many other metals at low concentration levels by ion exchange chromatography. The absorption spectra of PAN and metal–PAN chelates were recorded in the range from 500 nm to 600 nm and the chosen analytical wavelength was 550 nm because of the lowest absorption of PAN and the maximum absorption of all metal–PAN chelates.

The concentration of PAN reagent is reported to be important in metal determinations. Thus the complexation efficiency in terms of peak area of the metal–PAN complexes is dependent on the concentration of PAN; increasing the PAN concentration up to 0.3 $mmol\ L^{-1}$ increased the peak areas of the chelates [100]. Tadayon [102] found the

complexation efficiency increased with increasing ligand concentration up to 0.01 $mmol\ L^{-1}$ and then remained constant [102]. The effect of pH on the extraction of manganese was studied within the range 4 to 12, and showed that the absorbance increased in the range 4 to 9.5. Above pH of 9.5 the absorbance started to decrease [102]. The reason for less complexation under acidic conditions is protonation of oxygen and nitrogen whilst in strongly alkaline conditions the metal will take the hydroxide form, with less competition from protons and therefore the best pH is 9.5 [102].

For this project the PAN method was chosen for manganese determination and used with the on-bench system setup using microfluidic test chip to observe the behaviour of the solutions and time required for analysis.

4.4 Using the PAN reagent prepared with Triton X-100

4.4.1 Application of the PAN method on chip - Triton X-100

In order to make manganese measurements on the microfluidic platform the different designs of reagent additions and in cell diffusion were tested. Initial experiments on chip were performed using the PAN reagent prepared with Triton X-100 (chip design Figure 4.3).

The results were compared between the premixed solution, where sample and reagent are mixed before being introduced to the microfluidic chip, and where sample and reagent are introduced to the chip through separate channel inlets and directed to the measurement cell where the diffusion takes place. Voltage measurements from the sensor were taken after signal stabilisation (Table 4.1).

Table 4.1: On chip experiments. PAN - Triton X-100. Sample premixed with reagent.

On-chip measurements. PAN Triton X-100.		
Mn(II) [nM]	Rep	Voltage [V] [at 100 sec]
900	1	1.907
	2	1.453
	3	1.655
1000	1	1.677
	2	1.611
1800	1	1.657
	2	1.458

By comparing Figures 4.7 and 4.8 it can be clearly seen that the preformed Mn-PAN complex gave much noisier data in the chip than when the Mn-PAN complex was formed during diffusive mixing in the cell.

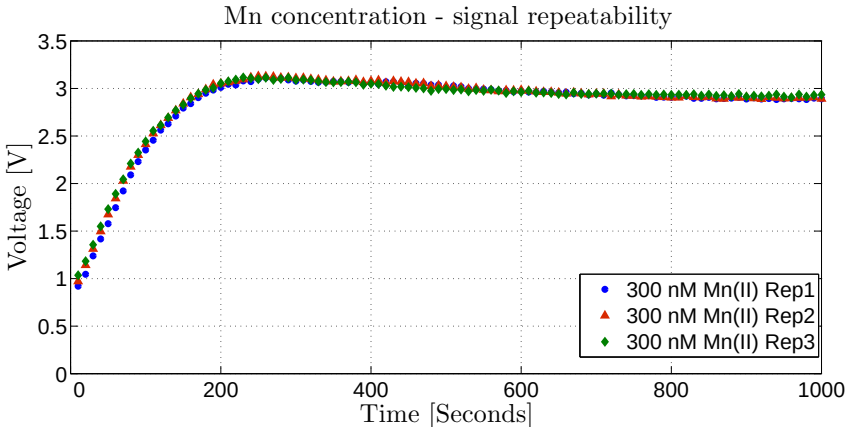

Figure 4.7: On chip measurements. PAN-Triton-X. Diffusion. 300 nM Mn(II) Replicates 1-3.

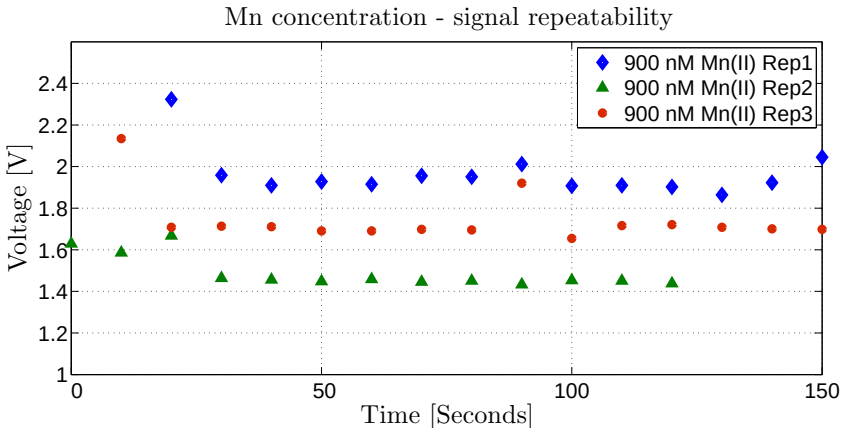

Figure 4.8: On chip measurements. PAN-Triton-X. Premixed. 900 nM Mn(II) Replicates 1-3.

The poor reproducibility and noise associated with measurement of preformed Mn-PAN solution indicated a problem not previously identified with the method that needed investigation.

Possible reasons for inconsistent results obtained from the manganese measurements on the chip using the PAN method are:

- light from outside of the system was affecting the detected signal

- difference in the pH of the solution after the sample and reagent are mixed

- detection or LED power source or connection failures

- reagent solution was not stable, not mixed fully, or otherwise non uniform

The light from outside of the system was not affecting the detected signal which was confirmed by comparing the output from the system with system covered / not covered from the outside light. The pH of the solution after the sample and reagent were mixed was checked and found to be 9.5, which is the correct pH for the method applied.

The chips are produced manually and therefore it is possible that the chip, LED and photodiode used for test experiments may not be performing correctly. To test the performance of the chip the method for iron analysis was applied on the chip (chip design Figure 4.5). The iron method was used in the past on the microfluidic chip and good results were obtained. The determination of Fe(II) was based on a colorimetric method where iron creates a colour complex with ferrozine with a maximum absorbance at 562 nm. This wavelength is very close to that of the Mn-PAN maximum and so

the same LED, detector and chip could be used. The 0.01 M ferrozine reagent was prepared in acetate buffer (Ferrozine for spectrophotometric determination of iron $\geqslant$ 97.0%; sodium acetate BioXtra $\geqslant$ 99.0%; acetic acid TraceSELECT Ultra $\geqslant$ 99.0%; from Sigma Aldrich). The Fe(II) standard solutions were prepared with 1 mM ammonium Fe(II) sulphate hexahydrate, and stabilised by addition of ascorbic acid solution.

The results from the iron measurements on the chip showed a good response and repeatability. The results are shown in Table 4.2.

Table 4.2: Iron measurements on the chip.

On-chip measurements		
Fe(II)	Rep	Voltage
250 nM	1	3.108
	2	3.074
500 nM	1	2.431
	2	2.307

The conclusion from this test is that the pre-concentration chip used for tests experiments is performing as expected.

One of the reasons for the signal being not consistent may be the behaviour of the PAN reagent. Experiments were performed using the PAN reagent prepared with extended mixing times. The mixing time during the preparation of the reagent in the original method reported by Chin et al. [40] is 8 hours. The mixing time was extended to 17 hours and 23 hours. Even after these changes in the reagent preparation the results obtained still showed inconsistent signals.

4.4.2 Observation of the PAN reagent using a microscope

Observations of PAN reagent using a microscope were performed in order to assess if the reagent was not fully dissolved or if the colloidal form was unstable with time.

For the reagent prepared with 5 mL Triton X-100 per 250 mL of PAN reagent solution and 8 hours mixing time, particles were visible under the microscope the day after preparation, and the reagent further changed with time with more visible particles seen after 48 hours.

For PAN reagent prepared with 15 mL Triton X-100 per 250 mL of PAN reagent and

8 hours mixing time only a few particles are visible under microscope and the reagent was not changing when the mixing time during preparation is extended from 8 hours to 23 hours.

The results are presented in Figures 4.9 to 4.12.

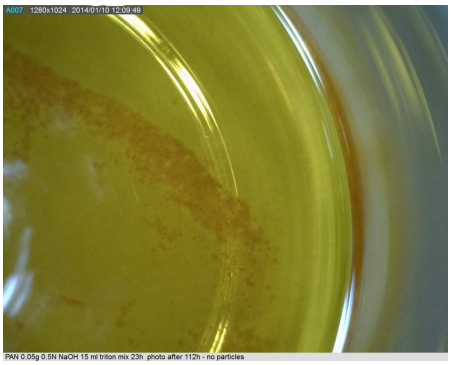

Figure 4.9: Observation under microscope. PAN Triton X-100, 8 hours mixing time, 48 hours after preparation. Bottom of flask shown (around 70 mm).

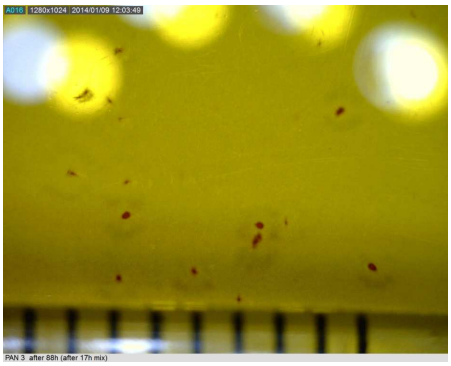

Figure 4.10: Observation under microscope. PAN Triton X-100, 17 hours mixing time, 48 hours after preparation. Scale shows 1 mm intervals.

Figure 4.11: Observation under microscope. PAN Triton X-100, 8 hours mixing time, 112 hours after preparation.

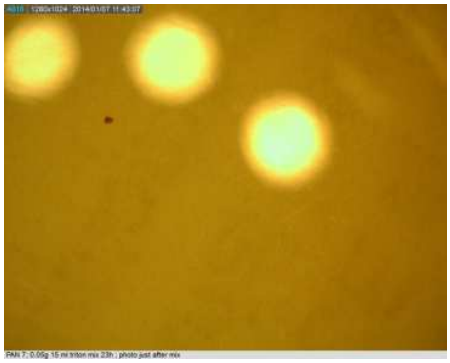

Figure 4.12: Observation under microscope. PAN Triton X-100, 23 hours mixing time, just after preparation.

The mixing time during preparation of reagent was extended from 8 hours to 23 hours. For all mixing times immediately after preparation of reagent the uniform orange reagent colour was present as in Figure 4.12. However within several hours for the majority of the reagents, micelle coagulation and particle formation was evident. Solutions which had a visually uniform color, when passed through the chip gave inconsistent results, indicating a problem was still present.

A further useful change to the method that should help with reagent stability is reduced concentration of PAN during PAN reagent preparation. The concentration of PAN used in the work reported by Chin et al. is 0.8 $mmolL^{-}$ ^{1}. This translates to 0.05 g of PAN per 250 mL of reagent solution [40].

The concentration of PAN used by Srijaranai et al. [100], in the work where PAN is used as the post column reagent for ion exchange chromatography of heavy metals in

environmental samples, is 0.3 $mmolL^{-1}$. Tadayon et al. [102], reported the determination and pre-concentration of manganese using an ionic liquid based micro-extraction technique in biological samples, with use of PAN at concentration 0.1 $mmolL^{-1}$. The concentration of PAN was reduced from 0.05 g PAN (0.8 $mmolL^{-1}$) to 0.025 g PAN (0.4 $mmolL^{-1}$) per 250 mL of reagent solution prepared and this concentration was used from this point for PAN reagent preparation.

4.4.3 PAN - Triton X-100 - spectrophotometric measurements

The experiments using the microfluidic chip demonstrated there were issues with the conventional PAN technique. Spectrophotometric measurements using 10 cm cell in a Hitachi U2800 double beam instrument were therefore performed in order to better characterise the behaviour of the Mn-PAN complex formation. The standard solution was prepared in 0.01 M HCl, MQ water or sea water. When sample was prepared in acid solution a buffer was added. The blank was a buffered acid solution and PAN reagent mixture, buffered seawater and and PAN reagent mixture or MQ water and PAN reagent mixture. PAN reagent was prepared with 15 mL Triton X-100 (total reagent volume 250 mL) and mixed for 23 hours. The PAN reagent (5 mL) was mixed with 50 mL of standard, and after mixing absorbance with time was measured with the 10 cm cell. The measurement gave absorbances to 4 d.ps.

It is shown that the absorbance of PAN complexes with manganese formed in this way are not stable and the observed absorbance value decreased with time (Figure 4.13 to 4.15). The results are given in Appendix A.

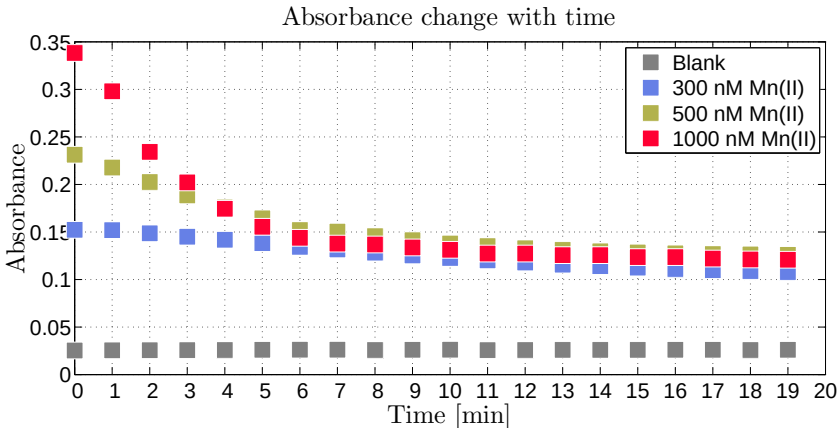

Figure 4.13: Spectrophotometric measurements of Mn-PAN with Triton X-100. Manganese standards were in 0.01 M HCl, and buffered to pH 9.5 with boric acid in 0.15 M NaOH. Blank – 0.01 M HCl buffered solution and PAN reagent mixture.

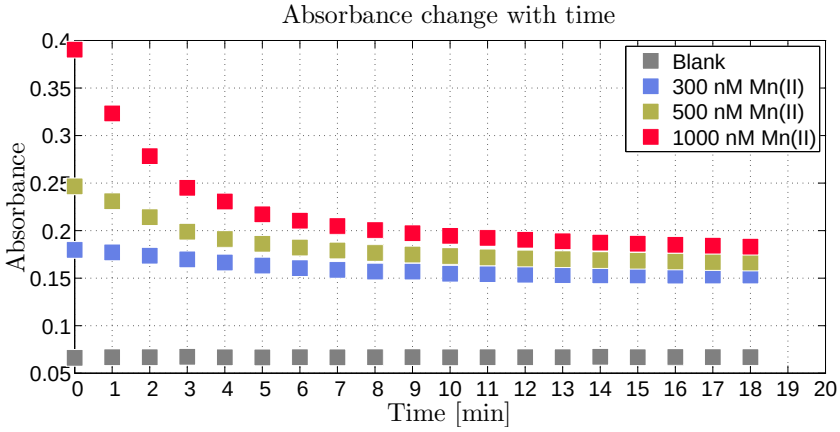

Figure 4.14: Spectrophotometric measurements of Mn-PAN with Triton X-100. Manganese standards were in seawater with pH adjusted to 8.0 using ammonia solution. Blank – sea water buffered solution and PAN reagent mixture.

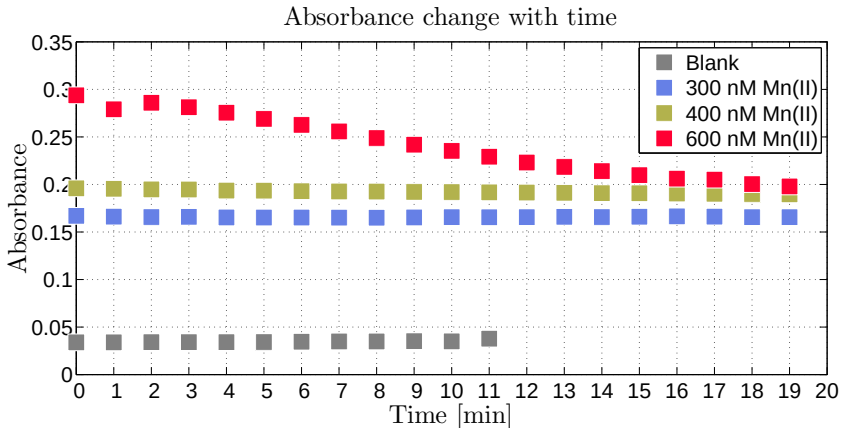

Figure 4.15: Spectrophotometric measurements of Mn-PAN with Triton X-100. Manganese sample is prepared in MQ (no buffer). Blank – MQ and PAN reagent mixture.

Experiments using a microscope showed significant changes with time of the Triton X-100 'stabilised' PAN-Mn through apparent combination of smaller colloids into larger particles. Experiments using a conventional spectrophotometer showed rapid changes in absorbance, presumably reflecting this lack of stability of the Triton X-100 solubilised PAN. As stability of the reagent in the LOAC system is very important an important conclusion from those experiments was that a new surfactant for the preparation of PAN reagent was needed.

4.5 Choice of alternative surfactant

Surfactants are commonly separated into four major groups, depending on their ionization or charge: anionic, cationic, nonionic and amphoteric. Anionic and cationic surfactants ionize when mixed with water due to their negative charge (anion) and positive charge (cations), respectively. Nonionic surfactants do not ionize in aqueous or water solutions, whereas amphoteric surfactants can be either anionic or cationic depending on the acidity of the solution. Detergents contain a hydrophilic "head" region and a hydrophobic "tail" region [103].

The structure of the sodium dodecyl sulfate (SDS) detergent, showing the hydrophilic and hydrophobic regions is presented in Figure 4.16. Figure 4.17 is a simple illustration of a sodium dodecyl sulfate micelle, with the hydrophobic tail attracted to the metal complex [103].

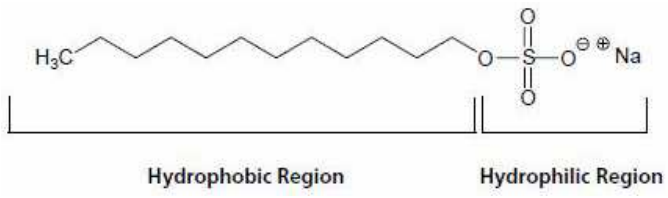

Figure 4.16: Structure of the anionic detergent sodium dodecyl sulfate (SDS), showing the hydrophilic and hydrophobic regions.

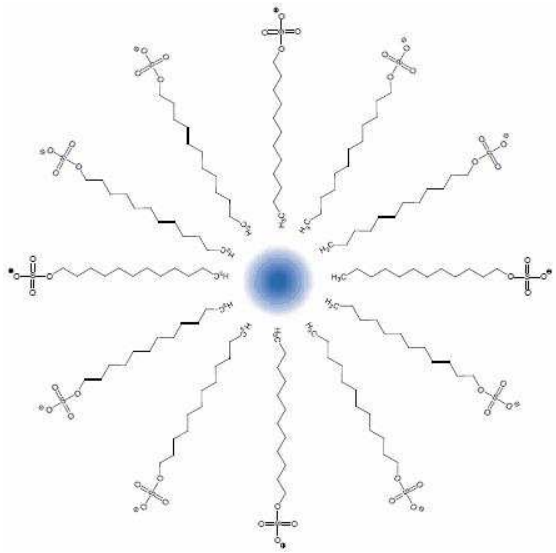

Figure 4.17: Simple illustration of a sodium dodecyl sulfate micelle, with the hydrophobic tail attracted to the metal complex.

Critical micelle concentration (CMC) is the concentration at which micelles begin to form, it is the maximum monomer concentration [103]. With increasing surfactant concentration, SDS molecules aggregate on the surface of the metal complex through Van Der Waals interactions at the hydrocarbon tails of the ligands in the metal complex and the SDS molecules [104]. These surface aggregates are called hemimicelles or admicelles. Above the CMC micelles of SDS will be formed in solution [104]. Hemimicelles or admicelles can trap molecules of PAN via the interactions between the exposed hydrocarbon tails in the hemi-micelles and the hydrophobic groups in the PAN [104].

Several different micelling agents have been reported for use with the PAN method, including SDS, Triton-100 and Tween-80 and these have been tested by Eskandari et al. [105]. It was reported that the Pd(II)-PAN complex was precipitated in Tween-80

immediately and in Triton-100 after 1 hour. In contrast, complexes of palladium and cobalt with PAN in SDS micellar media were stable and soluble for at least 3 days [105]. Higher stability and faster formation for the Ni(II) complex was observed in Tween 80 compared to Triton X-100 and was more sensitive than in SDS. Therefore those authors selected Tween-80 as the micellizing agent for further studies with Ni [106].

Agnihotri et al. [107] reported that the high solubilisation capacity of surfactants and micellar systems improves the sensitivity and selectivity of procedures considerably. Agnihotri et al. [107] reported the photometric determination of copper with PAN. In the presence of Triton X-100 the maximum increase in absorbance at 555 nm was observed. Although some of the PAN chelates in Triton X-100 provide higher molar absorptivities than those with SDS, SDS gave lower background absorbances and lower detection limits [100].

The performance of PAN in the presence of SDS, cetyltrimethylammonium chloride (CTAC), and Triton X-100 micelles was evaluated by Xia et al. for the detection of Zn(II), Co(II), Cd(II), and Mn(II) after separation by HPLC. The detection limits obtained with SDS were reported to be better, by up to 15-fold, than those obtained with CTAC and Triton X-100 [108].

The literature suggests that SDS is a suitable alternative to the Triton X-100 (as has been recommended by Chin et al. [40]), and so experiments were run to test this different solubilising agent for PAN.

4.6 PAN reagent prepared with SDS

4.6.1 PAN - SDS - off chip measurements

The PAN reagent was prepared (PAN-SDS reagent). 0.025 g of PAN was taken and added to 60 mL of 10 % SDS solution (sodium dodecyl sulfate solution, 10 % in H_2O, Sigma Aldrich), and stirred until PAN was dissolved. 100 mL boric acid buffer solution was added and made up to 250 mL volume with MQ. The buffer reagent was prepared with 0.618 g of boric acid (boric acid 99.999 % trace metal basic, Sigma Aldrich) dissolved in 100 mL of 0.1 M NaOH solution (sodium hydroxide 99.999 % trace metal basis, Sigma Aldrich).

Initial observations of the new PAN reagent were made using a microscope in order to assess if the particles were present (Figure 4.18 and 4.19).

Figure 4.18: Observation under microscope. PAN - SDS, 2 hours mixing time, after 1 day.

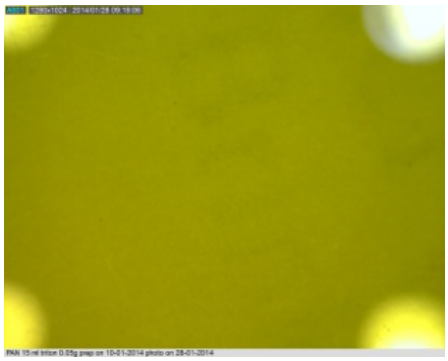

Figure 4.19: Observation under microscope. PAN - SDS, 2 hours mixing time, after 7 days.

Unlike the PAN-Triton X-100 mixture, the SDS based reagent showed no evidence for micelles coallescing and formation of visible particles.

Spectrophotometric calibrations were performed in order to characterise the behaviour of the PAN-SDS reagent over time. The standard solutions were prepared as described in section 2.1.

Data for standards in MQ, seawater and 0.02 M HCl are shown, and changes in absorbance with time were followed. The main objective here was to demonstrate the completeness of formation of Mn-PAN SDS and the reproducible nature of the measurements. (Final results are summarised and presented in Appendix A).

The results for spectrophotometric measurements using 10 cm cell in a Hitachi U2800 double beam instrument are given in Figures 4.20 to 4.22. PAN was prepared with SDS.

When standard sample was prepared in acid solution a buffer is added. The blank was buffered acid solution and PAN reagent mixture, buffered seawater and and PAN reagent mixture or MQ water and PAN reagent mixture, where the main source of the blank is the reagent solution.

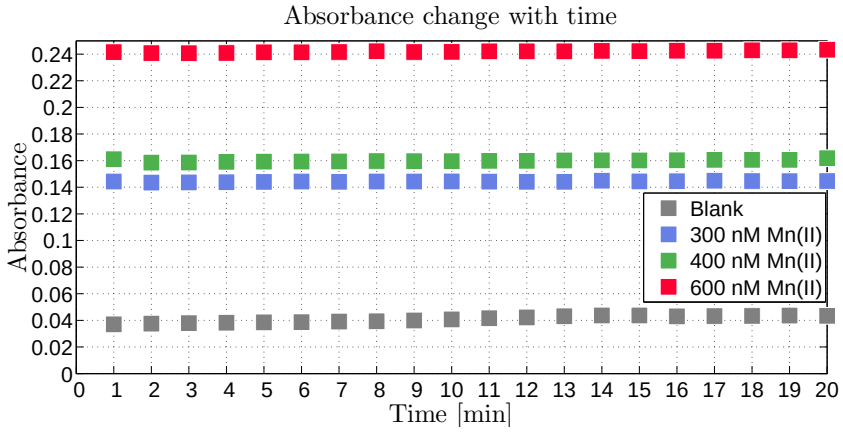

Figure 4.20: Spectrophotometric measurements. PAN-SDS. Sample in MQ. Blank, 300 nM, 400 nM and 600 nM. Blank – MQ and PAN reagent mixture.

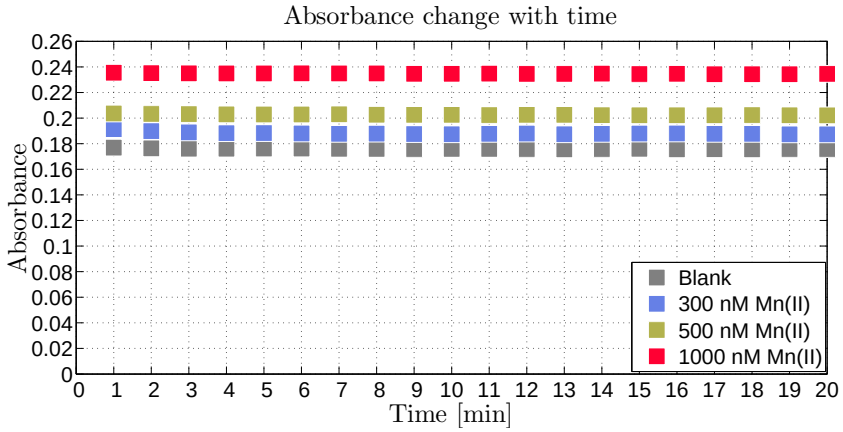

Figure 4.21: Spectrophotometric measurements. PAN-SDS. Sample in sea water. Blank, 300 nM, 500 nM and 1000 nM. Blank – sea water buffered solution and PAN reagent mixture.

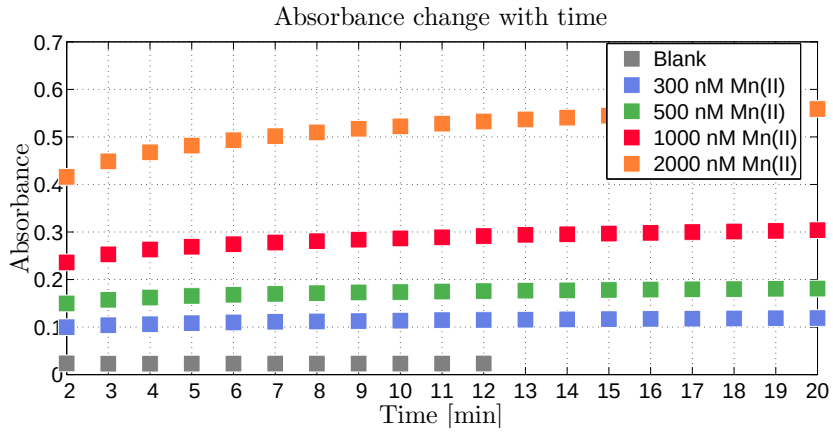

Figure 4.22: Spectrophotometric measurements. PAN-SDS. Sample in 0.02 M HCl. Blank, 300 nM, 500 nM, 1000 nM and 2000 nM. Blank – 0.02 M HCl buffered solution and PAN reagent mixture.

Results for 300nM, 500 nM, 1000 nM and 2000 nM manganese standards are shown (Figure 4.23 to 4.26).

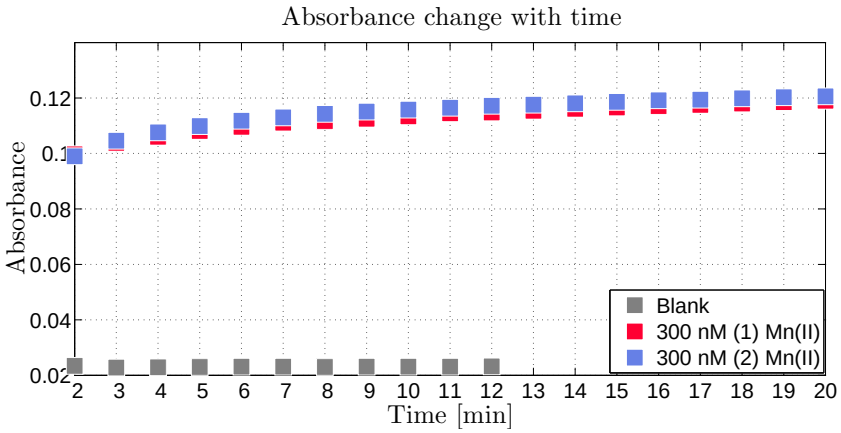

Figure 4.23: Spectrophotometric measurements. PAN-SDS. Sample in 0.02 M HCl. 300 nM Replicate 1 and Replicate 2. Blank – 0.02 M HCl buffered solution and PAN reagent mixture.

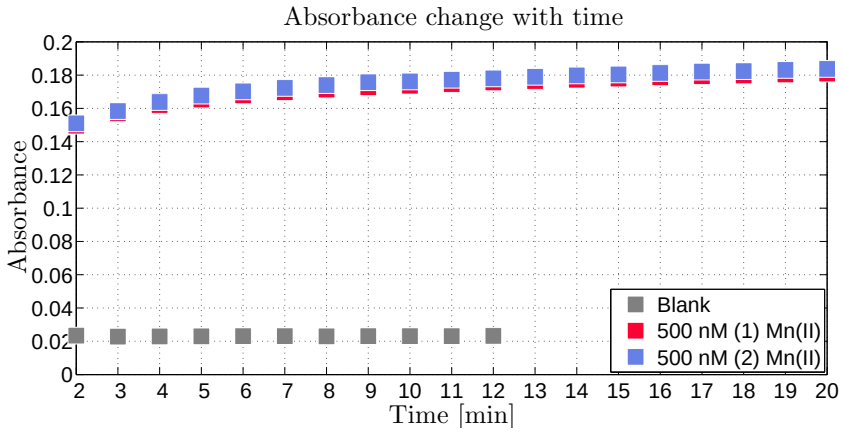

Figure 4.24: Spectrophotometric measurements. PAN-SDS. Sample in 0.02 M HCl. 500 nM Replicate 1 and Replicate 2. Blank – 0.02 M HCl buffered solution and PAN reagent mixture.

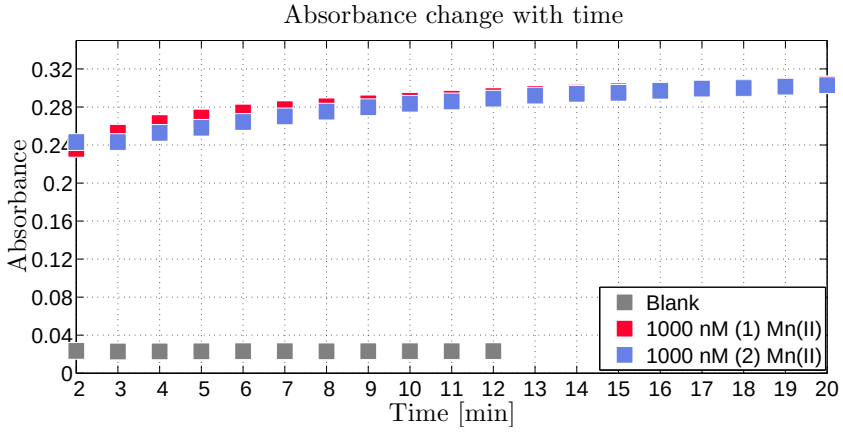

Figure 4.25: Spectrophotometric measurements. PAN-SDS. Sample in 0.02 M HCl. 1000 nM Replicate 1 and Replicate 2. Blank – 0.02 M HCl buffered solution and PAN reagent mixture.

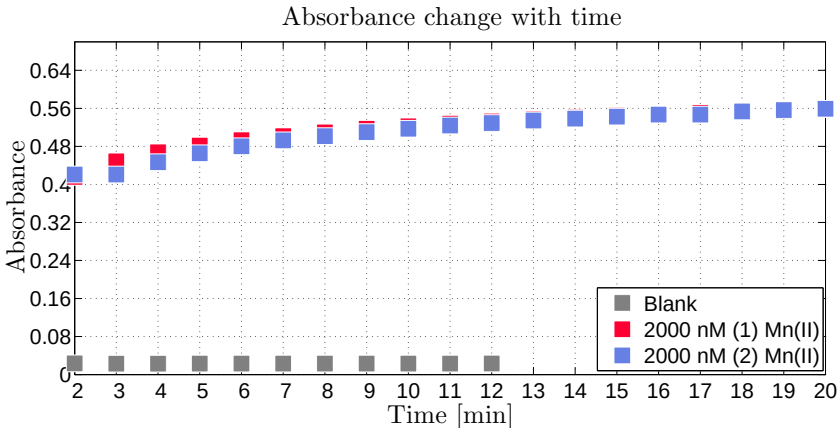

Figure 4.26: Spectrophotometric measurements. PAN-SDS. Sample in 0.02 M HCl. 2000 nM Replicate 1 and Replicate 2. Blank – 0.02 M HCl buffered solution and PAN reagent mixture.

The raw data are given in Appendix A. These data show that for the matrices tested the Mn-PAN formed rapidly and remained stable for at least 15 minutes.

4.6.2 PAN - SDS - method performance

Linearity is studied by preparing a series of different standards with concentrations of between 200 and 1000 nM for spectrophotometric analysis.

In this study the precision within a set of measurements was determined. The standard deviation was calculated from the absorbance values for replicates of a fixed concentration of manganese. The percent relative standard deviation was calculated. To assess the limit of detection an appropriate number of blanks were analysed and the standard deviation of these responses was calculated. In this study the limit of detection was calculated based on the standard deviation of the response and the slope of the calibration curve at levels approximating the LOD according to the formula LOD $= 3.0 \times (standarddeviation/slope)$ The calculated LOD value of 14 nM, and the values are presented Table 4.3.

Table 4.3: Spectrophotometric measurements. PAN SDS. Sample in 0.02 M HCl. Sample buffer 0.04 M NaOH.

Spectrophotometric measurements. PAN - SDS. 560 nm.							
Mn(II) [nM]	Rep	Abs	STD DEV	% RSD	Slope	R-squared	LOD [nM]
Blank	1	0.005979	0.001	19.49	0.2435	0.96	14
	2	0.004602					
	3	0.006737					
	4	0.007019					
	5	0.004667					
300	1	0.092313	0.003	2.68			
	2	0.098291					
	3	0.094766					
	4	0.098443					
	5	0.096286					
500	1	0.13786	0.001	1.08			
	2	0.138184					
	3	0.135881					
	4	0.134592					
	5	0.136751					
1000	1	0.241160	0.091	3.81			
	2	0.225866					
	3	0.230089					
	4	0.231544					
	5	0.217151					

Relative standard deviations for data collected for standards prepared with 0.02 M HCl varied between 19.49% and 1.08 %.

Linearity plots of absorbance values against the concentration of manganese in nM are presented in Figures 4.27 to 4.29. Calibration curves were constructed by plotting absorbance against the concentration in nM. Slope intercept and correlation coefficient values are presented in Table 4.4. The standards were prepared with MQ, 0.01 M and 0.02

M HCl solution and mixed with sample buffer and reagent in the ratio $10 : 1 : 1 v/v/v$. The sample buffer was prepared by dissolving boric acid in 0.15 M and 0.4 M NaOH solution respectively. For samples prepared with MQ no buffer was used.

Table 4.4: Off chip (560 nm) spectrophotometric calibration data.

Summary of off chip spectrophotometric calibration data. 560 nm.				
Matrix	Concentration range [nM]	Slope	R squared	Buffer system
MQ	300, 400, 600	0.2603	0.971	no buffer
0.01 M HCl	300, 500, 1000, 2000	0.2461	0.998	boric acid in 0.15 M NaOH
0.02 M HCl	200, 400, 500, 1000	0.2380	0.984	boric acid in 0.4 M NaOH

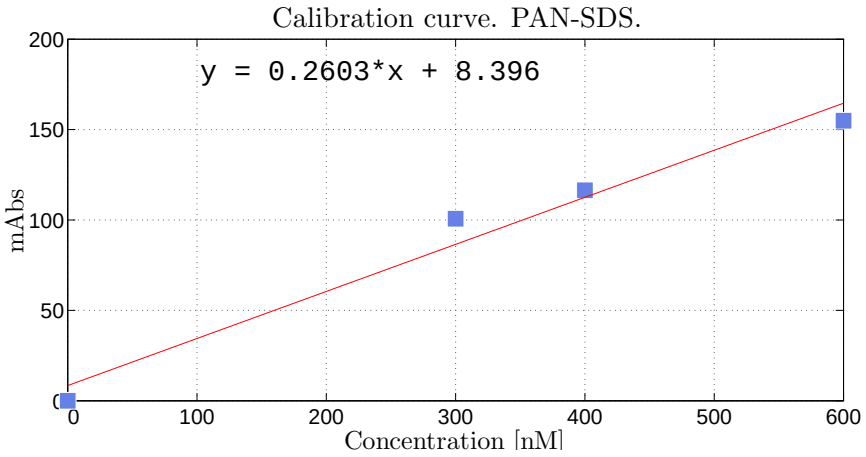

Figure 4.27: Spectrophotometric measurements. PAN SDS. 300 nM, 400 nM, 600 nM. Calibration. Samples in MQ. Blank – MQ and PAN reagent mixture.

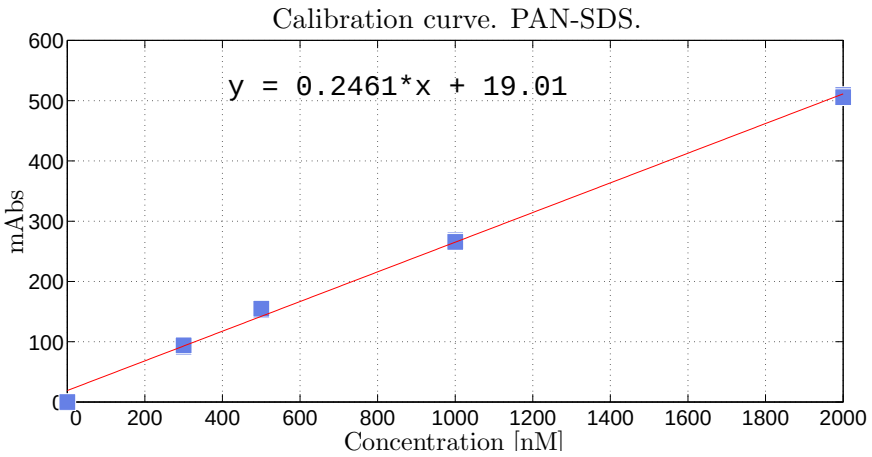

Figure 4.28: Spectrophotometric measurements. PAN SDS. 300 nM, 500 nM, 1000 nM and 2000 nM. Calibration. Samples in 0.01 M HCl. Blank – 0.01 M HCl buffered solution and PAN reagent mixture.

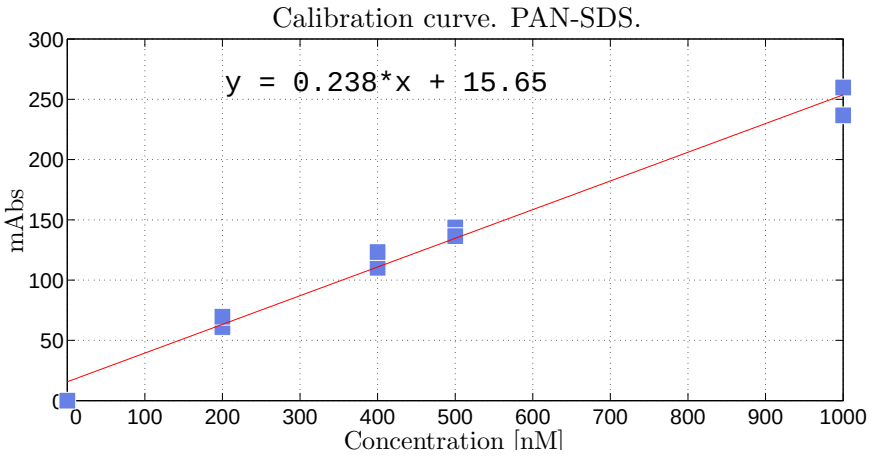

Figure 4.29: Spectrophotometric measurements. PAN SDS. 200 nM, 400 nM, 500 nM and 1000 nM. Calibration. Samples in 0.02 M HCl. Blank – 0.02 M HCl buffered solution and PAN reagent mixture.

PAN reagent is the major source of the blank in the method used, however during UV-VIS spectrophotometric measurements the blank sample was recorded as the background value and deducted automatically before standard measurements. To quantify the level of the blank the data reported in Table 4.3 were used and calibration slope was applied 0.2380 (Figure 4.29). Blank was calculated as about 24 nM.

The spectrophotometric measurements data used to construct the calibration curves

are shown in Table 4.5.

Table 4.5: The spectrophotometric measurements data used to construct the calibration curves.

Spectrophotometric calibration data Off chip measurements								
Matrix								
MQ			0.01 M HCl			0.02 M HCl		
Concentration Mn(II) [nM]	Rep	mAbs	Concentration Mn(II) [nM]	Rep	mAbs	Concentration Mn(II) [nM]	Rep	mAbs
300	1	100.7	300	1	91.6	200	1	61.0
400	1	116.4		2	94.0		2	69.6
600	1	154.9	500	1	152.4	400	1	110.2
-	-	-		2	154.8		2	123.2
-	-	-	1000	1	268.3	500	1	143.6
-	-	-		2	265.6		2	136.4
-	-	-	2000	1	509.2	1000	1	259.7
-	-	-		2	509.8		2	236.7

Section 4.6.3 reports the application of the improved assay in a lab on chip format.

4.6.3 Application of PAN method on chip - PAN - SDS

Experiments were performed on chip using PAN-SDS regent. Manganese standards at different concentrations were prepared and used for manganese determination on chip (as described in section 2.1). Samples were introduced as described in section 4.2.1.

The PAN–Mn complex absorbs at 560 nm and the LED used in the chip is centered on 572 nm (full width half maximum ~ 30 nm), therefore the off chip spectrophotometric results with 10 cm cell are reported for 572 nm together with on chip results (10 cm optical cell) (Table 4.6) (Figures 4.30 and 4.31 and 4.32).

Table 4.6: Summary of off chip and on chip spectrophotometric calibration data (10 cm cell).

Summary of off chip and on chip spectrophotometric calibration data.				
Matrix 0.02 M HCl	Concentration range [nM]	Slope	R-squared	Buffer system
Off chip 572 nm	200, 400, 500, 1000	0.0917	0.992	boric acid in 0.4 M NaOH
On chip	200, 400, 500, 1000	0.1085	0.928	boric acid in 0.4 M NaOH

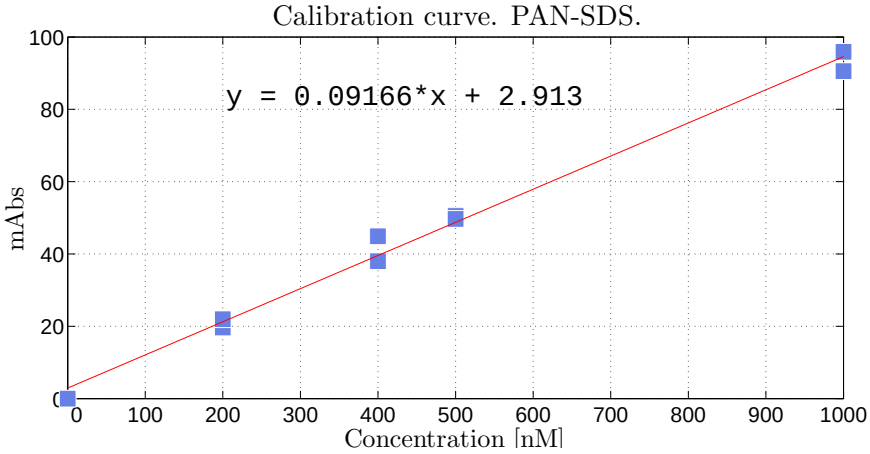

Figure 4.30: Spectrophotometric measurements. PAN SDS. 200 nM, 400 nM, 500 nM and 1000 nM. Calibration. Samples in 0.02 M HCl. 572 nm. Off chip. Blank – 0.02 M HCl buffered solution and PAN reagent mixture.

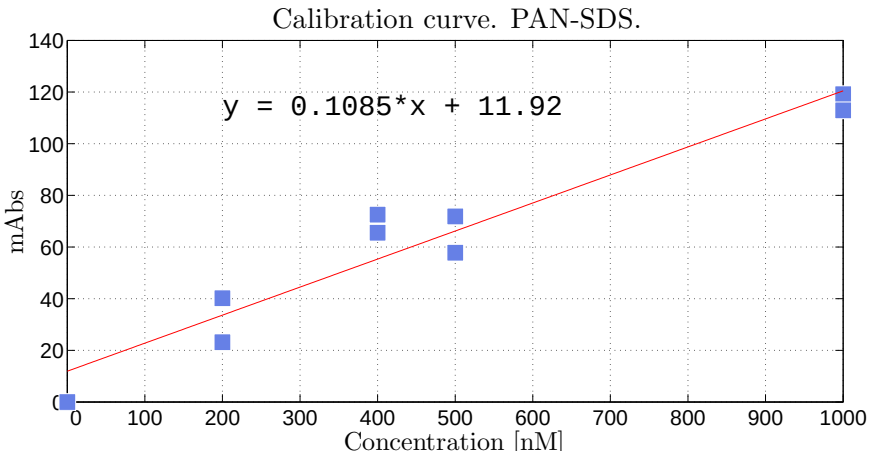

Figure 4.31: Spectrophotometric measurements. PAN SDS. 200 nM, 400 nM, 500 nM and 1000 nM. Calibration. Samples in 0.02 M HCl. On chip. Blank – MQ.

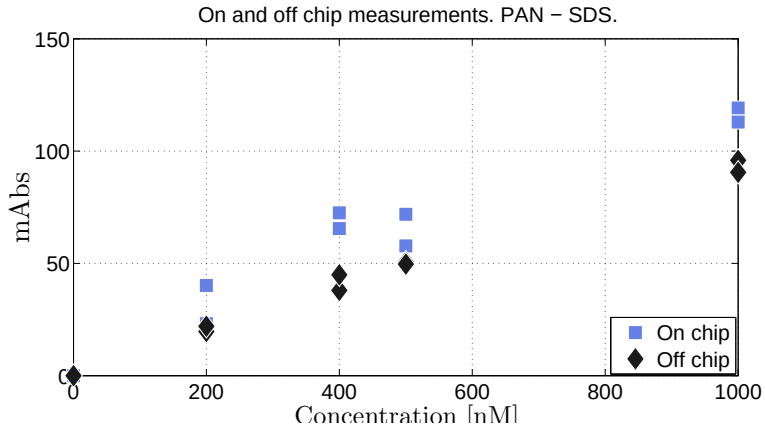

Figure 4.32: Spectrophotometric on and off chip measurements. PAN SDS.

The spectrophotometric measurements data used to construct the calibration curves are shown in Table 4.7.

Table 4.7: Spectrophotometric calibration data. On and off chip measurements (572 nm).

Spectrophotometric calibration data On and off chip measurements (572 nm)					
On chip			Off chip		
Concentration Mn(II) [nM]	Rep	mAbs	Concentration Mn(II) [nM]	Rep	mAbs
200	1	23.2	200	1	19.7
	2	40.2		2	22.0
400	1	65.5	400	1	38.0
	2	72.5		2	44.9
500	1	71.9	500	1	50.5
	2	57.8		2	49.7
1000	1	119.2	1000	1	95.9
	2	112.9		2	90.6

The voltage response from analysed standard solutions on chip was recorded and the results are shown in Figures 4.33 and 4.34, showing the response for 500 nM and 1000 nM manganese standards. Note that here the graphs are showing voltage (transmittance) against concentration, not absorbance.

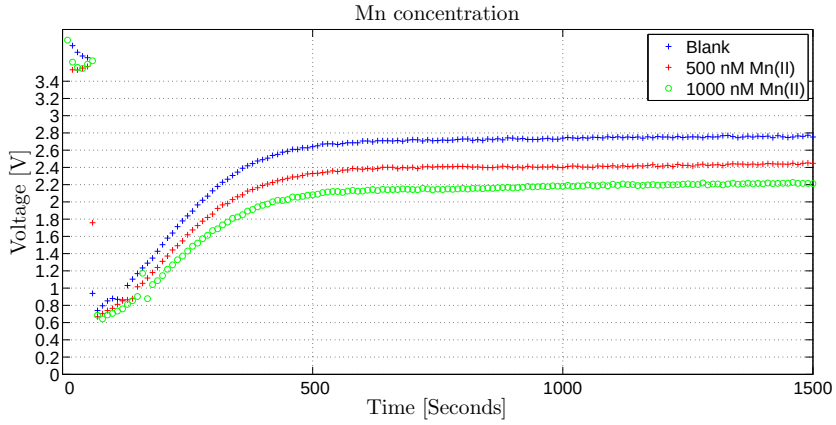

Figure 4.33: On chip measurements. PAN SDS. Blank, 500 nM, 1000 nM. Blank – 0.02 M HCl buffered solution and PAN reagent mixture.

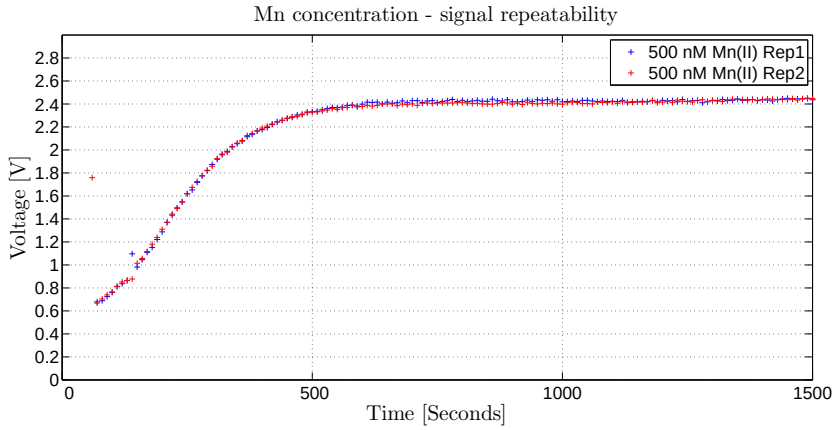

Figure 4.34: On chip measurements. PAN SDS. 500 nM.

The sample and reagent were introduced to the chip and the data show that a consistent signal was obtained in the experiments for the samples diffused in the measurement cell.

Drift is the long-term change in the average signal when no changes have been made by the operator to the main controls of the instrument. Drift can be caused by a variety of factors including for example change in temperature of the chip system being used, or variability in the power supply output. The noise could be improved if needed by smoothing algorithms [109]. Drift in these types of system is best allowed for by regular calibration and if necessary the data corrected for this long term change.

The calibration curve created for on-chip measurements with no pre-concentration, see Figure 5.16 on page 123 (slope value 0.1386). For information the calibration data were used to convert the drift voltage values presented on Figure 4.34 into Mn(II) concentrations (Figure 4.35).

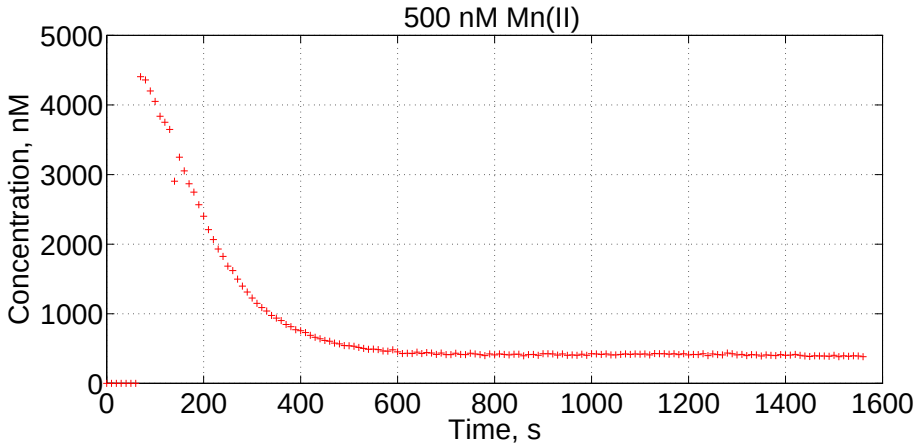

Figure 4.35: On chip measurements. PAN SDS. 500 nM. Voltage values converted to Mn(II) concentrations.

4.7 Summary and conclusions

In both on chip and off chip spectrophotometer measurements of manganese with the PAN method reported by Chin et al. [40] significant variability was observed both between repeats and over time.

To test the performance of the chip the iron method used in the past on the chip was used and good results were obtained. The conclusion from this test was that the chip used for test experiments was performing as expected.

The PAN Triton X-100 reagent was observed under the microscope and showed the reagent was forming particles. Absorbance measurements of manganese standards were performed using a UV-VIS spectrophotometer and results proved the absorbance values of the standards analysed were rapidly changing and the absorbance values for standard solutions at higher concentration were most affected.

The PAN reagent was prepared with a bigger volume of Triton X-100 solution (15 mL as opposed to 5 mL per 250 mL of reagent). The reagent did not appear to form particles with time after increasing the volume of surfactant added, and the mixing time during reagent preparation. However tests were performed on chip and the results showed that the values obtained from the same standard solution were not repeatable. The absorbance of manganese standards premixed with PAN reagent prepared with 15 mL of Triton X-100 were then measured using a bench UV-VIS spectrophotometer. The

results showed that absorbance values fell over time.

The SDS surfactant has been reported in the literature as suitable for use with the PAN method and this surfactant was chosen as an alternative to Triton X-100 for PAN reagent preparation. Absorbance measurements of manganese standards using a UV-VIS spectrophotometer with PAN reagent prepared with SDS solution gave stable absorbances over at least 15 minutes. A good calibration curve was obtained with good precision and LOD values.

The PAN reagent prepared with SDS solution was used for manganese standard measurements on the microfluidic chip with good response in relation to concentration of standards used (voltage values for Blank, 500 nM and 1000 nM of manganese). Given the superior performance of the SDS over Triton X-100, this was used in the subsequent development of the system.

Chapter 5

On-bench Lab on a Chip spectrophotometric manganese analyser with pre-concentration

Contents

5.1 Introduction . . . 105
5.2 System parts and materials . . . 106
5.2.1 Microfluidic chip - optical cell optimisation . . . 107
5.2.2 System design . . . 110
5.3 System performance . . . 117
5.4 Pump system tests . . . 126
5.5 Optimisation of elution . . . 136
5.6 System tests and calibration . . . 145
5.7 Summary and conclusions . . . 155

5.1 Introduction

With the tests of the PAN colorimetric determination on chip completed, as described in Chapter 4, the next stages were the design of the analyser chip and construction of the on-bench system for manganese determination with PAN. Some aspects of the design needed to be optimised on simpler chips prior to building of the final analytical

system. This was followed by system tests, optimisation of the elution stage and analysis of manganese standards and a certified reference material.

5.2 System parts and materials

The fabrication methods and components of the microfluidic device used for manganese determination follow the general procedures in Chapter 2 with the additional incorporation of the resin column.

For the purpose of this project I designed and produced test microfluidic chips following the above procedure. The microfluidic chips are designed using Autodesk Inventor Professional software. The production and building of the chip is based on the materials reported by Floquet at al. [72].

The prototypes of the microfluidic pre-concentration chip used for the manganese pre-concentration and detection was designed with all on-chip microchannels being 150 μm wide and 300 μm deep, except the 100 mm long optical absorption cell where both 500 μm and 600 μm width channels were tested, both channels were 300 μm deep.

The solutions were directed into the chip through the channels and flows were controlled with Hamilton Syringe Pumps (schematic of the system shown in Figure 5.1). The direction of flow of fluids through the system was controlled with solenoid valves (Lee Products 300 Series) and the sensor as a whole was managed by a LabView program, prepared by Victoire Rerolle and later modified by Jeroen Broeders, with data collection using a National Instruments NI 6009 card.

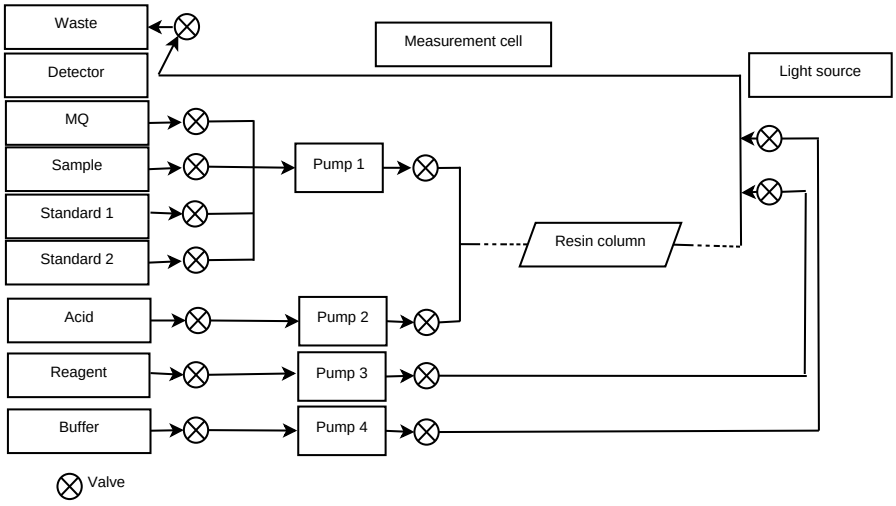

Figure 5.1: Diagram showing the solutions directed into the chip with Hamilton Syringe Pumps used to control the flows.

The pre-concentration part of the system used Toyopearl 650AF resin, packed into a micro-column of 20 μL internal volume (see Chapter 3). The resin material was packed in the PTFE tube (0.8 mm ID) and held in place with polypropylene frits. The column was attached to the chip with plastic tubing and 0.25 inch Delrin connectors (see Chapter 4). All other tubing used in the system was 0.3 mm id PTFE.

5.2.1 Microfluidic chip - optical cell optimisation

The first stage in the preparation of the manganese analyser was the design and optimisation of the main component of the system, the microfluidic chip. The reagent and sample (or standard or blank) are pumped simultaneously into the optofluidic cell. Because of the low Reynolds number the flow is laminar and mixing between adjacent streams is by diffusion only. In this particular implementation the diffusive mixing and reaction takes place with the flow stopped. The diffusion time (t) increases with width of the channel:

$t = w^2/D$

where: w - width of the channel; D - diffusivity of the diffusing molecule

An important factor affecting the time required for the solutions to fully mix in the measurement channel in the chip is the width of the measurement cell. Therefore experiments were performed to observe the response obtained from a MQ-dye solution analysed on chip with measurement cell of 500 μm and 600 μm width. Greater widths

of cell lead to excessive diffusion times, and narrower widths reduce the light passing through the cell but give quicker diffusive mixing times. The total time for full color development is a function of the time taken to achieve diffusive mixing, and the reaction kinetics. Previous work [62] suggested that about 500 μm width should be best.

Design of the chip used for the experiments with 500 μm cell width is shown in Figure 5.2. The chip was designed and produced by Alexander Beaton. The middle cell is 500 μm wide and this cell was used for measurements. In Figure 5.2 round features at the end of channels represent fluid connector inlets/outlets, small rectangles to the right photodiodes, and to the left of the measurement cell are LEDs.

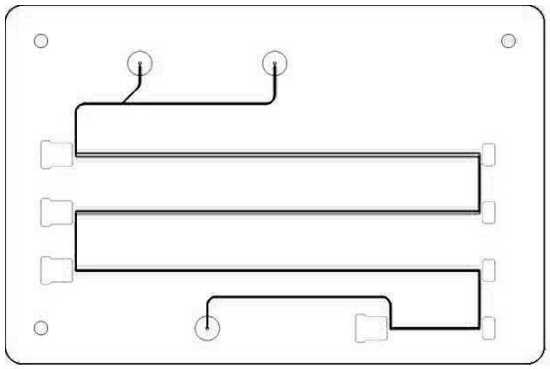

Figure 5.2: Test chip design with measurement cell 500 μm wide.

The chip used for the experiments with a 600 μm cell width is shown in Figure 4.3 in subsection 4.2.1 as the other channels on the chip in Figure 5.2 were not functioning.

The response from the MQ water diffused with MQ-red dye solution on chip with the 500 μm cell is shown in Figure 5.3.

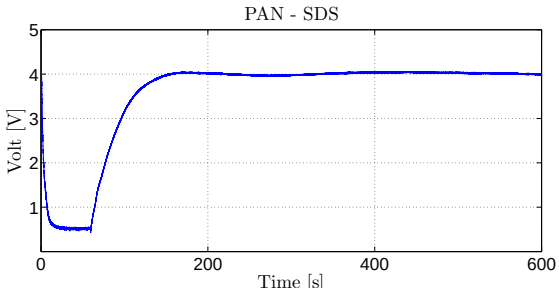

Figure 5.3: Test chip - measurement cell 500 μm wide. MQ water diffused with MQ-red dye solution.

The response from the MQ water diffused with MQ-red dye solution on chip with the measurements cell 600 μm wide is shown in Figure 5.4.

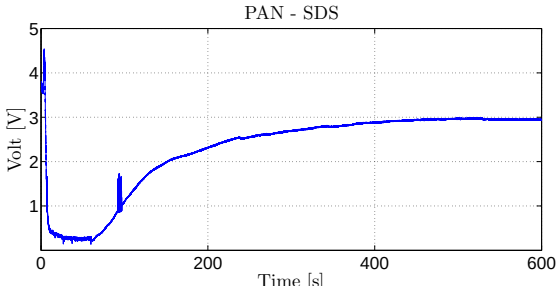

Figure 5.4: Test chip - measurement cell 600 μm wide. MQ water diffused with MQ-red dye solution.

High absorption at first 10 - 60 seconds which then decreases to a steady state value (Figure 5.3 and 5.4) was the time when the sequence was started and the solutions were flowing through the chip. The end of the steady response and the beginning of the rise of the signal is when the flow was stopped and the solutions started diffusing in the measurement cell. Higher light output for MQ and MQ-dye solution in 500 μm channel was the result of the LED current set up and the way the chip was produced.

The response recorded after the diffusion time from both chips is presented in Table 5.1.

Table 5.1: The response from the MQ water diffused with MQ-red dye solution on chip with the measurements cell 600 μm and 500 μm wide

Results from tests on chip with 500 μm and 600 μm cell width. Response recorded after diffusion time.				
Time [seconds]	500 μm		600 μm	
	MQ	MQ-dye	MQ	MQ-dye
500	-	-	3.333 V	2.964 V
200	4.255 V	4.003 V	-	-

The results clearly show that when the solutions diffuse and react in the 500 μm cell a shorter diffusion time is required for the solution to mix in the measurement cell and the signal to stabilise (about 200 seconds for 500 μm cell and about 500 seconds for 600 μm cell).

As a result of these experiments the chip with the 500 μm width measurement cell was chosen for the final design of the manganese analyser. Smaller width of the channel could be tested for future systems. With this stage completed, the next steps were planning the operation of the system and the design of the microfluidic chip for manganese determinations with the pre-concentration column.

5.2.2 System design

In the initial plan the idea was to build an in-situ system in which the chip was directly coupled to a Sensors Group designed piston pump. Therefore a diagram was created to show how the solutions are directed in the system, the valves used to control the flow of solutions, and pumps to withdraw and inject each solution through the microfluidic unit (Figure 5.5).

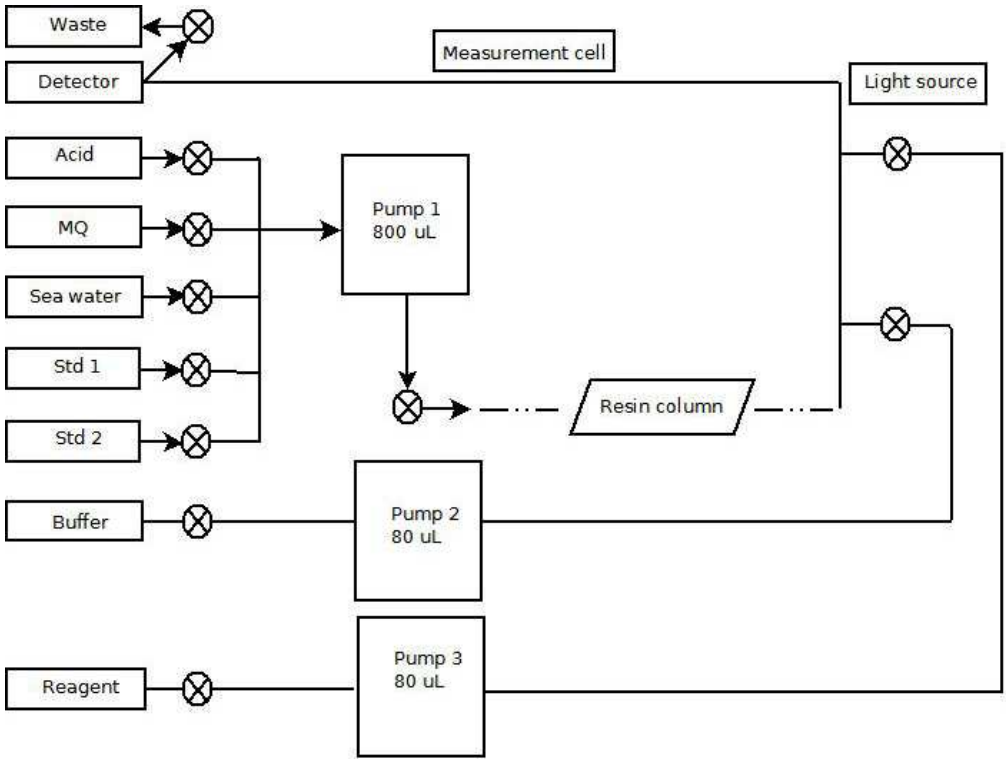

Figure 5.5: Diagram showing the flow of solutions in the system with pumps and valves (crosses in circles).

After the plan of the system was created, I then designed a suitable microfluidic chip, shown in Figure 5.6. The design of the chip incorporates the space to implement the custom designed pump, in the middle of the unit. The curved top and bottom edges were to allow easy installation in a pressure case needed for in-situ deployment.

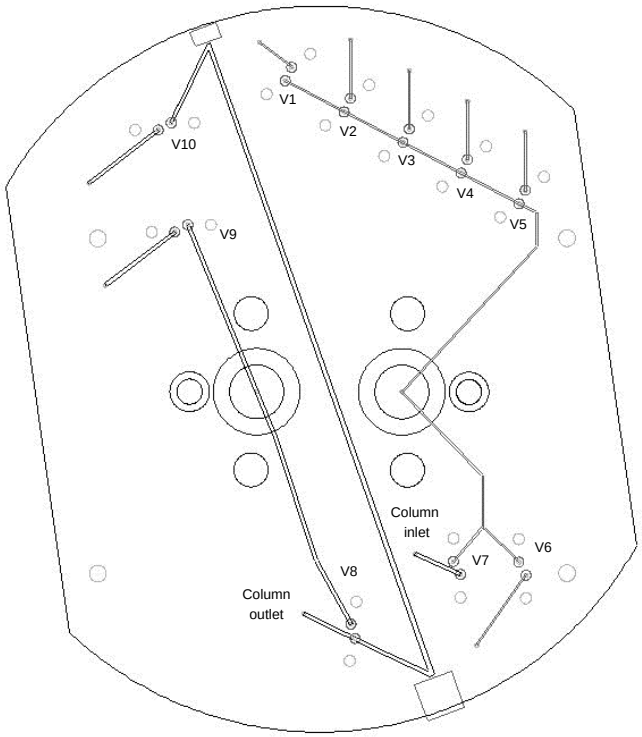

Figure 5.6: The first design for on bench chip with the custom designed pump implemented on the chip. Top to bottom distance was around 120 mm.

In this proposed design the sequence for valve and pump operation for the system with built in pump was prepared and the steps of analysis were planned. In this sequence the solutions are withdrawn from the containers and injected into the microfluidic unit. The pump consists of two 800 μL volume barrels and two 80 μL volume barrels. The big barrels may be used to pump MQ, standards, sample and acid solution and the small barrel to pump the reagent. The sample and the reagent are introduced to the measurement cell and the data are recorded during the diffusion time.

However, there were important reasons why it was not possible to build the in-situ system with built in pumps at this stage of the project. There was not enough time to build the in-situ system, within the short project time frame, as the building of such system requires work from many members of the Sensors Group in addition to my input. The decision was made to start with the on-bench version of the system using bench top

Harvard syringe pumps to pump the solutions through the system, instead of the custom made in situ pump. The system was operated with a LabView program, rather than the custom made software used in earlier devices [62]. The chip design and production process is detailed in Chapters 2 and above. Initial designs used a serpentine mixer in addition to in cell diffusion, but these were not used because of problems with flushing the mixing unit between samples. My final design of the chip for on-bench manganese determination is presented in Figure 5.7. The circular shape was to facilitate manufacture in the Sensors Group by Gregory Slavik.

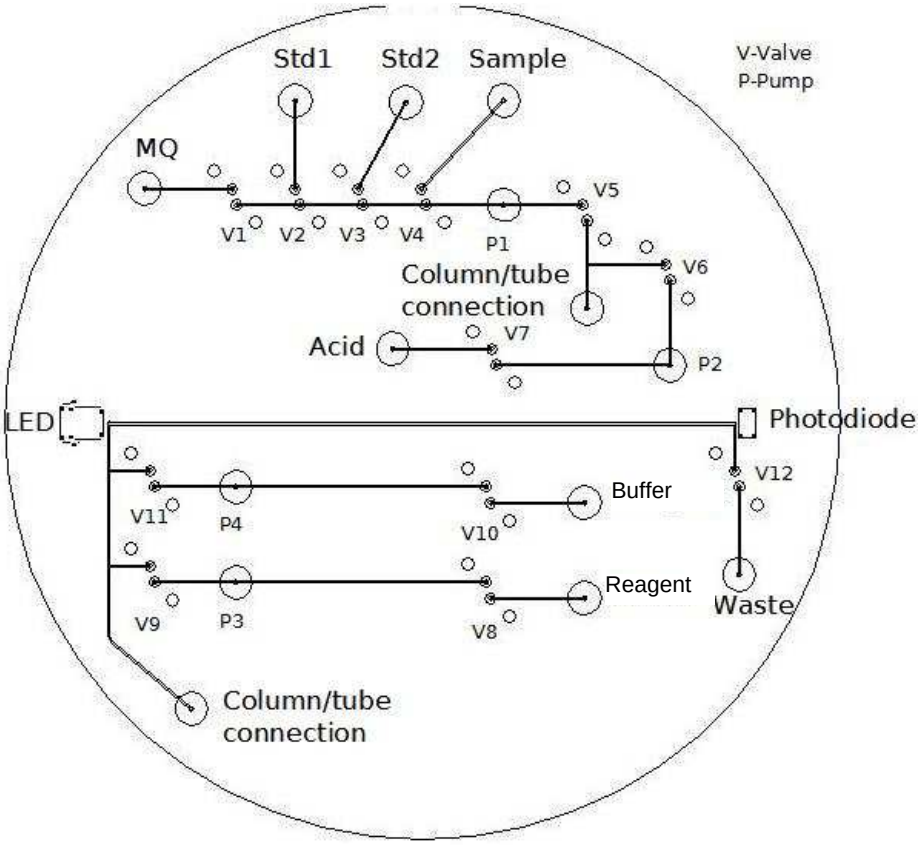

Figure 5.7: Final design for on bench chip for use with syringe pumps. P = Hamilton Syringe pump inlet, V = Lee valves.

In the operation sequence the solutions are withdrawn from the blood-bag containers and injected to the microfluidic unit (with appropriate valves opened or closed). The four syringe Hamilton pumps are used to withdraw and inject the solutions. Pump 1 is used to pump MQ, standards and sample with volume of the syringe 1000 μL. Pump

2 is used to pump acid solution with volume of the syringe 500 μL. Pump 3 is used to pump the reagent with volume of the syringe 250 μL. Pump 4 is used to pump the buffer solution with volume of the syringe 250 μL.

In the first step of the sequence valve 1 is open and MQ is withdrawn into syringe 1, then valve 1 is closed and valves 5 and 12 opened and MQ is injected into the system to clean the channels. This stage is repeated multiple times. The next stage is to withdraw the solutions (syringe 1), standard or sample (standard 1 - valve 2 open, standard 2 - valve 3 open, sample - valve 4 open) and then to inject solution into the system (valves 5 and 12 open) and through the pre-concentration column and the measurement cell to the waste outlet (valve 12). In the next stage the acid solution is withdrawn into syringe 2 with valve 7 open, the reagent is withdrawn into syringe 3 with valve 8 open, and the buffer solution is withdrawn into syringe 4 with valve 10 open. The acid, reagent and the buffer are injected into the system at the same time (valve 6, 9 and 11 open, syringes 2, 3 and 4 pumped). The sample, reagent and buffer are introduced to the measurement cell at ratio of 10:1:1 v/v/v with the flow stopped and the data are recorded during the diffusion and reaction time.

The internal volumes of the channels were calculated before the sequence of operation was finally decided upon (Table 5.2).

Table 5.2: Internal volumes of the channels

Channels - internal volumes			
Channel between start and end point	Length $[mm]$	Width and depth of the channel $[\mu m]$	Volume $[\mu L]$
measurement cell	100.0	500/300	15
from column outlet to start of measurement cell	50.3	300/300	5
between acid valve (V6) and column inlet	19.5	300/300	2
between buffer pump outlet (P3) and measurement cell	28.0	300/300	3
between acid valve (V6) and start of measurement cell	31.4	300	3
between acid valve (V6) and end of measurement cell	46.4	300	4
internal column (resin)	-	-	20
between the column outlet and the chip	-	-	4.7
between the column inlet and the chip	-	-	4.7

The sequence for valve and pump operation for the on-bench system is presented in Table 5.3.

Table 5.3: Sequence of operation for the system, with final volumes used

On bench system. Syringe pumps. Operation sequence. Solutions, pumps and valves.							
Solution	Valve open (pump withdrawing)	Valve open (pump injecting)	Pump	Withdrawing (W) Injecting (I)	Volume $[\mu L]$ (Example)	Flow $[\mu L/\text{min}]$ (Example)	Comments
MQ	V 1	-	P 1	W	1000	600	-
	-	V 5, V 12	P 1	I	1000	600	-
Standard 1 (Standard 2)	V 2 (V 3) (V 4)	-	P 1	W	1000	600	-
(Sample)	-	V 5, V 12	P1	I	1000	200	-
Acid	V 7		P 2		300	600	
Buffer	V 10	-	P 4	W	30	60	-
Reagent	V 8		P 3		30	60	
Acid			P 2		300	600	
Buffer	-	V 6, V 9, V 11, V 12	P 4	I	30	60	-
Reagent			P 3		30	60	
-	-	-	-	-	-	-	Diffusion
MQ	V 1	-	P 1	W	1000	600	-
	-	V 5, V 12	P 1	I	1000	600	-

With the chip produced and the set-up of the system for on-bench manganese determination completed, the next stage was to test the performance of the system by making measurements with the Mn-PAN chemistry.

5.3 System performance

The initial experiments were performed with no pre-concentration to check on response and color formation; the resin column was replaced by a plastic tube.

The manganese standards were prepared with 0.02 M HCl and mixed with sample buffer and the reagent solution (see Chapter 4 for preparation details). A premixed solution of manganese standard, buffer and reagent in the ratio 10:1:1 v/v/v was introduced into the measurement cell. Data were collected for 500 nM and 1000 nM manganese standards. The results in Figure 5.8 show responses corresponding to the manganese concentrations analysed. The values recorded showed significant variability (data in Appendix B Table B1).

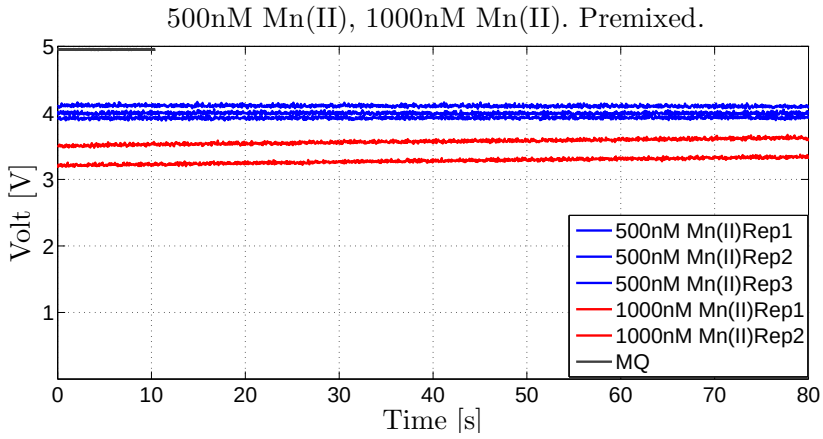

Figure 5.8: Mn standard measurements (500 nM and 1000 nM) with PAN-SDS. Solutions premixed before injecting in to the chip.

The calibration curve was created for on-chip measurements with no pre-concentration, see Figure 5.16 on page 123 (slope value 0.1386). For information the calibration data were used to convert the drift voltage values presented on Figure 5.8 into Mn(II) concentrations (Figure 5.9).

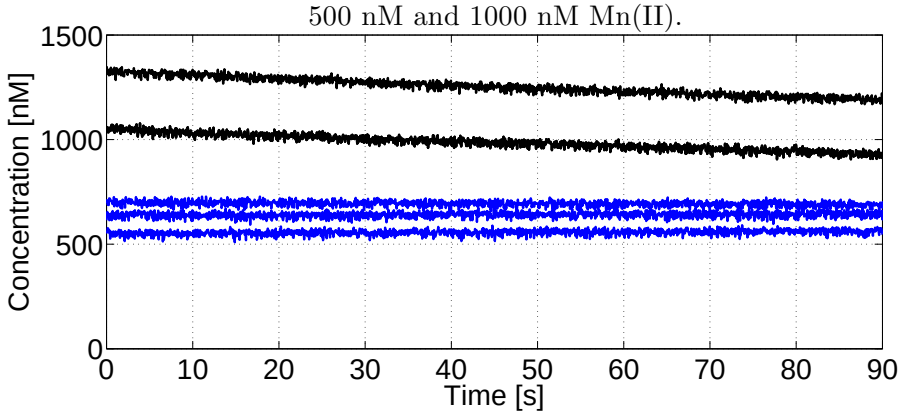

Figure 5.9: Mn standard measurements (500 nM and 1000 nM) with PAN-SDS. Solutions premixed before injecting in to the chip. Voltage values converted to nM concentrations.

The next stage was to test if similar results were obtained when the solutions where introduced to the microfluidic unit at the designed ratio and the diffusion occurred in the measurement cell. The manganese standard samples were prepared and introduced to the chip to mix with the sample buffer and the reagent solution. The data were collected over the diffusion time, which was 480 seconds. The measurement was repeated four times and the results obtained are shown in Figure 5.10 (data in Appendix B Table B2).

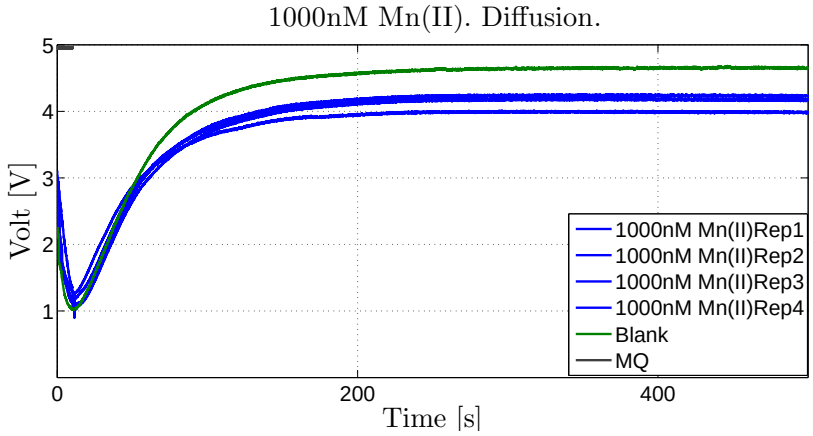

Figure 5.10: Mn standards measurements PAN-SDS. Solutions diffused in the measurement cell of the the chip. Blank and 1000 nM. Blank – 0.02 M HCl buffered solution and PAN reagent mixture.

The experiment showed that the results were comparable with values measured for

the premixed solutions with still significant variability. Further experiments with other standards all showed significant variability in the standards run.

The tests performed on the system also demonstrated that there was an interference coming from the system electronics. There was a signal change when the valves used in the system were operated (Figure 5.11).

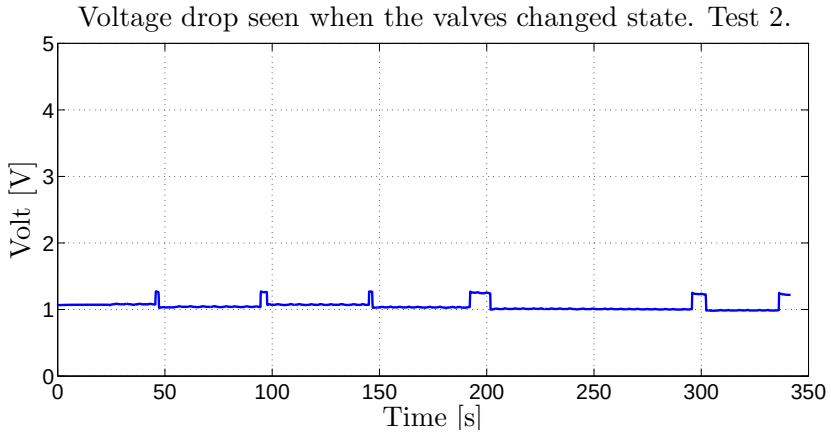

Figure 5.11: MQ-dye measurement. Response recorded when valves turn on/off.

The valves and the LED were powered with a power supply and connected through 2 valve driver boards and 1 constant current LED board. The LED was driven by the constant current supply, which gave good stability as long as the power supply remained stable. The power supply for the LED drive and the valves was shared, so the very small voltage drop seen when the valves changed state changed the supply voltage enough on the LED that the output changed noticeably to the TAOS. The LED was connected to a separate power supply and the problem was solved and there was no signal change with the valves operation.

After the initial measurements performed using Chip 1, the photodiode in the chip was broken and the chip could not be used for further experiments and a new microfluidic unit was prepared.

With the new unit prepared and installed in the on-bench system, the next stage was to test the performance and record the voltage response for MQ, blank and manganese standard solutions. The manganese standards were prepared in 0.02 M HCl (see Chapter 2) and introduced to the chip to mix with the sample buffer and the reagent solution.

The blank measurements were repeated 4 times and 500 nM manganese standard

measurements were repeated 3 times. The results are presented in Figure 5.12 (data in Appendix B Table B3).

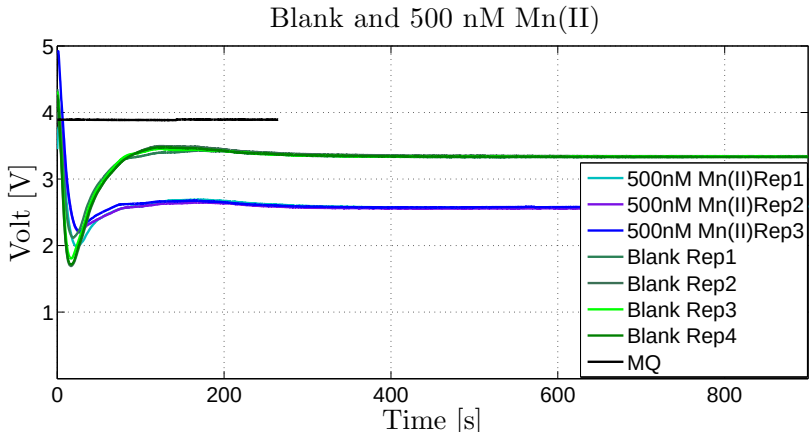

Figure 5.12: Manganese standard measurements PAN-SDS. Solutions diffused in the measurement cell of the the chip. Blank and 500 nM. Blank – 0.02 M HCl buffered solution and PAN reagent mixture.

The LED currents were adjusted prior to, and then kept constant throughout the experiments. The blank measurements were performed and repeated and the relative standard deviation between the measurements was calculated to be 1.99 % The results are presented in Figure 5.13 (Table B4, Appendix B).

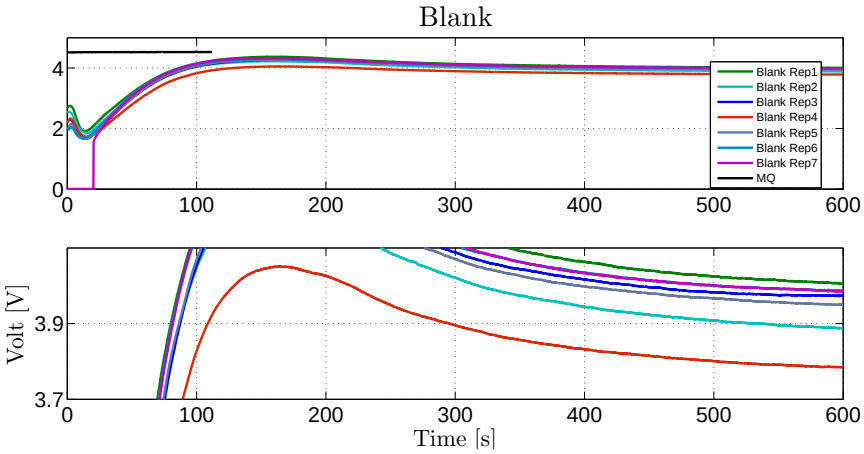

Figure 5.13: Blank measurements PAN-SDS. Solutions diffused in the measurement cell of the chip. Blank – 0.02 M HCl buffered solution and PAN reagent mixture.

The subsequent experiments included measurements of manganese standards, at 500

nM (RSD = 3.74 % n=6) and 1000 nM (RSD = 7.23 % n=8). The experiments show there is still significant variability with significant outliers (Tables 5.4 and 5.5, Figures 5.14 and 5.15).

Table 5.4: Mn standards measurements PAN-SDS. Solutions diffused in the measurement cell of the the chip. 500 nM. Figure 5.14.

On-chip measurements PAN-SDS				
Sample	Rep	Volt	STD DEV	%RSD
MQ	1	4.302	-	-
500 [nM] Mn(II)	1	3.196		
	2	3.132	0.12	3.75
	3	3.310		
	4	0.005	(not included in calc.)	
	5	3.398		
	6	3.464		
	7	3.273		
	8	0.004	(not included in calc.)	

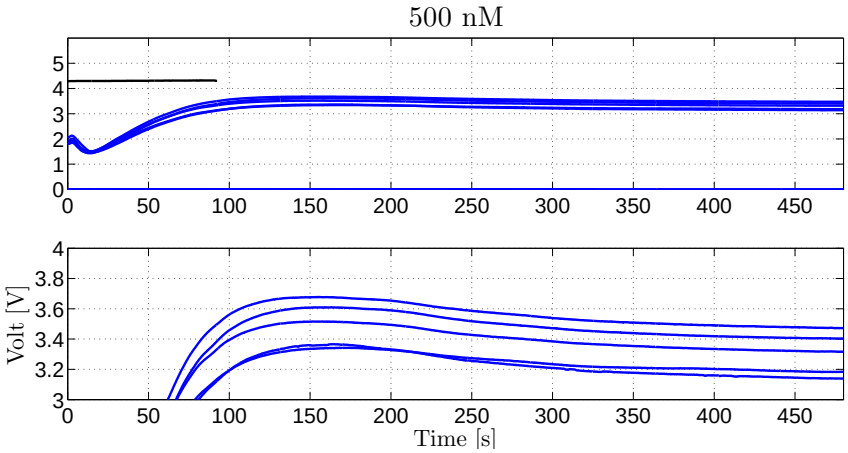

Figure 5.14: Mn standards measurements PAN-SDS. Solutions diffused in the measurement cell of the the chip. 500 nM Replicates 1-7.

Table 5.5: Mn standards measurements PAN-SDS. Solutions diffused in the measurement cell of the the chip. 1000 nM. Figure 5.15.

On-chip measurements PAN-SDS				
Sample	Rep	Volt	STD DEV	%RSD
MQ	1	4.281	-	-
	1	3.009		
	2	2.842		
	3	3.000		
1000	4	2.820		
[nM]	5	2.914	0.17	5.53
Mn(II)	6	3.187		
	7	3.308		
	8	3.046		

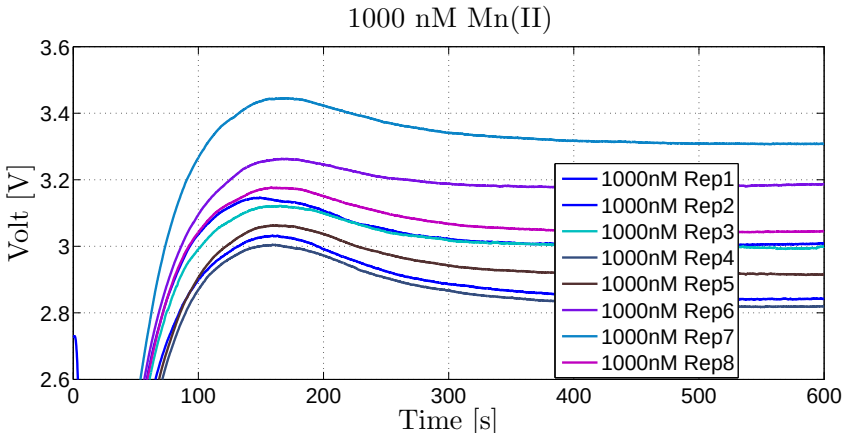

Figure 5.15: Mn standard measurements PAN-SDS. Solutions diffused in the measurement cell of the the chip. 1000 nM Replicates 1-8. Expanded y axis.

The results from measurements of manganese standards performed on the system with no pre-concentration were used to construct the calibration curve and calculate the LOD. The data are shown in Table 5.6 and Figure 5.16.

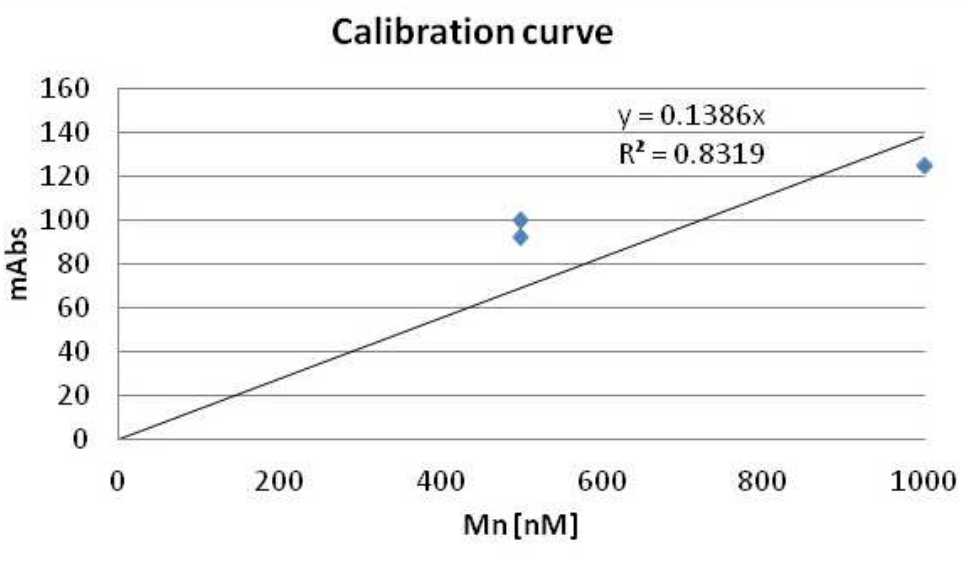

Figure 5.16: Calibration curve. No pre-concentration. Blank – MQ.

Table 5.6: On chip experiments. No pre-concentration.

Results from test on system with no pre-concentration On chip measurements						
Sample	Rep	mV	T	mAbs	Slope	R-squared
MQ	-	4954	-	-	-	-
Blank	1	4558	0.920	36.182		
	2	4568	0.922	35.230		
	3	4565	0.921	35.515		
	4	4528	0.914	39.050		
500 nM Mn(II)	1	4007	0.809	55.622	0.1386	0.832
	2	3938	0.795	63.153		
1000 nM Mn(II)	1	3717	0.750	88.311		
	2	3707	0.748	89.452		

The blank measurements were used to calculate the RSD at 4.79 % and the LOD which was about 38 nM (3SD).

Calculations were performed to predict how the pre-concentration factor would theoretically change with the volume of the sample and the resulting possible changes for the LOD. The predicted LOD value was calculated by dividing the LOD reported for the system (38 nM) by the pre-concentration factor (Table 5.7).

Table 5.7: Relation between the volume of the sample and the pre-concentration factor and the resulting theoretical LOD

Theoretical LOD calculated using the pre-concentration factor			
Sample volume [μL]	Acid volume [μL]	Pre-concentration factor	LOD [nM]
1000	300	3.33	11.40
	150	6.67	5.70
	50	20.00	1.90
2000	300	6.67	5.70
	150	13.33	2.85
	50	40.00	0.95
3000	300	10.00	3.80
	150	20.00	1.90
	50	60.00	0.63
5000	300	16.67	2.28
	150	33.33	1.14
	50	100.00	0.38
6000	300	20.00	1.90
	150	40.00	0.95
	50	120.00	0.32

When the volume of the eluting acid would be 50 μL and the sample volume 6000 μL the pre-concentration factor calculated was 120 with calculated theoretical LOD of 0.32 nM.

The data collected during the experiments assessing the performance of the system (subsection 5.3 System performance) were used to quantify the variability between the results in terms of manganese concentration using the calibration curve (data in Table 5.6). The variability reported for data sets was calculated between the highest and the lowest Volt value. The calculated difference would correspond to: in Figure 5.8 – about 190 nM for 1000 nM standard (n=2) with %RSD 12.61; in Figure 5.10 – about 280 nM for 1000 nM standard (n=4) with %RSD 30.34; in Figure 5.12 – about 60 nM for 500 nM standard (n=3) with %RSD 4.16; in Figure 5.14 – about 315 nM for 500 nM standard (n=6) with %RSD 32.98; in Figure 5.15 – about 500 nM for 1000 nM standard (n=7) with %RSD 29.86.

Milani et al. [62] reports first autonomous analyser for the routine in-situ determination of dissolved Fe(II) and manganese in aquatic environments. The sensor uses microfluidic Lab-On-A-Chip technology and mixes reagents and samples in-line by diffusion. In the described system manganese can be measured with a frequency of up to 6 samples per hour with limits of detection of 27 nM for Fe(II), 2.1 % precision (n=20) and 28 nM for manganese, 2.4 % precision (n=19).

The spectrophotometric method used by Milani et al. [62] was modified with the use of different surfactant. The theoretical LOD reported for the system used with modified method is 38 nM with no pre-concentration. However due to the system error / variability between the results the current system does not allow for accurate assessment of values of LOD of the system.

The next stage was to perform tests on the pumping system. The following experiments were designed to test the system without the use of the chemical method, to exclude this variable and not waste chemical reagents, by using MQ water coloured with red food dye solution.

In the initial experiment the MQ-dye solution was pumped using pump 4 (the pump used in the analyser to pump buffer solution). The measurements were repeated 11 times. The results are shown in Figure 5.17 and the RSD calculated was 1.58 % (Table B5, Appendix B);(additional data in Tables B6 - B9, Appendix B).

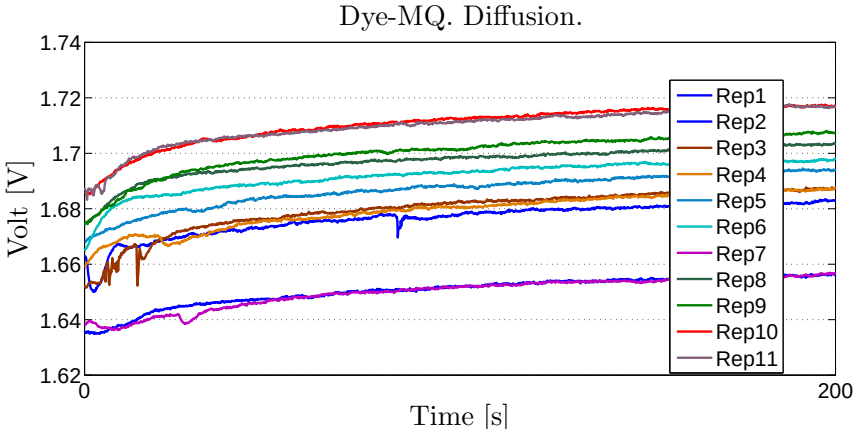

Figure 5.17: Dye-MQ measurements. Rep 1-11. Expanded y axis.

In subsequent experiments the MQ-dye solution was pumped through the system using pumps 2, 3 and 4 separately and simultaneously and each pump was set to a flow

rate of 60 $\mu L/min$. The results are shown in Table 5.8.

Table 5.8: Pump tests using dye solution. Pump number and the solutions pumped in the system for manganese determination are listed for information: pump 1 – MQ, standatd, sample; pump 2 – acid solution; pump 3 – reagent; pump 4 – buffer.

Pump tests. Dye-MQ.

Pump	Flow $\mu L/min$	Rep	% RSD
2	60	n=11	1.58
3		n=4	0.75
4		n=5	1.24
2,3,4		n=6	4.14

The experiments using the MQ-dye solution demonstrated the variability between the pumps. For example the variability (calculated between the highest and the lowest Volt value in terms of manganese concentration would correspond to value about 250 nM (for samples between 500 nM and 1000 nM (value calculated using data from Table 5.6, by taking the difference (0.3 V), and calculating corresponding manganese concentration using the calibration curve.) Whilst RSDs overall look good, the problem of outliers is still there suggesting potentially a problem with the pumps.

5.4 Pump system tests

To test the performance of the Hamilton syringe pumps, accuracy was tested by pumping specific volumes of solution and weighing the mass pumped. MQ water was pumped through the system with pumps 2,3 and 4 separately and then simultaneously (60 or 600 $\mu L/min$) and the water was collected when exiting the system through the waste line. The weight measurements were made and the results are shown in Table 5.9 to 5.15. An assumed density of water of 1.000 g/mL was used in the calculations. The density of water at lab temperature (20 °C) is 0.99883 g/mL, and so any variation in error caused by density difference would be less than 0.12 % of the volume.

In the experiment where only pump 2 was tested the error calculated was between 1.1 % and 2.1 % (n=3). The results are summarised in Table 5.9.

Table 5.9: Pump test. Pump 2 used at flow rate 600 $\mu L/min$ for 60 seconds.

Pump Test Experiment 1				
Pump 2	Flow rate 600 $\mu L/min$	Total Volume 600 μL	% Error	Volume Error μL
Rep	Mass [g]	mass % of volume pumped		
1	0.5924	98.7	1.3	7.8
2	0.5933	98.9	1.1	6.6
3	0.5876	97.9	2.1	12.6

In the experiments where only pump 3 was tested the calculated error was 2.2 % and 2.5 % (n=2). The results are summarised in Table 5.10.

Table 5.10: Pump test. Pump 3 used at flow rate 60 $\mu L/min$ for 200 seconds.

Pump Test Experiment 2				
Pump 3	Flow rate 60 $\mu L/min$	Total Volume 200 μL	% Error	Volume Error μL
Rep	Mass [g]	mass % of volume pumped		
1	0.1955	97.8	2.2	4.4
2	0.1950	97.5	2.5	5.0

In the experiments where only pump 4 was tested the calculated error was 6.2 % and 1.3 % (n=2). The results are summarised in Table 5.11.

Table 5.11: Pump test. Pump 4 used at flow rate 60 $\mu L/min$ for 200 seconds.

Pump Test Experiment 3				
Pump	Flow rate	Total volume		
Pump 4	$60\mu L/min$	$200\mu L$		
Rep	Mass [g]	Mass % of volume pumped	% Error	Volume Error [μL]
1	0.1875	93.8	6.2	12.4
2	0.1973	98.7	1.3	2.6

The experiment was performed where pumps 2 and 3 were used. Pump 2 with flow 600 $\mu L/min$ and pump 3 with flow 60 $\mu L/min$ to obtain a ratio 10:1 v/v, as used in the analyser system. The calculated error was between 1.4 % and 30.6 % (n=5), which corresponds to volume variation between 9.2 μL and 202.0 μL (total volume 660 μL. The results are summarised in Table 5.12.

Table 5.12: Pump test. Pump 2, flow 600 $\mu L/min$, pump 3, flow 60 $\mu L/min$ used simultaneously for 60 seconds.

Pump Test Experiment 4				
Pump	Flow rate	Total volume		
Pump 2 Pump 3	600 μL/min 60 μL/min	660 μL		
Rep	Mass [g]	Mass % of volume pumped	% Error	Volume Error [μL]
1	0.6511	98.6	1.4	9.2
2	0.6343	96.1	3.9	25.7
3	0.5921	89.7	10.3	68.0
4	0.4583	69.4	30.6	202.0
5	0.6501	98.5	1.5	9.9

The experiment was performed where pumps 2 and 4 were used. Pump 2 with flow 600 $\mu L/min$ and pump 4 with flow 60 $\mu L/min$ to obtain ratio 10:1 v/v, as used in the analyser system. The calculated error was between 1.3 % and 16.9 % (n=5), which corresponds to volumes between 9.9 μL and 111.5 μL (total volume 660 μL. The results

are summarised in Table 5.13.

Table 5.13: Pump test. Pump 2, flow 600 $\mu L/min$, pump 4, flow 60 $\mu L/min$ used simultaneously for 60 seconds.

Pump Test Experiment 5				
Pump	Flow rate	Total volume		
Pump 2 Pump 4	600 $\mu L/min$ 60 $\mu L/min$	660 μL		
Rep	Mass [g]	Mass % of volume pumped	% Error	Volume Error [μL]
1	0.6414	97.2	2.8	18.5
2	0.6023	91.3	8.7	57.4
3	0.6171	93.5	6.5	42.9
4	0.5486	83.1	16.9	111.5
5	0.6511	98.7	1.3	9.9

In the following experiment pump 2 was set to 600 $\mu L/min$ and pump 3 and 4 to 60 $\mu L/min$ to obtain the ratio 10:1:1 v/v/v as it is used in manganese determination experiments with the PAN method. The data collected show the error was between 1.2 % and 3.3 % (n=5) which corresponds to volumes between 8.6 μL and 23.8 μL for a total volume of 720 μL. The results are summarised in Table 5.14.

Table 5.14: Pump test. Pump 2, flow 600 $\mu L/min$, pump 3 and 4, flow 60 $\mu L/min$ used simultaneously for 60 seconds.

Pump Test Experiment 6				
Pump	Flow rate	Total volume		
Pump 2	600 $\mu L/min$			
Pump 3	60 $\mu L/min$	720 μL		
Pump 4	60 $\mu L/min$			
Rep	Mass [g]	Mass % of volume pumped	% Error	Volume Error [μL]
1	0.6966	96.7	3.3	23.8
2	0.7051	97.9	2.1	15.1
3	0.7004	97.3	2.7	19.4
4	0.7112	98.8	1.2	8.6
5	0.7094	98.5	1.5	10.8

The experiment was performed with all 3 pumps 2, 3 and 4 were used with the same flow set to 60 $\mu L/min$. The data collected show the error was between 1.2 % and 3.5 % (n=4) which corresponds to volumes between 7.2 μL and 21.0 μL in a total volume of 600 μL. Data are summarised in Table 5.15.

Table 5.15: Pump test. Pump 2, 3 and 4 used simultaneously at flow rate 60 $\mu L/min$ for 200 seconds.

Pump Test Experiment 7				
Pump	Flow rate	Total volume		
Pump 2	60 $\mu L/min$			
Pump 3	60 $\mu L/min$	600 μL		
Pump 4	60 $\mu L/min$			
Rep	Mass [g]	Mass % of volume pumped	% Error	Volume Error [μL]
1	0.5885	98.1	1.9	11.4
2	0.5790	96.5	3.5	21.0
3	0.5930	98.8	1.2	7.2
4	0.5916	98.6	1.4	8.4

The above results show that the error in the system as a result of the pump operation may be as high as 30.6 % and is not reproducible for all pumps used. Errors of this magnitude will affect the results as the ratio of solutions meeting and diffusing in the measurement cell is altered. When the volume ratio of solutions is not consistent, this will also result in the change of the pH of the mixed solution.

The biggest effect on the pH of the mixture is the volume of the buffer solution. Therefore the experiment was performed to determine how the change in the pH of the sample - buffer - reagent mix is affected by the change in the buffer volume.

The experiments were performed where the volume of the buffer in the sample - buffer - reagent mix was altered, with smaller volume of the buffer solution added to each sample and pH of the resulting sample-mix recorded. The % error was calculated representing the volume of the buffer. The results are summarised in Table 5.16 and 5.17.

Table 5.16: Boric acid buffer volume error and its impact on pH change. Boric acid dissolved in 0.4 M NaOH.

Buffer Volume Error - pH change. Sample buffer prepared in 0.4 M NaOH.				
Eluting acid Volume [μL]	Sample Buffer Volume [μL]	Buffer deducted Volume [μL]	Buffer deducted [%]	Acid and Buffer mix pH
5000	500	0.0	0.0	9.5
5000	495	5.0	1.0	6.0

Table 5.17: Boric acid buffer volume error and its impact on pH change. Boric acid dissolved in 0.5 M NaOH

Buffer Volume Error - pH change. Sample buffer prepared in 0.5 M NaOH.				
Eluting acid Volume [μL]	Sample Buffer Volume [μL]	Buffer deducted Volume [μL]	Buffer deducted [%]	Acid and Buffer mix pH
5000	500	0.0	0.0	11.0
5000	495	5.0	1	10.0
5000	490	10.0	2	10.0
5000	480	20.0	4	10.0
5000	470	30.0	6	9.5
5000	460	40.0	8	9.0
5000	450	50.0	10	6.5
5000	400	100.0	20	5.0

The results show that a 1.0 % error in the volume of the buffer in the mix results in a pH change from 9.5 to 6.0 (Table 5.16). At pH 6 colour development will be impeded with the PAN method (see Chapter 2). The buffer solution was prepared where boric acid was dissolved with 0.5 M NaOH (buffer B), to replace the boric acid buffer prepared with 0.4 M NaOH (buffer A) used in previous experiments to achieve higher pH of the sample - buffer - reagent mix. The pH measurements were repeated with the buffer B added to the sample and reagent mix. The results demonstrated that 6 to 8 % error in the volume of the buffer added still allowed the pH to stay above or equal to 9.0 (Table

5.17). As pH 9.0 - 9.5 is required for PAN method, the buffer B was used from this point on in future experiments. This approach allowed continuation of the experiments with the existing pump performance, despite the errors in volumes.

The response from the blank solution was measured on the system and repeated 5 times. The RSD for the blank sample was calculated to be 0.75 % (Figure 5.18, Table B10 in Appendix B).

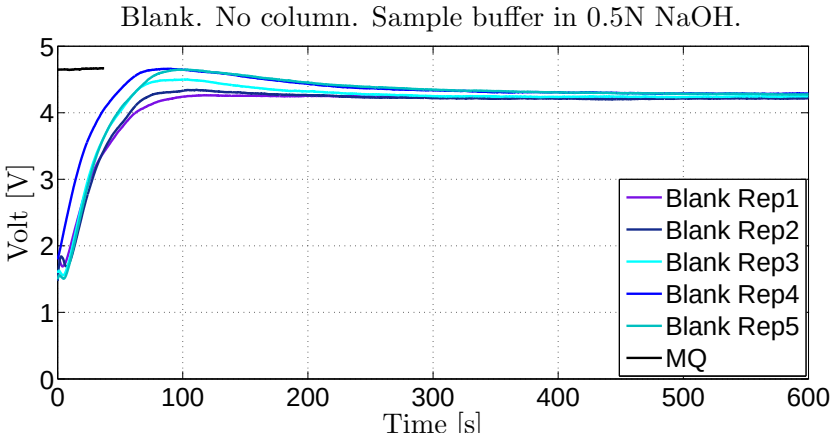

Figure 5.18: Blank measurements. Solutions diffused in the measurement cell of the chip. Boric acid buffer in 0.5 M NaOH. Replicates 1-5.

The measurement of a 2000 nM standard (n=6) gave a RSD of 15.93 % Results are presented in Figure 5.19 (Table B11, Appendix B).

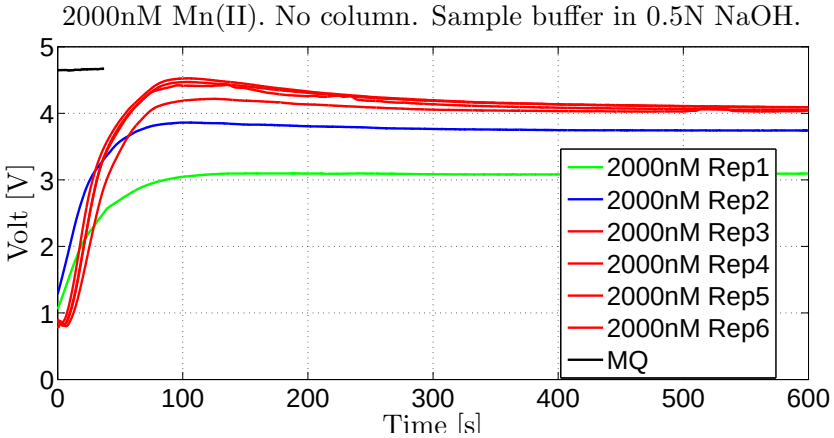

Figure 5.19: Manganese standards measurements. 2000 nM. Solutions diffused in the measurement cell of the chip. Boric acid buffer in 0.5 M NaOH. Replicates 1-6.

This experiment demonstrated that value measured for the 2000 nM standard recorded was below 3 Volt for the first two measurements and higher Volt values were obtained for the following measurements, as high as the blank value. These higher values recorded may be the result of the pump error and lower pH of the mixed solution.

Subsequent experiments using 2000 nM standards showed the same pattern of low Volt values recorded for the first few measurements and higher values for the following measurements. The results show the same pattern for the next three repeated sequences Figure 5.20 to 5.22 (Tables B12 to B14 in Appendix B).

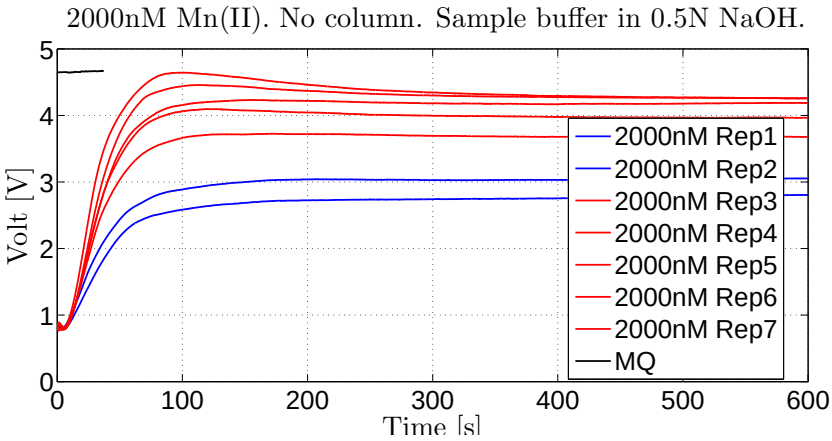

Figure 5.20: Manganese standards measurements. 2000 nM. Solutions diffused in the measurement cell of the chip. Boric acid buffer in 0.5 M NaOH. Replicates 1-7.

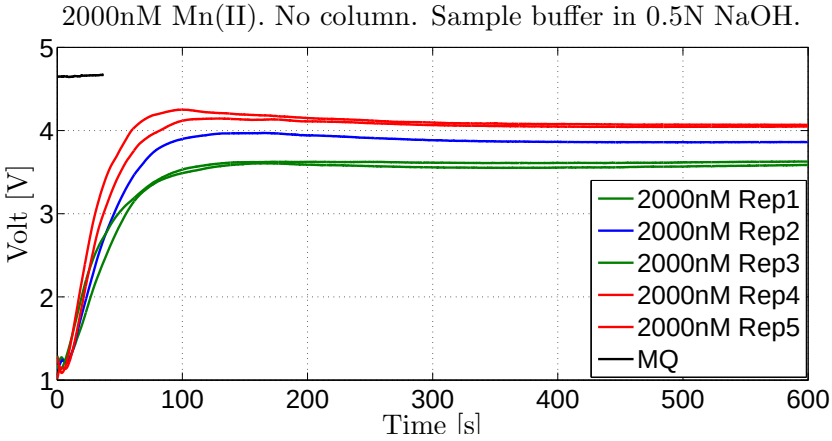

Figure 5.21: Manganese standards measurements. 2000 nM. Solutions diffused in the measurement cell of the chip. Boric acid buffer in 0.5 M NaOH. Replicates 1-5.

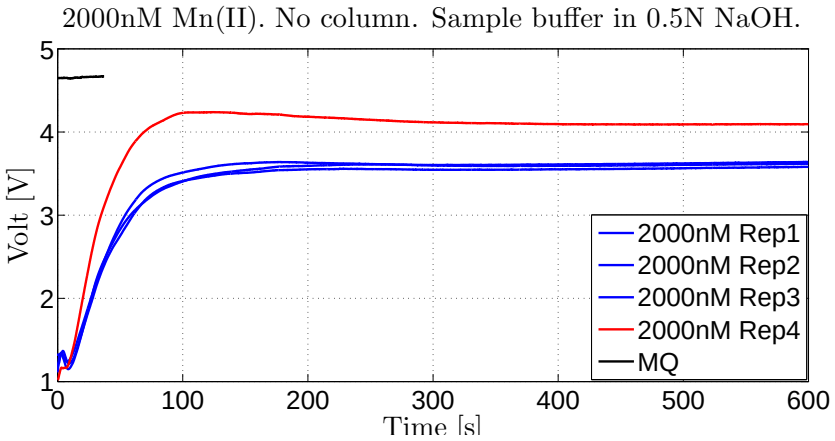

Figure 5.22: Manganese standards measurements. 2000 nM. Solutions diffused in the measurement cell of the chip. Boric acid buffer in 0.5 M NaOH. Replicates 1-4.

Variability between the results collected during the experiments (subsection 5.4 Pump system tests) was quantified in terms of manganese concentration using the calibration curve (data in Table 5.6). The variability reported for data sets was calculated between the highest and the lowest Volt value for 2000 nM standard. The calculated difference would correspond to: in Figure 5.19 – about 875 nM (n=6) with %RSD 194.35; in Figure 5.20 – about 1300 nM (n=7) with %RSD 92.04; in Figure 5.21 – about 395 nM (n=5) with %RSD 111.96; in Figure 5.22 – about 400 nM (n=4) with %RSD 38.06.

The %RSD calculated for the 2000 nM standard measurements for pumped systems was as high as 194.35 % and for manual system %RSD was calculated as 38.06 %.

Thus despite changes to the buffer partially compensating for errors in volumes observed, there was clearly still unacceptable variability in response that seems to be related to the pumps. Reasons for the variability in the volumes dispensed include: 1) air being withdrawn with the sample into the syringe altering the volume of the liquid injected as the results of compression of the gas, 2) piston shaking or leaking, 3) a fault with the pump mechanism.

The LabView program used for the manganese determinations was changed to allow for a pause in the measurement sequence before the solutions are injected into the microfluidic unit. When the sequence was paused, the syringes were filled manually and care was taken to make sure the syringe was fully filled with no air bubbles visibly present. The results are presented in Figure 5.23 (Table B15 in Appendix B).

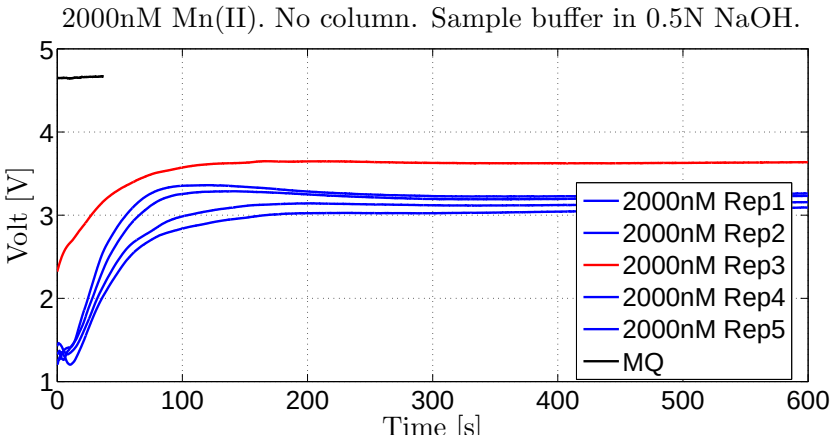

Figure 5.23: Manganese standards measurements. 2000 nM. Withdrawn manually. Solutions diffused in the measurement cell of the chip. Boric acid buffer in 0.5 M NaOH. Replicates 1-5.

The calculated difference between the results (Figure 5.23) quantified in terms of manganese concentration would correspond to about 135 nM; 1165 nM less than highest value reported (Figure 5.20) and 260 nM less than lowest value reported (Figure 5.21).

This approach made a positive difference and the results did not show changes in voltages from lower to higher in repeated measurements of manganese standard as previously observed. Whilst the manual operation seemed to improve the performance of the system, there is the possibility that this was just coincidence. As the result of this experiment the solutions were taken up manually for all subsequent experiments performed on the system. The work was continued with the existing set-up and modifications to minimise errors.

In the future the in-situ analyser will have a custom made pump located directly on the microfluidic chip and this should eliminate the error caused by the pump system used in the current set-up.

5.5 Optimisation of elution

Whilst the elution profile of manganese from the Toyopearl resin had been examined independently (see Chapter 3), it was not clear how incorporating the resin column into the final chip design might impact this elution process.

As the total volume of eluent needed to fully remove the manganese from the resin

(about 500 μL, see Chapter 3) far exceeded the volume in the optical cell (15 μL), it was important to investigate the signal obtained with decreased total eluent volume, to optimise the sensitivity of the system. The profile of the elution showed that most of the manganese (about 80 %) was eluted in about 35 μL volume of eluent (see Chapter 3).

To observe the elution profile when the manganese sample was eluted from the column on chip the LabView sequence was adjusted so that the eluting acid solution was injected in 10 steps (about 480 seconds wait time between each step). The elution injections were optimised by changing the volume of the acid and comparing results. A small volume of acid was used for the elution in each step (see below).

The first experiments were run with 1500 nM and 2500 nM Mn standards, with 1000 μL of standard solution loaded on the column and 900 μL acid volume used for elution, which corresponds to 90 μL of acid in each step (Figure 5.24 and 5.25) (Table B16 and B17 in Appendix B).

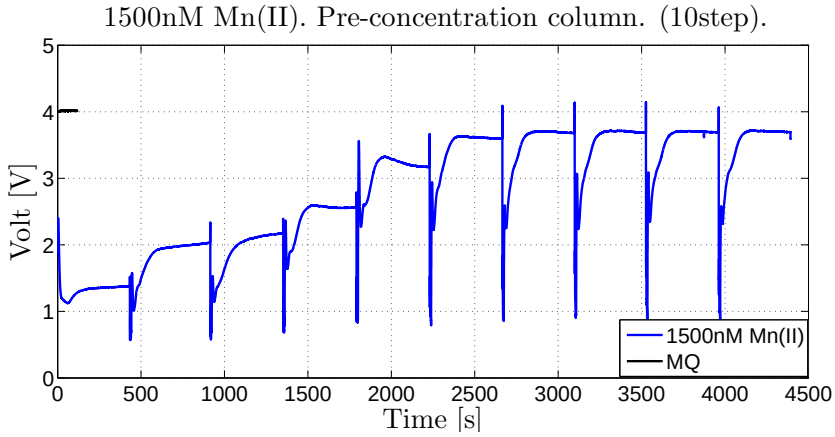

Figure 5.24: Eluted manganese standard measurements. 1500 nM. Solutions diffused in the measurement cell of the chip. Boric acid buffer in 0.5 M NaOH. 10 steps. 900 μL acid volume.

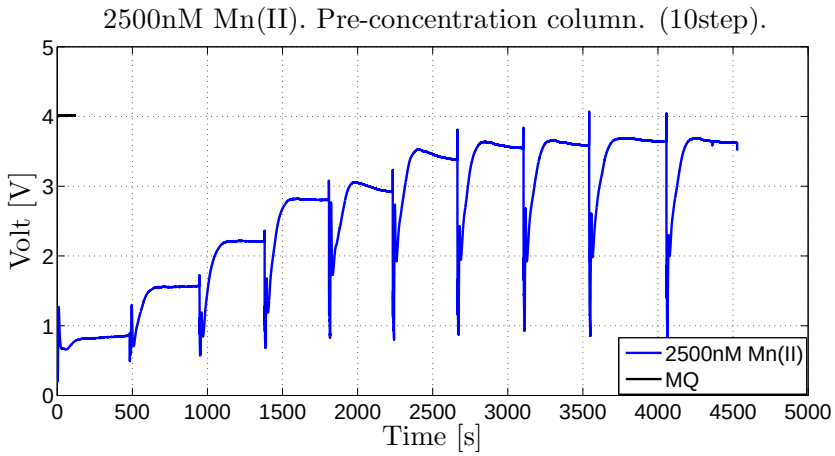

Figure 5.25: Eluted manganese standard measurements. 2500 nM. Solutions diffused in the measurement cell of the chip. Boric acid buffer in 0.5 M NaOH. 10 steps. 900 μL acid volume.

Note that in these figures, voltage (i.e. transmission) is shown and so a low voltage means high manganese concentration.

The results for 1500 nM and 2500 nM manganese standard measurements eluted with 900 μL acid volume are summarised in Table 5.18.

Table 5.18: The results for 1500 nM and 2500 nM manganese standard measurements eluted with 900 μL acid volume.

Eluted manganese standard measurements.				
Total eluting acid volume μL.	Eluting acid volume per step $[\mu L]$	Step	1500 nM Mn(II) [V]	2500 nM Mn(II) [V]
900	90	1	1.399	0.621
		2	1.571	0.813
		3	2.208	1.040
		4	2.803	1.433
		5	2.915	0.834
		6	3.373	1.164
		7	3.544	1.092
		8	3.579	1.681
		9	3.642	2.133
		10	3.619	2.556

The results show the full elution of manganese within around 600 μL of acid solution for 1500 nM standard.

To assess if all manganese was eluted from the column the Volt values recorded for each step were compared to the value obtained for the blank solution (3.752 V). The Volt value recorded close to the blank value suggests that all manganese was eluted for 1500 nM standard.

To observe more accurately the first part of the elution profile, a lower volume of the eluting acid was used, which corresponds to a lower volume of the acid in each step of elution measured.

The measurements of 2500 nM standard were taken with 400 μL eluting acid, which corresponds to 40 μL of acid in each step (Figure 5.26, Table B18 in Appendix B).

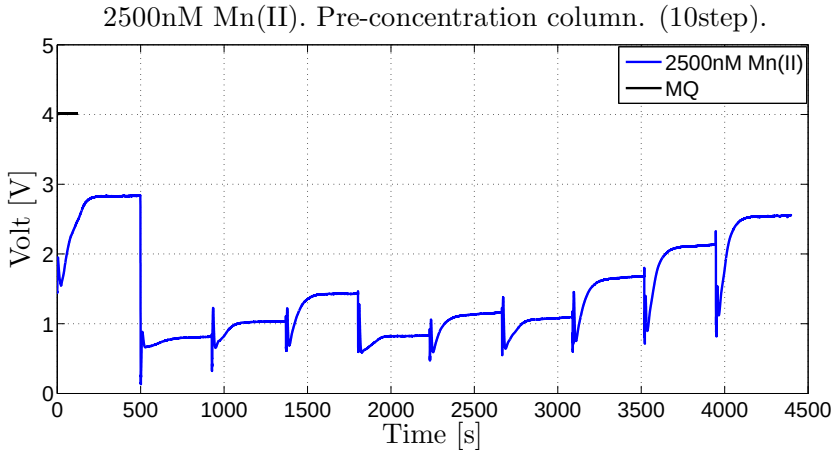

Figure 5.26: Eluted manganese standard measurements. 2500 nM. Solutions diffused in the measurement cell of the chip. Boric acid buffer in 0.5 M NaOH. 10 steps. 400 μL acid volume.

The results for 2500 nM manganese standard measurements eluted with 900 μL and 400 μL acid volume are summarised in Table 5.19.

Table 5.19: The results for 2500 nM manganese standard measurements eluted with 900 μL and 400 μL acid volume.

Eluted manganese standard measurements.							
2500 nM Mn(II)				2500 nM Mn(II)			
Total eluting acid volume [μL]	Eluting acid volume per step [μL]	Step	[V]	Total eluting acid volume [μL]	Eluting acid volume per step [μL]	Step	[V]
900	90	1	0.621	400	40	1	2.837
		2	1.571			2	0.813
		3	2.208			3	1.040
		4	2.803			4	1.433
		5	2.915			5	0.834
		6	3.373			6	1.164
		7	3.544			7	1.092
		8	3.579			8	1.681
		9	3.642			9	2.133
		10	3.619			10	2.556

To observe the volume of the acid needed for full elution at lower standard concentrations the 500 nM and 250 nM standards were prepared and the measurements were taken with 300 μL acid, which corresponds to 30 μL of acid in each step (Figure 5.27 and Figure 5.28) (Tables B19 and B20 in Appendix B).

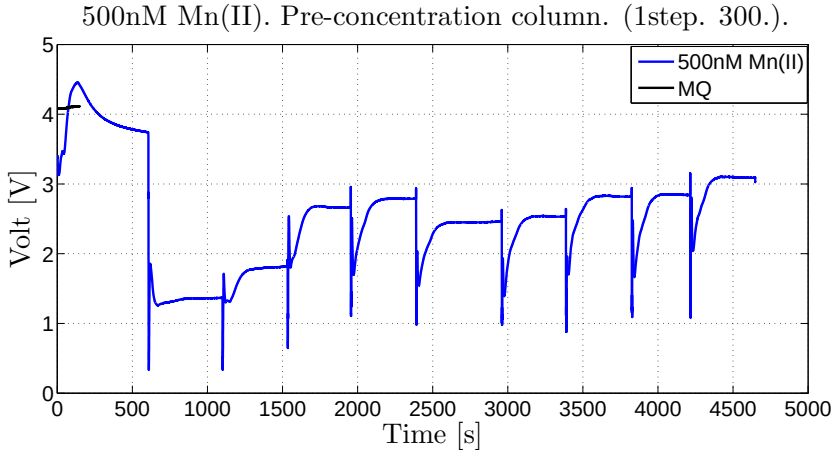

Figure 5.27: Eluted manganese standard measurements. 500 nM. Solutions diffused in the measurement cell of the chip. Boric acid buffer in 0.5 M NaOH. 10 steps. 300 μL acid volume.

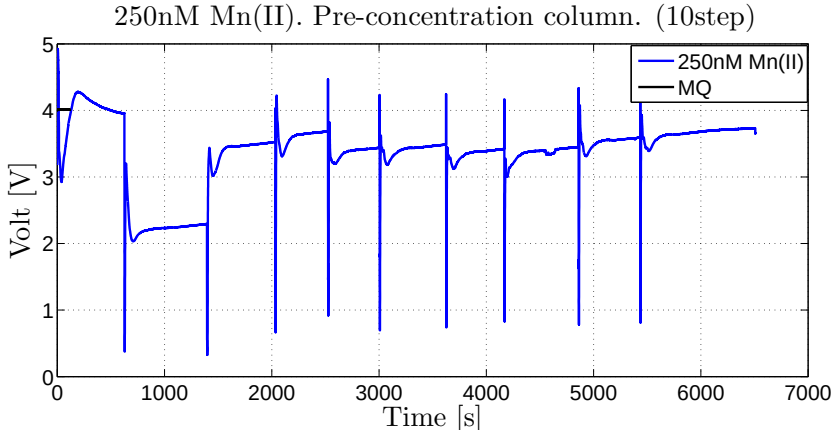

Figure 5.28: Eluted manganese standard measurements. 250 nM. Solutions diffused in the measurement cell of the chip. Boric acid buffer in 0.5 M NaOH. 10 steps. 300 μL acid volume.

The results for 250 nM and 500 nM manganese standard measurements eluted with 300 μL acid volume are summarised in Table 5.20.

Table 5.20: The results for 250 nM and 500 nM manganese standard measurements eluted with 300 μL acid volume.

Eluted manganese standard measurements.				
Total eluting acid volume μL.	Eluting acid volume per step $[\mu L]$	Step	250 nM Mn(II) [V]	500 nM Mn(II) [V]
300	30	1	3.956	3.741
		2	2.295	1.365
		3	3.524	1.818
		4	3.688	2.660
		5	3.440	2.788
		6	3.486	2.465
		7	3.422	2.531
		8	3.451	2.821
		9	3.440	2.841
		10	3.731	3.092

The results for the samples eluted with smaller volumes of the acid solution show that for the first step of the elution the Volt response recorded is high. This may be the result of: a pumping error where the solutions were not mixed in the ratio required and the pH needed was not obtained; problem with column elution; or dispersion prior to the detection cell. The internal volume of the channels in the chip is about 60 μL including the attached column and the measurement cell.

To confirm that the pH of the mixed solution at each step of the elution sequence is correct the pH measurements were made using 300 μL volume of the acid, which corresponds to 30 μL volume for each step, and with 600 μL volume of the acid, which corresponds to 60 μL volume for each step. The results are summarised in Tables 5.21 and 5.22.

Table 5.21: pH measurements. 10 steps, each step 30 μL

pH measurements. Eluting acid volume 300 μL.		
Step	Acid volume $[\mu L]$	pH
1	30	7.5
2	60	7.0
3	90	7.0
4	120	7.0
5	150	9.5
6	180	10.0
7	210	10.0
8	240	9.0
9	270	9.0
10	300	9.0

Table 5.22: pH measurements. 10 steps, each step 60 μL

pH measurements. Total eluting acid volume 600 μL.		
Step	Acid volume $[\mu L]$	pH
1	60	7.0
2	120	8.0
3	180	11.5
4	240	11.0
5	300	9.0
6	360	9.0
7	420	9.0
8	480	9.0
9	540	9.0
10	600	9.0

The experiments demonstrated that for the first 120 μL of the solution mix passing through the chip (collected from the waste outlet after the measurement cell), the pH value recorded was not high enough. The results from measurements with 900 μL acid volume show highest sensitivity for the first 90 μL injection. However, the results from

measurements with 300 μL acid volume show that the minimum volume of the acid that had to be used to obtain the required pH, was 150 μL or above. For the next experiments, the total volume of the eluting acid was chosen to be 300 μL and the measurements were performed with manganese standards and a standard reference material.

The results from measurements of manganese standards performed on the system with pre-concentration and 10 step elution are shown in Table 5.23.

Table 5.23: On chip measurements with pre-concentration and 10 step elution. 90 μL eluting acid

Results from test on system with pre-concentration On chip measurements. 10 step elution.						
Sample	Rep	mV	T	mAbs	Slope	R-squared
MQ	-	4043	-	-	-	-
Blank	1	3708	0.917	37.447		
	2	3677	0.909	41.210		
1500 nM Mn(II)	1	1399	0.321	453.644	0.3078	0.994
2500 nM Mn(II)	1	621	0.154	774,229		

The data shown in the table were the results collected after the first elution step, which corresponds to 90 μL acid solution and 480 seconds wait time.

5.6 System tests and calibration

After the experiment with volume of the eluting acid was completed, the next stages were to use the LabView system with the sequence programmed to pump the total eluting acid volume in one step, and analyse manganese standards and a certified reference material.

In the operation sequence the solutions were withdrawn from the reservoirs and injected into the microfluidic unit (with appropriate valves opened or closed). The four syringe Hamilton pumps were used to withdraw by hand and then inject the solutions. Pump 1 was used to pump MQ, standards and sample with volume of the syringe 1000 μL. Pump 2 was used to pump acid solution with the volume of the syringe 500 μL. Pump 3 was used to pump the reagent with volume of the syringe 250 μL. Pump 4 was

used to pump the buffer solution with volume of the syringe 250 μL.

In first step of the sequence the channels in the chip are cleaned with 500 μL MQ at flow rate of 600 $\mu L/min$, and this step was repeated 6 times. In the next stage the standard was withdrawn (1000 μL) at around 600 $\mu L/min$ and injected at 200 μL. Then the 300 μL acid solution was withdrawn at around 600 $\mu L/min$. The reagent (30 μL volume) and the buffer (30 μL volume) solution is withdrawn at around 600 $\mu L/min$. The acid, reagent and the buffer were injected to the system at the same time. The acid solutions at a flow rate of 600 $\mu L/min$ and the reagent and buffer solutions at flow rates of 60 $\mu L/min$ were pumped through the chip.

The sample, reagent and buffer were introduced to the measurement cell at ratio 10:1:1 v/v/v and the data were recorded during the diffusion time.

The above volumes and flow rates sum up to around 1180 seconds (19 minutes and 40 seconds) for withdrawing and injecting the solutions and for the diffusion time and 600 seconds for cleaning the system (10 minutes). The time required in the system for the valves and pumps operation in the LabView program is not counted as these count only for a few seconds each. The above volumes sum up to 1360 μL of reagent waste and 3000 μL of waste from system cleaning per sample. In future system designs the MQ volume used to clean the system and the diffusion time may be reduced.

The manganese standards were prepared at 1000 nM and 300 nM. The measurements were performed with 300 μL acid used for the elution (one step elution), repeated a number of times for each sample (blank, 300 nM and 1000 nM). The data were recorded after the solutions had diffused in the measurement cell for 480 seconds for each measurement taken. The results are shown in Figure 5.29 to 5.31.

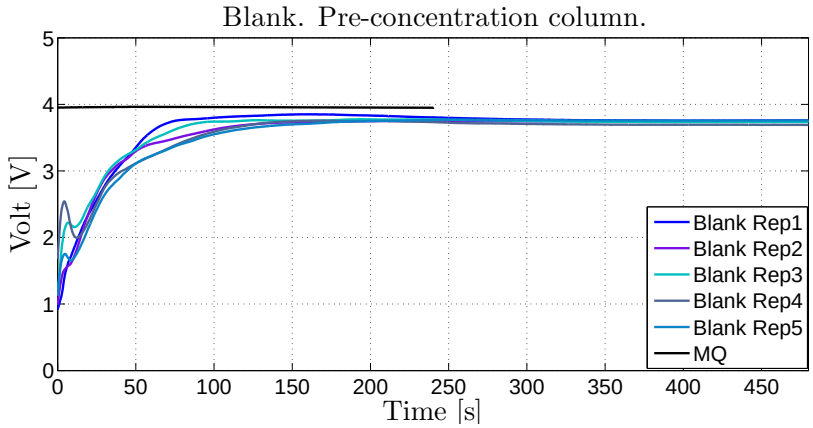

Figure 5.29: Blank measurements. Solutions diffused in the measurement cell of the chip. Replicates 1-5. Sample buffer in 0.5 M NaOH. 1 step. 300 μL acid volume.

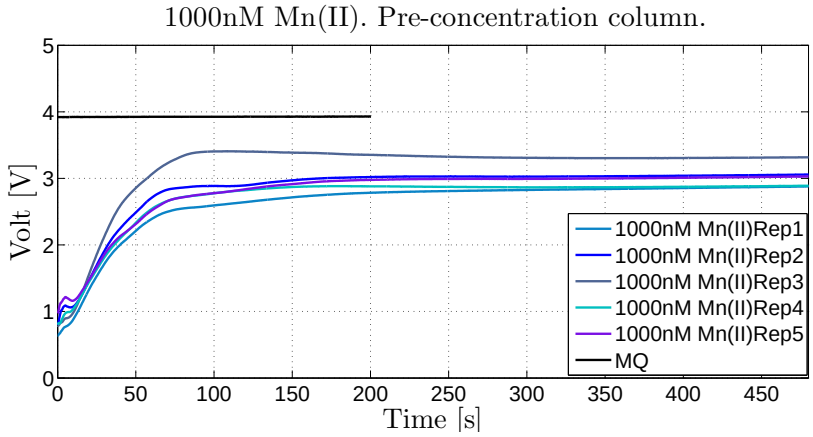

Figure 5.30: 1000 nM measurements. Solutions diffused in the measurement cell of the chip. Replicates 1-5. Boric acid buffer in 0.5 M NaOH. 1 step. 300 μL acid volume.

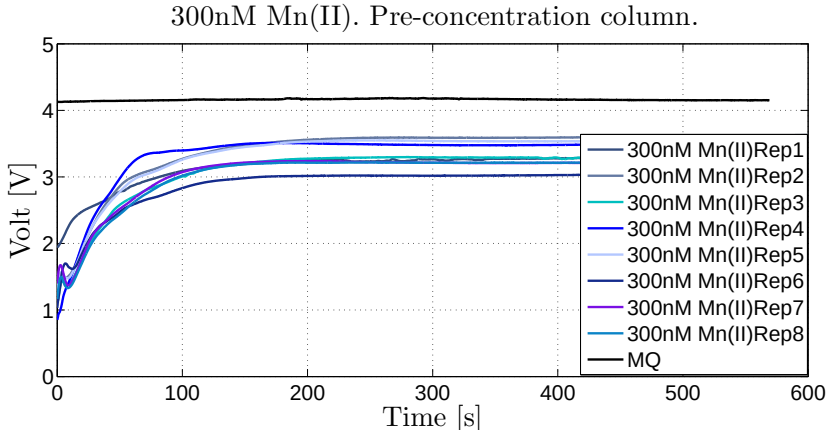

Figure 5.31: 300 nM measurements. Solutions diffused in the measurement cell of the chip. Replicates 1-8. Boric acid buffer in 0.5 M NaOH. 1 step. 300 μL acid volume.

The calibration curve is presented in Figure 5.32 with the slope value calculated $y = 0.1058x$ and R - squared = 0.9896. Results from on-chip measurements with pre-concentration (one step elution) and data used for the calibration are in Table 5.24.

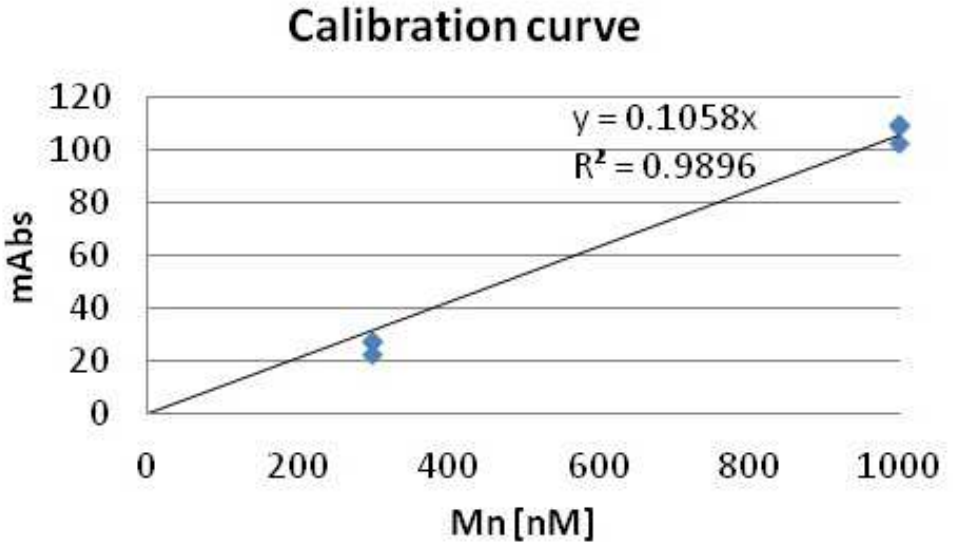

Figure 5.32: Calibration. On-chip measurements with pre-concentration. Blank – MQ.

Table 5.24: On-chip measurements with pre-concentration

Results from test on developed system On chip measurements										
Sample	Rep	Volt	STD DEV	% RSD	mV	T	mAbs	Comment	Slope	R-squared
MQ	-	3.949	-	-	-	-	-	-	-	-
Blank	1	3.773	0.03	0.86	3773	0.955	19.717			
	2	3.772			3772	0.955	19.894			
	3	3.745			3745	0.948	22.983			
	4	3.698			3698	0.936	28.527			
	5	3.771			3771	0.955	20.030			
MQ	-	4.154	-	-	-	-	-	-	0.1058	0.9896
300 nM Mn(II)	1	3.630	0.06	1.60	3630	0.919	36.258	outlier		
	2	3.516			3516	0.890	50.188	-		
	3	3.560			3560	0.901	44.742	-		
	4	3.630			3630	0.919	36.258	outlier		
	5	3.517			3517	0.891	50.021	-		
MQ	-	3.929	-	-	-	-	-	-		
1000 nM Mn(II)	1	2.916	0.08	2.69	2916	0.738	131.449	-		
	2	3.086			3086	0.781	106.817	outlier		
	3	2.914			2914	0.738	131.754	-		
	4	3.057			3057	0.774	110.962	outlier		
	5	2.960			2960	0.750	124.876	-		

The LOD was calculated at 106 nM, calculated as three times the standard deviation of the blank (σ = 35.46 nM). The LOD was calculated using the slope value ($y = 0.1058x$). Data are reported in Table 5.24 Note that when the one of the reported values (replicate 4) was an outlier, the standard deviation was σ = 14.77 nM and the LOD was calculated at 44 nM.

The summary of results from on chip measurements with and without pre-concentration are shown in Table 5.25.

Table 5.25: On chip measurements with and withouth pre-concentration.

On chip measurements with and without the preconcentartion		
No pre-concentration 1 step 300 μL acid volume		
Sample	Rep	mAbs
Blank	-	36.5
500 nM	1	55.6
	2	63.2
1000 nM	1	88.3
	2	89.5
Pre-concentration 1 step 300 μL acid volume		
Sample	Rep	mAbs
Blank	-	22.2
300 nM	1	50.2
	2	44.7
	3	50.0
1000 nM	1	131.4
	2	131.8
	3	124.9
Pre-concentration 10 step 90 μL acid volume		
Sample		mAbs
Blank		39.4
1500 nM		453.6
2500 nM		774.2

The sensitivity of the system was improved with pre-concentration. The results show that when the pre-concentration step elution method was used, where the manganese was eluted from the column with multiple steps of small acid volume and wait time between each step, the absorbance values recorded were higher comparing to one step elution.

The absorbance value recorded for 1000 nM standard for measurement with no pre-concentration was 88.9 (300 μL acid volume) and for measurement with pre-concentration with 1 step elution was 129.4 (300 μL acid volume). The absorbance value for 1000 nM standard for measurement with pre-concentration with 10 step elution was calculated using the slope value (0.3078) as 307.8 (90 μL acid volume). The absorbance values compared with the value recorded for 10 step elution were 2.4 times higher comparing to 1 step elution, and 3.5 times higher comparing to value recorded for measurements with no pre-concentration.

In order to quantify the amount of manganese in step elution for the 1500 nM standard the calibration (y=0.3078x) was applied and the response in each step (90 μL aliquot) was used to calculate the nM concentration. The results are shown in Table 5.26.

Table 5.26: On chip measurements. 10 step elution. (a) 1 mL manganese standard solution was loaded on the column equal to 1.5 nanomoles of manganese (one mL of 1500nM = 1.5 nmoles). (b) Eluted with 90 μL volume of acid in each step so for each step manganese concentration was calculated taking into account the 90 μL volume of eluting acid. The volume of the measurement cell was 15 μL.

On chip measurements with pre-concentration. 10 step elution.							
Sample	Step	V	mV	T	mAbs	nanomoles/ L	nanomoles/ 90 μL (b)
MQ	-	4.043	4043				
Blank	-	3.693	3693	0.913			
Mn(II) (a)	1	1.299	1299	0.321	453.644	1474	0.1326
	2	2.134	2134	0.528	238.085	774	0.0696
	3	2.201	2201	0.544	224.799	730	0.0657
	4	2.562	2562	0.634	158.674	516	0.0464
	5	2.256	2256	0.558	213.904	695	0.0625
	6	2.600	2600	0.643	152.431	495	0.0446
	7	3.686	3686	0.912	0.789	3	0.0002
	8	3.686	3686	0.912	0.801	3	0.0002
	9	3.693	3693	0.914	0.000	0	0.0000
	10	3.694	3694	0.914	0.000	0	0.0000

The total mass of manganese recovered was 0.422 nanomoles relative to 1.5 nanomoles loaded on the column, giving a yield of 28.1 %. The apparent low yield most probably reflects a large fraction of the manganese passing through the analytical cell prior to the final 15 μL of the first 90 μL going through the cell being measured. In future tests, smaller elution volumes should be used; in the present work the elution volume of 90 μL was dictated by the equipment available.

A certified reference material was tested. SLEW-2 was used as certified reference material (SLEW-2 estuarine water certified reference material for trace metals; manganese concentration 17.1 $\mu g/L$). The pH of SLEW-2 was adjusted to 8.0 using ammonia solution. The certified concentration of Mn(II) in the SLEW-2 standard is 311 nM. Results from tests on the developed system are given in Table 5.27 (Figure 5.33).

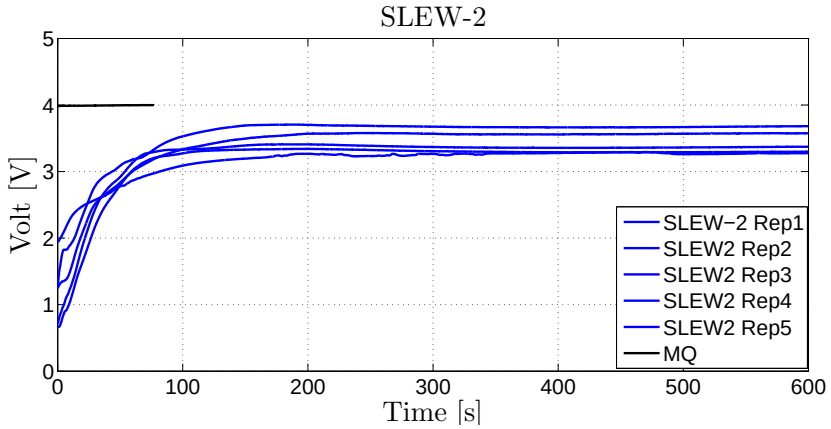

Figure 5.33: SLEW-2 measurements. Solutions diffused in the measurement cell of the chip. Rep 1-5. Boric acid buffer in 0.5 M NaOH. 1 step. 300 μL acid volume.

Table 5.27: Results from test on developed system. SLEW-2.

Results from test on developed system On chip measurements								
Sample	Rep	Volt	STD DEV	% RSD	mV	T	mAbs	nM
MQ	-	3.997	-	-	-	-	-	-
SLEW-2	1	3.371	0.16	4.67	3371	0.843	53.979	510
	2	3.622			3622	0.906	22.789	215
	3	3.277			3276	0.820	66.261	626
	4	3.298			3298	0.825	63.487	600
	5	3.575			3575	0.894	28.461	269

The system combining pre-concentration and colorimetric determination of the manganese using PAN-SDS provided a sensible calibration curve with reasonable precision for replicate standards measured. The values obtained for the SLEW-2 CRM were however very variable. There were several significant outliers still that most probably reflect continued problems with the pumps used, and with the CRM perhaps pH adjustment of the heavily acidified solution. The relative standard deviation of 5 measurements calculated for nM values reported in the Table 5.27 is 42.9 %. The mean calculated from the 5 measurements reported is 444 nM, it is 133 nM more that certified value of the reference standard used.

Improvements will include better pump systems, as discussed earlier, and methods to ensure consistent elution of the manganese in as small volume as possible.

5.7 Summary and conclusions

The objectives of this study were to use the LOAC system with pre-concentration for manganese determination with PAN chemistry. The microfluidic unit was designed and on-bench system was built. After the system was set-up for use for manganese determination, the reagents and samples were prepared and initial tests were performed without the pre-concentration. The results from the tests performed demonstrated that the data obtained were not consistent. Experiments were performed using red dye solution and MQ water to test the performance of the pumping system, and the response without PAN chemistry. The results demonstrated the error resulted from the volume of the solutions pumped by the syringe pumps used in the system. As a result of these experiments the preparation of the buffer solution used in the determination method was adjusted to allow for bigger error in volume of the buffer solution pumped. This adjustment made it possible to obtain the pH of the sample - buffer - reagent mix to be high enough, 9.0 or above, for the PAN method. After the manganese system was tested and the adjustments were made with major system errors characterised, the pre-concentration column was installed on the microfluidic unit. The subsequent experiments included the determination of manganese with the pre-concentration and optimisation of the volume of the acid solution used in the elution stage of manganese determination. The volume of the acid was chosen appropriate for the existing system. The manganese standards and certified reference material were analysed, with calibration curve plotted and LOD and precision numbers reported for the system.

The major results are listed below.

- Pump error remains a problem and the precision is 3.74 % - 7.23 % without pre-concentration and 0.86 % - 2.69 % with pre-concentration.

- Pump error and possibly dispersion in the column / chip causes deviation in the pH of the eluent output.

- The best results were obtained for small step elution cycles when the pre-concentration step elution method was used, where the manganese was eluted from the column with multiple steps of small acid volume and wait time between each step.

- Multi step elution method improves sensitivity comparing to one step elution with about 2.4 times improvement over 300 μL of step elution.

- The theoretical LOD with current system using 50 μL eluent and 6 mL sample is 0.3 nM which could be improved to 0.003 nM if the average pump standard deviation was reduced from about 12 % to less than 0.1 % as in the in-situ systems.

The system in its current form was used to demonstrate the principle of the pre-concentration on the chip, however the analyser does require further work to eliminate the pump error and make other improvements. Further work and suggested improvements and changes to the system are presented in Chapter 6.

Chapter 6

Conclusions and future directions

Contents

6.1 Summary of achievements 157
6.2 Recommendations for future work 159

6.1 Summary of achievements

The work presented in this thesis can be divided into the following four categories that address the main objectives in Chapter 1:

1. Collection and presentation of recent research related to different aspects of manganese determination.

2. Optimisation of the extraction of manganese from seawater with Toyopearl iminodiacetate resin.

3. Modification of the existing PAN method used for manganese determination and presentation of micelling agents reported for use with the PAN method published in the scientific literature.

4. Adaptation of the modified PAN method for use on the microfluidic unit with pre-concentration.

Whilst the system presented in this thesis is in the development stage and hence drawing definite conclusions regarding the behaviour of the system from the results produced to date is not possible, the author made several observations with regards to the

existing methods, advantages of the newly developed method, advantages of the application of pre-concentration and importance of the optimisation findings, as well as advantages and limitations of the developed LOAC system. The main achievements are listed below.

1. This thesis provides an overview of different laboratory based manganese determination methods as well as in-situ systems developed and used in marine waters for manganese determination in real time. The thesis includes the reported techniques using Toyopearl iminodiacetate resin for pre-concentration of manganese in water samples.

2. The method published by Chin et al. [40] was modified by implementing a new solubilising agent for PAN reagent preparation. The results proved the superior performance of the SDS surfactant over Triton X-100 surfactant when used with the PAN reagent. The PAN SDS method provides the measurements of the absorbance of manganese standards showing the absorbance values stable in time for at least 15 minutes. Additionally the PAN SDS reagent proves to be stable for at least 8 weeks and possibly longer. The modified method was used for manganese determination with calibration curves constructed and precision between the set of measurements determined and the LOD of the method assessed. For appropriate evaluation of the reagent lifetime more observations will need to be undertaken over a longer time. The extended lifetime of the reagent is a clear advantage when planning long-term deployments of the LOAC device.

3. The addition of the chelating resin pre-concentration step is a further improvement of the measurement technique. The implementation of the pre-concentration using iminodiacetate Toyopearl resin improves the sensitivity and eliminates or reduces the possibility of interferences from the matrix and other elements. Optimised conditions of the extraction of manganese from seawater with the Toyopearl iminodiacetate resin were developed using a Mn-54 tracer.

4. It has been found that the efficiency of adsorption of the manganese on to the resin is influenced by the flow rate of the sample stream when the manganese is absorbed on the resin material. Manganese recovery at flow rates higher than 0.2 mL/min was low (about 70 % at flow rate 0.5 mL/min). This observation suggests that the optimal flow rate required for full recovery of the manganese from the column is 0.2 mL/min.

5. Looking at the elution optimisation results from different acid concentrations tested it becomes apparent that the eluting acid solution may be prepared at a very low concentration of 0.001 M when HCl is used. This concentration of the eluting acid is sufficient for full elution of manganese of the resin, this was the lowest concentration

tested. The concentration of the eluting acid solution applied for manganese measurements in this thesis is 0.02 M HCl. This choice was directed by the requirements of the PAN method and its coupling with the LOAC system.

6. The suggested pre-concentration technique is suitable for trace metal determination and this pre-concentration technique can be easily incorporated into a LOAC system.

7. This thesis reports the adaptation of the modified PAN method on the chip and proves the concept of on-chip pre-concentration. The design and production methods of the microfluidic chip, that builds on the existing technology in the Sensors Group at Southampton, and the operation procedure of the bench-top LOAC manganese determination system with the resin column implemented on the chip are described. The LOAC system coupled with the resin column and PAN chemistry was used for manganese determinations with a calibration curve constructed and precision between the set of measurements determined and the LOD of the method reported.

6.2 Recommendations for future work

LOAC technology is still in development stage with different aspects of design, manufacturing, operation and control and more research, development and especially validation are required to ensure that LOAC systems achieve their full potential. The research presented in this thesis creates a reference and framework for other researchers to continue the work on the improved LOAC sensing technology where pre-concentration of the analyte is included.

Suggested ways forward are:

1. In order to obtain a device providing good precision the most urgent improvement of the system is the implementation of the custom designed syringe pump developed by the Sensors Group at NOC, Southampton. The custom designed pump will be located directly on the microfluidic chip and this should eliminate the errors caused by the pump system used in the current set-up, and reduce the air bubbles problem.

2. With the new pump system implemented additional optimisation experiments can be performed focusing on the best eluting acid volume to provide maximum signal response in the cell.

3. From the point of view of the sensitivity of the analyser and the limit of detection

the blank value needs to be reduced. This can be achieved by removing the interfering matrix with the use of the resin columns. Contamination control methods need to be rigorously applied.

4. The PAN–Mn complex absorbs at 560 nm and the LED used in the current system is centered on 572 nm. It is suggested to use an LED more compatible with the PAN-Mn complex maximum absorption in future microfluidic units that are produced.

5. From the point of view of the system performance over time it is important to investigate whether the strong acidic and basic solutions used in the determination method are affecting the internal surface of the chip and the components of the system in direct contact with the solutions used.

6. The implementation of in line mixing of sample and reagent rather that diffusive mixing in the cell in the chip can improve the mixing time and reduce the time needed for the measurements.

7. The resin may be locked inside the chip. The resin would be immobilized in the resin channel with polypropylene frits or similar constraints.

Appendix A

Data for Chapter 4

Table A.1: Spectrophotometric measurements. PAN Triton X-100. Sample in 0.01 M HCl, sample buffer boric acid in 0.15 M NaOH.

Spectrophotometric measurements PAN Triton X-100 Sample in 0.01 M HCl								
	Blank		300 [nM] Mn(II)		500 [nM] Mn(II)		1000 [nM] Mn(II)	
Min	Abs 560 nm	pH	Abs 560 nm	pH	Abs 560 nm	pH	Abs 560 nm	pH
1	0.0253	9.69	0.1522	9.67	0.2312	9.78	0.3382	9.67
2	0.0255	9.69	0.1519	9.68	0.2178	9.78	0.2980	9.67
3	0.0256	9.70	0.1486	9.68	0.2025	9.79	0.2342	9.68
4	0.0257	9.70	0.1450	9.68	0.1885	9.79	0.2021	9.68
5	0.0258	9.69	0.1418	9.68	0.1757	9.79	0.1744	9.68
6	0.0260	9.69	0.1382	9.68	0.1643	9.79	0.1554	9.68
7	0.0261	9.69	0.1343	9.68	0.1520	9.79	0.1438	9.68
8	0.0261	9.69	0.1316	9.68	0.1504	9.78	0.1377	9.68
9	0.0258	9.68	0.1282	9.68	0.1456	9.78	0.1368	9.68
10	0.0260	9.68	0.1253	9.68	0.1414	9.78	0.1337	9.68
11	0.0261	9.68	0.1226	9.68	0.1378	9.78	0.1312	9.68
12	0.0257	9.68	0.1201	9.68	0.1351	9.78	0.1273	9.68
13	0.0258	9.68	0.1179	9.68	0.1329	9.78	0.1273	9.68
14	0.0259	9.68	0.1156	9.67	0.1311	9.78	0.1256	9.68
15	0.0259	9.68	0.1140	9.67	0.1297	9.78	0.1256	9.68
16	0.0259	9.68	0.1125	9.67	0.1284	9.78	0.1235	9.67
17	0.0260	9.68	0.1110	9.67	0.1275	9.78	0.1235	9.67
18	0.0260	9.68	0.1098	9.67	0.1268	9.78	0.1220	9.67
19	0.0258	9.68	0.1088	9.67	0.1263	9.78	0.1211	9.67
20	0.0260	9.68	0.1078	9.66	0.1259	9.78	0.1208	9.67

Table A.2: Spectrophotometric measurements. PAN Triton X-100. Sample in seawater pH 8.0.

Spectrophotometric measurements PAN Triton X-100 Sample in sea water pH 8.0								
	Blank		300 [nM] Mn(II)		500 [nM] Mn(II)		1000 [nM] Mn(II)	
Min	Abs 560 nm	pH	Abs 560 nm	pH	Abs 560 nm	pH	Abs 560 nm	pH
1	0.0661	8.86	0.1810	8.78	0.2547	8.80	0.4328	8.78
2	0.0661	8.86	0.1797	8.78	0.2465	8.80	0.3903	8.78
3	0.0668	8.86	0.1771	8.80	0.2309	8.80	0.3232	8.80
4	0.0668	8.86	0.1735	8.80	0.2141	8.81	0.2783	8.81
5	0.0672	8.86	0.1697	8.82	0.1988	8.81	0.2450	8.81
6	0.0667	8.86	0.1664	8.82	0.1911	8.81	0.2306	8.81
7	0.0666	8.86	0.1632	8.82	0.1861	8.81	0.2171	8.81
8	0.0668	8.86	0.1605	8.82	0.1821	8.81	0.2104	8.82
9	0.0667	8.86	0.1586	8.82	0.1790	8.81	0.2048	8.82
10	0.0668	8.86	0.1569	8.82	0.1765	8.81	0.2006	8.82
11	0.0669	8.85	0.1569	8.82	0.1748	8.81	0.1973	8.82
12	0.0667	8.85	0.1546	8.82	0.1732	8.81	0.1945	8.82
13	0.0668	8.85	0.1542	8.82	0.1718	8.81	0.1923	8.82
14	0.0668	8.85	0.1536	8.83	0.1707	8.81	0.1903	8.82
15	0.0668	8.85	0.1532	8.83	0.1699	8.81	0.1888	8.82
16	0.0672	8.85	0.1530	8.83	0.1690	8.81	0.1873	8.82
17	0.0668	8.85	0.1528	8.83	0.1683	8.81	0.1862	8.82
18	0.0670	8.84	0.1526	8.83	0.1675	8.81	0.1850	8.82
19	0.0669	8.84	0.1527	8.83	0.1669	8.81	0.1841	8.81
20	0.0669	8.84	0.1527	8.83	0.1664	8.81	0.1831	9.67

Table A.3: Spectrophotometric measurements. PAN Triton X-100. Sample in MQ.

Spectrophotometric measurements PAN Triton X-100 Sample in MQ				
	Blank	300 [nM] Mn(II)	400 [nM] Mn(II)	600 [nM] Mn(II)
Min	Abs 560 nm	Abs 560 nm	Abs 560 nm	Abs 560 nm
1	0.0339	0.1669	0.1959	0.2937
2	0.0339	0.1661	0.1954	0.2790
3	0.0341	0.1657	0.1948	0.2859
4	0.0341	0.1659	0.1947	0.2812
5	0.0341	0.1653	0.1935	0.2754
6	0.0342	0.1652	0.1934	0.2689
7	0.0345	0.1652	0.1929	0.2626
8	0.0348	0.1651	0.1926	0.2557
9	0.0348	0.1650	0.1925	0.2488
10	0.0351	0.1653	0.1921	0.2418
11	0.0349	0.1656	0.1920	0.2352
12	0.0377	0.1655	0.1917	0.2291
13	-	0.1656	0.1915	0.2230
14	-	0.1659	0.1912	0.2184
15	-	0.1657	0.1908	0.2140
16	-	0.1660	0.1907	0.2098
17	-	0.1664	0.1904	0.2061
18	-	0.1661	0.1901	0.2050
19	-	0.1656	0.1899	0.2004
20		0.1656	0.1896	0.1979

Table A.4: Spectrophotometric off chip measurements. PAN SDS. Sample in seawater pH 8.0

Spectrophotometric measurements PAN - SDS Sample in seawater								
	Blank		300 [nM] Mn(II)		500 [nM] Mn(II)		1000 [nM] Mn(II)	
Min	Abs 560 nm	pH	Abs 560 nm	pH	Abs 560 nm	pH	Abs 560 nm	pH
1	0.1769	8.86	0.1914	8.82	0.2036	8.86	0.2354	8.77
2	0.1764	8.86	0.1898	8.82	0.2032	8.85	0.2351	8.77
3	0.1761	8.88	0.1888	8.82	0.2031	8.85	0.2350	8.85
4	0.1761	8.89	0.1882	8.82	0.2029	8.85	0.2349	8.85
5	0.1762	8.89	0.1883	8.82	0.2028	8.85	0.2349	8.85
6	0.1762	8.89	0.1880	8.86	0.2028	8.85	0.235	8.86
7	0.1760	8.89	0.1877	8.86	0.203	8.85	0.2349	8.86
8	0.1759	8.89	0.1878	8.86	0.2026	8.85	0.2349	8.86
9	0.1758	8.89	01875	8.86	0.2025	8.85	0.2346	8.87
10	0.1759	8.89	0.1874	8.86	0.2025	8.85	0.2346	8.87
11	0.1759	8.89	0.1877	8.86	0.2024	8.85	0.2347	8.87
12	0.1758	8.89	0.1879	8.86	0.2025	8.85	0.2345	8.86
13	0.1756	8.89	0.1874	8.86	0.2025	8.85	0.2345	8.86
14	0.1758	8.88	0.1877	8.86	0.2023	8.85	0.2347	8.86
15	0.1760	8.88	0.1879	8.86	0.2022	8.85	0.2344	8.86
16	0.1756	8.88	0.1880	8.86	0.2022	8.85	0.2346	8.86
17	0.1757	8.88	0.1877	8.86	0.2022	8.85	0.2346	8.86
18	0.1759	8.88	0.1877	8.86	0.2024	8.85	0.2343	8.86
19	0.1758	8.88	0.1873	8.85	0.2022	8.85	0.2343	8.86
20	0.1758	8.88	0.1873	8.85	0.2021	8.85	0.2345	8.86

Table A.5: Spectrophotometric off chip measurements. PAN SDS. Sample in 0.02 M HCl. Sample buffer boric acid in 0.4 M NaOH. Part 1/2

Spectrophotometric measurements PAN - SDS Sample in 0.02 M HCl										
	Blank		300 [nM] Mn(II) Rep1		300 [nM] Mn(II) Rep2		500 [nM] Mn(II) Rep1		500 [nM] Mn(II) Rep2	
Min	Abs 560 nm	pH	Abs 560 nm	pH	Abs 560 nm	pH	Abs 560 nm	pH	Abs 560 nm	pH
1	0.0234	9.71	0.0997	9.63	0.0990	9.58	0.1496	9.66	0.1510	9.64
2	0.0228	9.71	0.1038	9.63	0.1046	9.60	0.1572	9.66	0.1584	9.64
3	0.0229	9.75	0.1060	9.63	0.1076	9.60	0.162	9.66	0.1638	9.64
4	0.0230	9.76	0.1081	9.63	0.1099	9.66	0.1653	9.67	0.1677	9.64
5	0.0231	9.76	0.1096	9.63	0.1118	9.67	0.1678	9.67	0.1702	9.65
6	0.0231	9.75	0.1111	9.62	0.1130	9.68	0.1697	9.67	0.1723	9.65
7	0.0230	9.75	0.1117	9.62	0.1143	9.68	0.1713	9.67	0.1740	9.65
8	0.0231	9.76	0.1125	9.62	0.1151	9.69	0.1727	9.67	0.1757	9.65
9	0.0231	9.76	0.1134	9.62	0.1158	9.69	0.1736	9.67	0.1762	9.65
10	0.0231	9.76	0.1145	9.62	0.1165	9.69	0.1746	9.67	0.1772	9.65
11	0.0232	9.76	0.1148	9.62	0.1172	9.69	0.1756	9.67	0.1780	9.65
12	-	-	0.1154	9.62	0.1176	9.69	0.1764	9.68	0.1790	9.65
13	-	-	0.1161	9.61	0.1181	9.70	0.1772	9.68	0.1798	9.65
14	-	-	0.1166	9.61	0.1186	9.70	0.1779	9.68	0.1804	9.65
15	-	-	0.1171	9.61	0.1192	9.70	0.1787	9.68	0.1813	9.65
16	-	-	0.1175	9.61	0.1194	9.70	0.1793	9.68	0.1821	9.65
17	-	-	0.1180	9.61	0.1199	9.70	0.1798	9.68	0.1824	9.65
18	-	-	0.1185	9.60	0.1203	9.70	0.1804	9.68	0.1831	9.65
19	-	-	0.1190	9.60	0.1206	9.70	0.1809	9.68	0.1837	9.65
20	-	-	0.1193	9.60	0.1209	9.69	0.1816	9.68	0.1843	9.65

Table A.6: Spectrophotometric off chip measurements. PAN SDS. Sample in 0.02 M HCl. Sample buffer boric acid in 0.4 M NaOH. Part 2/2

Spectrophotometric measurements PAN - SDS Sample in 0.02 M HCl								
	1000 [nM] Mn(II) Rep1		1000 [nM] Mn(II) Rep2		2000 [nM] Mn(II) Rep1		2000 [nM] Mn(II) Rep2	
Min	Abs 560 nm	pH	Abs 560 nm	pH	Abs 560 nm	pH	Abs 560 nm	pH
1	0.2360	9.70	0.2431	9.74	0.4159	9.64	0.4209	9.65
2	0.2528	9.73	0.2431	9.74	0.4486	9.64	0.4209	9.65
3	0.2631	9.74	0.2527	9.74	0.4677	9.64	0.4466	9.65
4	0.2689	9.74	0.2581	9.76	0.4816	9.66	0.4656	9.67
5	0.2742	9.74	0.2642	9.76	0.4931	9.67	0.4803	9.67
6	0.2777	9.75	0.2701	9.76	0.5015	9.67	0.4926	9.68
7	0.2807	9.75	0.2751	9.76	0.5094	9.97	0.5016	9.68
8	0.2838	9.75	0.2798	9.76	0.5171	9.67	0.5100	9.68
9	0.2865	9.75	0.2834	9.76	0.5222	9.68	0.5171	9.68
10	0.2887	9.75	0.2859	9.76	0.5278	9.68	0.5239	9.69
11	0.2915	9.75	0.2888	9.76	0.5324	9.68	0.5290	9.69
12	0.2938	9.75	0.292	9.76	0.5368	9.68	0.5344	9.69
13	0.2951	9.75	0.2938	9.76	0.5404	9.68	0.5385	9.69
14	0.2965	9.75	0.2949	9.76	0.5446	9.69	0.5426	9.69
15	0.2981	9.75	0.297	9.76	0.5480	9.69	0.5468	9.69
16	0.2999	9.75	0.2993	9.76	0.5507	9.69	0.5468	9.69
17	0.3009	9.75	0.2999	9.76	0.5535	9.70	0.5535	9.69
18	0.3022	9.75	0.3014	9.76	0.5563	9.70	0.5564	9.68
19	0.3039	9.75	0.3029	9.76	0.5586	9.71	0.5591	9.68
20	0.3047	9.75	0.3043	9.76	0.5611	9.72	0.5621	9.68

Appendix B

Data for Chapter 5

Table B.1: Data - Figure 5.8

On-chip measurements PAN-SDS			
Sample	Rep	Volt	STD DEV
MQ	1	4.954	-
Blank	1	4.949	-
500 [nM]	1	4.076	0.15
	2	4.237	
	3	3.938	
1000 [nM]	1	3.625	0.15
	2	3.410	

Table B.2: Data - Figure 5.10

On-chip measurements PAN-SDS				
Sample	Rep	Volt	STD DEV	%RSD
MQ	1	4.953	-	-
Blank	1	4.660	-	-
1000 [nM]	1	3.868	0.31	7.31
	2	3.983		
	3	4.171		
	4	4.235		

Table B.3: Data - Figure 5.12

On-chip measurements PAN-SDS				
Sample	Rep	Volt	STD DEV	%RSD
MQ	1	3.891	-	-
Blank	1	3.331	0.01	0.17
	2	3.335		
	3	3.344		
	4	3.332		
500 [nM]	1	2.582	0.03	11.25
	2	2.633		
	3	2.593		

Table B.4: Data - Figure 5.13

On-chip measurements PAN-SDS				
Sample	Rep	Volt	STD DEV	%RSD
MQ	1	4.528	-	-
Blank	1	4.007	0.08	1.99
	2	3.888		
	3	3.975		
	4	3.784		
	5	0.005	(not included in calc.)	
	6	3.950		
	7	3.985		
	8	3.985		
	9	0.005	(not included in calc.)	

Table B.5: Data - Figure 5.17

On-chip measurements PAN-SDS				
Sample	Rep	Volt	STD DEV	%RSD
MQ	1	4.459	-	-
Dye	1	1.661	0.03	1.58
	2	1.686		
	3	1.690		
	4	1.693		
	5	1.700		
	6	1.702		
	7	1.661		
	8	1.707		
	9	1.754		
	10	1.720		
	11	1.720		

Table B.6: MQ-Dye experiment data

On-chip measurements PAN-SDS				
Sample	Rep	Volt	STD DEV	%RSD
MQ	1	4.459	-	-
Dye	1	3.373	0.05	1.38
	2	3.294		
	3	3.385		
	4	3.374		
	5	3.421		

Table B.7: MQ-Dye experiment data

On-chip measurements PAN-SDS				
Sample	Rep	Volt	STD DEV	%RSD
MQ	1	4.476	-	-
Dye	1	2.707	0.11	4.14
	2	2.647		
	3	2.552		
	4	2.851		
	5	2.751		

Table B.8: MQ-Dye experiment data

On-chip measurements PAN-SDS				
Sample	Rep	Volt	STD DEV	%RSD
MQ	1	4.390	-	-
Dye	1	3.900	0.05	1.24
	2	3.893		
	3	3.994		
	4	3.981		
	5	3.958		
	6	4.009		

Table B.9: MQ-Dye experiment data

On-chip measurements PAN-SDS				
Sample	Rep	Volt	STD DEV	%RSD
MQ	1	4.421	-	-
Dye	1	2.826	0.02	0.75
	2	2.878		
	3	2.859		
	4	2.855		

Table B.10: Data - Figure 5.18

On-chip measurements PAN-SDS				
Sample	Rep	Volt	STD DEV	%RSD
MQ	1	4.671	-	-
Blank	1	4.221	0.03	0.75
	2	4.217		
	3	4.248		
	4	4.290		
	5	4.274		

Table B.11: Data - Figure 5.19

On - chip measurements PAN-SDS		
Sample	Rep	Volt
MQ	1	4.288
	2	4.433
2000 nM	1	3.094
	2	3.742
	3	4.046
	4	4.049
	5	4.092
	6	4.091

Table B.12: Data - Figure 5.20

On - chip measurements PAN-SDS		
Sample	Rep	Volt
MQ	1	4.671
2000 nM	1	2.804
	2	3.055
	3	3.677
	4	3.965
	5	4.187
	6	4.259
	7	3.298

Table B.13: Data - Figure 5.21

On - chip measurements PAN-SDS		
Sample	Rep	Volt
MQ	1	4.288
	2	4.433
2000 nM	1	3.586
	2	3.862
	3	3.626
	4	4.049
	5	4.069

Table B.14: Data - Figure 5.22

On - chip measurements PAN-SDS		
Sample	Rep	Volt
MQ	1	4.288
	2	4.433
2000 nM	1	3.620
	2	3.581
	3	3.640
	4	4.069

Table B.15: Data - Figure 5.23

On - chip measurements PAN-SDS		
Sample	Rep	Volt
MQ	1	4.288
2000 nM	1	3.208
	2	3.117
	3	3.674
	4	3.254
	5	3.139

Table B.16: Data - Figure 5.24

On-chip measurements PAN-SDS		
Sample	Step	Volt
MQ	-	4.013
1500 [nM]	1	1.399
	2	2.134
	3	2.201
	4	2.562
	5	3.256
	6	3.599
	7	3.686
	8	3.686
	9	3.693
	10	3.694

Table B.17: Data - Figure 5.25

On-chip measurements PAN-SDS		
Sample	Step	Volt
MQ	-	4.013
	1	2.837
	2	0.812
	3	1.039
	4	1.433
2500	5	0.834
[nM]	6	1.164
	7	1.092
	8	1.681
	9	2.133
	10	2.556

Table B.18: Data - Figure 5.26

On-chip measurements PAN-SDS		
Sample	Step	Volt
MQ	-	4.013
	1	0.621
	2	1.571
	3	2.208
	4	2.803
2500	5	2.915
[nM]	6	3.373
	7	3.544
	8	3.579
	9	3.642
	10	3.619

Table B.19: Data - Figure 5.27

On-chip measurements PAN-SDS		
Sample	Step	Volt
MQ	-	4.115
	1	3.741
	2	1.365
	3	1.818
	4	2.660
500	5	2.788
[nM]	6	2.464
	7	2.531
	8	2.821
	9	2.841
	10	3.092

Table B.20: Data - Figure 5.28

On-chip measurements PAN-SDS		
Sample	Step	Volt
MQ	-	4.111
	1	3.956
	2	2.295
	3	3.524
	4	3.688
250	5	3.440
[nM]	6	3.486
	7	3.422
	8	3.451
	9	3.440
	10	3.731

Bibliography

[1] J. T. M. de Jong, M. Boye, M. D. Gelado-Caballero, K. R. Timmermans, M. J. W. VeldhuiS, R. F. Nolting, C. M. G. van den Berg, and H. J. W. de Baar, "Inputs of iron, manganese and aluminium to surface waters of the Northeast Atlantic Ocean and the European continental shelf," *Marine Chemistry*, vol. 107, pp. 120–142, OCT 30 2007.

[2] N. Morley, P. Statham, and J. Burton, "Dissolved trace-metals in the southwestern Indian Ocean," *Deep-Sea Research Part I - Oceanographic Research Papers*, vol. 40, pp. 1043–1062, MAY 1993.

[3] L. Coo, T. Cardwell, R. Cattrall, and S. Kolev, "Spectrophotometric study of the solubility and the protolytic properties of 1-(2-pyridylazo)-2-naphthol in different ethanol-water solutions," *Analytica Chimica Acta*, vol. 360, pp. 153–159, MAR 10 1998.

[4] http://www.hc-sc.gc.ca/ewh-semt/contaminants/radiation/surveill/sodium eng.php.

[5] F. Morel and N. Price, "The biogeochemical cycles of trace metals in the oceans," *Science*, vol. 300, pp. 944–947, MAY 9 2003.

[6] S. Iwata and J. Barber, "Structure of photosystem II and molecular architecture of the oxygen-evolving centre," *Current Opinion In Structural Biology*, vol. 14, pp. 447–453, AUG 2004.

[7] J. Barber, "Photosystem II: the water-splitting enzyme of photosynthesis," *Cold Spring Harbor symposia on quantitative biology*, 2012.

[8] L. Brand, W. Sunda, and R. Guillard, "Limitation of marine-phytoplankton reproductive rates by zinc, manganese and iron," *Limnology and Oceanography*, vol. 28, no. 6, pp. 1182–1198, 1983.

[9] P. Saager, H. Debaar, and P. Burkill, "Manganese and iron in Indian Ocean," *Geochemica et Cosmochimica Acta*, vol. 53, pp. 2259–2267, SEP 1989.

[10] K. Bruland, J. Donat, and D. Hutchins, "Interactive influences of bioactive trace-metals on biological production in oceanic waters," *Limnology and Oceanography*, vol. 36, pp. 1555–1577, DEC 1991.

[11] P. W. Boyd and M. J. Ellwood, "The biogeochemical cycle of iron in the ocean," *Nature Geoscience*, vol. 3, pp. 675–682, OCT 2010.

[12] R. Middag, H. J. W. de Baar, P. Laan, P. H. Cai, and J. C. van Ooijen, "Dissolved manganese in the Atlantic sector of the Southern Ocean," *Deep-Sea Research Part A - Oceanographic Research Papers*, vol. 58, pp. 2661–2677, DEC 15 2011.

[13] G. Luther, B. Sundby, B. Lewis, P. Brendel, and N. Silverberg, "Interactions of manganese with the nitrogen cycle: Alternative pathways to dinitrogen," *Geochimica et Cosmochimica Acta*, vol. 61, pp. 4043–4052, OCT 1997.

[14] T. Doi, H. Obata, and M. Maruo, "Shipboard analysis of picomolar levels of manganese in seawater by chelating resin concentration and chemiluminescence detection," *Analytical and Bioanalytical Chemistry*, vol. 378, pp. 1288–1293, MAR 2004.

[15] J. H. Martin, "Glacial-Interglacial CO2 change: the iron hyphothesis," *Paleoceanography*, vol. 5, no. 1, pp. 1–13, 1990.

[16] G. Klinkhammer, H. Elderfield, and A. Hudson, "Rare-earth elements in seawater near hydrothermal vents," *Nature*, vol. 305, no. 5931, pp. 185–188, 1983.

[17] Y. Hongo, H. Obata, T. Gamo, M. Nakaseama, J. Ishibashi, U. Konno, S. Saegusa, S. Ohkubo, and U. Tsunogai, "Rare earth elements in the hydrothermal system at Okinawa Trough back-arc basin," *Geochemical Journal*, vol. 41, no. 1, pp. 1–15, 2007.

[18] J. Martin and G. Knauer, "Manganese cycling in Northeast Pacific waters," *Earth And Planetary Science Letters*, vol. 51, no. 2, pp. 266–274, 1980.

[19] W. Sunda. and S. Huntsman, "Photoreduction of manganese oxides in seawater," *Marine Chemistry*, vol. 46, pp. 133–152, APR 1994.

[20] L. Neretin, C. Pohl, G. Jost, T. Leipe, and F. Pollehne, "Manganese cycling in the Gotland Deep, Baltic Sea," *Marine Chemistry*, vol. 82, pp. 125–143, AUG 2003.

[21] W. Sunda and S. Huntsman, "Control of Cd concentrations in a coastal diatom by interactions among free ionic Cd, Zn, and Mn in seawater," *Environmental Science And Technology*, vol. 32, pp. 2961–2968, OCT 1 1998.

[22] W. Landing and K. Bruland, "Manganese in the north Pacific," *Earth and Planetary Science Letters*, vol. 49, no. 1, pp. 45–56, 1980.

[23] P. Statham and J. Burton, "Dissolved manganese in the North Atlantic Ocean, 0-35 degrees-N," *Earth and Planetary Science Letters*, vol. 79, pp. 55–65, AUG 1986.

[24] A. Tappin, D. Hydes, J. Burton, and P. Statham, "Concentrations, distributions and seasonal variability of dissolved Cd, Co, Cu, Mn, Ni, Pb and Zn in the English-Channel," *Continental Shelf Research*, vol. 13, pp. 941–969, AUG-SEP 1993.

[25] A. E. Noble, C. H. Lamborg, D. C. Ohnemus, P. J. Lam, T. J. Goepfert, C. I. Measures, C. H. Frame, K. L. Casciotti, G. R. DiTullio, J. Jennings, and M. A. Saito, "Basin-scale inputs of cobalt, iron, and manganese from the Benguela-Angola front to the South Atlantic Ocean," *Limnology and Oceanography*, vol. 57, pp. 989–1010, JUL 2012.

[26] K. Mandernack and B. Tebo, "Manganese scavenging and oxidation at hydrothermalal vents and in vent plumes," *Geochimica Et Cosmochimica Acta*, vol. 57, pp. 3907–3923, AUG 1993.

[27] W. Sunda and S. Huntsman, "Effect of sunlight on redox cycles of manganese in the southwestern saragasso sea," *Deep-Sea Research Part A - Oceanographic Research Papers*, vol. 35, pp. 1297–1317, AUG 1988.

[28] Z. Chase, K. Johnson, V. Elrod, J. Plant, S. Fitzwater, L. Pickell, and C. Sakamoto, "Manganese and iron distributions off central California influenced by upwelling and shelf width," *Marine Chemistry*, vol. 95, pp. 235–254, JUN 1 2005.

[29] P. Statham, D. Connelly, C. German, T. Brand, J. Overnell, E. Bulukin, N. Millard, S. McPhail, M. Pebody, J. Perrett, M. Squire, P. Stevenson, and A. Webb, "Spatially complex distribution of dissolved manganese in a fjord as revealed by high-resolution in situ sensing using the autonomous underwater vehicle autosub," *Environmental Science and Technology*, vol. 39, pp. 9440–9445, DEC 15 2005.

[30] P. Statham, P. Yeats, and W. Landing, "Manganese in the eastern Atlantic Ocean: processes influencing deep and surface water distributions," *Marine Chemistry*, vol. 61, pp. 55–68, JUN 1998.

[31] W. Landing and K. Bruland, "The contrasting biogeochemistry of iron and manganese in the Pacific Ocean," *Geochemica et Cosmochimica Acta*, vol. 51, pp. 29–43, JAN 1987.

[32] E. Bucciarelli, S. Blain, and P. Treguer, "Iron and manganese in the wake of the Kerguelen Islands (Southern Ocean)," *Marine Chemistry*, vol. 73, pp. 21–36, JAN 2001.

[33] T. Crompton, *Preconcentration Techniques for Natural and Treated Waters. High Sensitivity Determination of Organic and Organometallic Compounds, Cations and Anions.* London: Spon Press, 2003.

[34] A. G. Howard and P. J. Statham, *Inorganic trace analysis: philosophy and practice.* John Wiley and Sons Inc., 1993.

[35] S. Song and A. Singh, "On-chip sample preconcentration for integrated microfluidic analysis," *Analytical and Bioanalytical Chemistry*, vol. 384, pp. 41–43, JAN 2006.

[36] D. Kara, "The Use of Chelating Solid Phase Materials in Flow Injection Systems: A Review," *Analytical Letters*, vol. 44, no. 1-3, pp. 457–482, 2011.

[37] J. Resing and M. Mottl, "Determination of manganese in seawater using flow injection analysis with on-line preconcentration and spectrophotometric detection," *Analytical Chemistry*, vol. 64, pp. 2682–2687, NOV 15 1992.

[38] J. Olafsson, "The semi-automated determination of manganese in sea water with leuco-malachite green," *Science of the environment*, vol. 49, pp. 101–113, MAR 1986.

[39] A. M. Aguilar-Islas, J. A. Resing, and K. W. Bruland, "Catalytically enhanced spectrophotometric determination of manganese in seawater by flow-injection analysis with a commercially available resin for on-line preconcentration," *Limnology and Oceanography - Methods*, vol. 4, pp. 105–113, APR 2006.

[40] C. Chin, K. Johnson, and K. Coale, "Spectrophotometric determination of dissolved manganese in natural waters with 1-(2-pyridylazo)-naphthol - application

to analysis in situ in hydrothermal plumes," *Marine Chemistry*, vol. 37, pp. 65–82, MAR 1992.

[41] K. Warnken, D. Tang, G. Gill, and P. Santschi, "Performance optimization of a commercially available iminodiacetate resin for the determination of Mn, Ni, Cu, Cd and Pb by on-line preconcentration inductively coupled plasma-mass spectrometry," *Analytica Chimica Acta*, vol. 423, pp. 265–276, NOV 1 2000.

[42] D. V. Biller and K. W. Bruland, "Analysis of Mn, Fe, Co, Ni, Cu, Zn, Cd, and Pb in seawater using the Nobias-chelate PA1 resin and magnetic sector inductively coupled plasma mass spectrometry (ICP-MS)," *Marine Chemistry*, vol. 130, pp. 12–20, FEB 20 2012.

[43] A. Milne, W. Landing, M. Bizimis, and P. Morton, "Determination of Mn, Fe, Co, Ni, Cu, Zn, Cd and Pb in seawater using high resolution magnetic sector inductively coupled mass spectrometry (HR-ICP-MS)," *Analytica Chimica Acta*, vol. 665, pp. 200–207, APR 30 2010.

[44] M. Khajeh and E. Sanchooli, "Synthesis of ion-selective imprinted polymer for manganese removal from environmental water," *Polymer Bulletin*, vol. 67, pp. 413–425, JUL 2011.

[45] Y. Yamini, N. Amiri, and M. Karimi, "Determination of trace elements in natural water using X-ray fluorescence spectrometry after preconcentration with powdered silica gel," *X-Ray Spectrometry*, vol. 38, pp. 474–478, NOV-DEC 2009.

[46] K. Coale, C. Ccin, G. Massoth, K. Johnson, and E. Barber, "In situ chemical mapping of dissolved iron and manganese in hydrothermal plumes," *Nature*, vol. 352, pp. 325–328, JUL 25 1991.

[47] B. Chiswell, G. Rauchle, and M. Pascoe, "Spectrophotometric methods for the determination of manganese," *Talanta*, vol. 37, pp. 237–259, FEB 1990.

[48] K. Okamura, T. Gamo, H. Obata, E. Nakayama, H. Karatani, and Y. Nozaki, "Selective and sensitive determination of trace manganese in sea water by flow through technique using luminol hydrogen peroxide chemiluminescence detection," *Analytica Chimica Acta*, vol. 377, pp. 125–131, DEC 31 1998.

[49] M. Mowlem, S. Hartman, S. Harrison, and K. Larkin, "Intercomparison of biogeochemical sensors at ocean observatories," tech. rep., EUR-OCEANS report for WP2.1., 2008.

[50] E. Achterberg, T. Holland, A. Bowie, R. Fauzi, C. Mantoura, and P. Worsfold, "Determination of iron in seawater," *Analytica Chimica Acta*, vol. 442, pp. 1–14, AUG 31 2001.

[51] M. Mowlem and V. Chavagnac, "Micro system technology for marine measurement," *Oceans 2006, Vols 1-4: 845-850.*, 2006.

[52] K. Johnson, C. Beehler, C. Sakamoto, and J. Childress, "In situ measurements of chemical distributions in deep sea hydrothermal vent field," *Science*, vol. 231, pp. 1139–1141, MAR 7 1986.

[53] C. Chin, K. Coale, V. Elrod, K. Johnson, G. Massoth, and E. Baker, "In situ observations of dissolved iron and manganese in hydrothermal vent plumes, Juan-De-Fuca Ridge," *Journal of Geophysical Research - Solid Earth*, vol. 99, pp. 4969–4984, MAR 10 1994.

[54] G. Massoth, E. Baker, R. Feely, J. Lupton, R. Collier, J. Gendron, K. Roe, S. Maenner, and J. Resing, "Manganese and iron in hydrothermal plumes resulting from the 1996 Gorda Ridge Event," *Deep-Sea Research Part I - Oceanographic Research Papers*, vol. 45, no. 12, pp. 2683–2712, 1998.

[55] G. Klinkhammer, "Fiber optic spectrophotometers for in situ measurements in the oceans - the ZAPS probe," *Marine Chemistry*, vol. 47, pp. 13–20, SEP 1994.

[56] T. Chapin, H. Jannasch, and K. Johnson, "In situ osmotic analyzer for the year-long continuous determination of Fe in hydrothermal systems," *Analytica Chimica Acta*, vol. 463, pp. 265–274, JUL 22 2002.

[57] P. Statham, D. Connelly, C. German, E. Bulukin, N. Millard, S. McPhail, M. Pebody, J. Perrett, M. Squires, P. Stevenson, and A. Webb, "Mapping the 3D spatial distribution of dissolved manganese in coastal waters using an in situ analyser and the autonomous underwater vehicle Autosub," *Underwater Technology*, vol. 25, pp. 129–134, SPR 2003.

[58] P. Sarradin, N. Le Bris, C. Le Gall, and P. Rodier, "Fe analysis by the ferrozine method: Adaptation to FIA towards in situ analysis in hydrothermal environment," *Talanta*, vol. 66, pp. 1131–1138, JUN 15 2005.

[59] R. Vuillemin, D. Le Roux, P. Dorval, K. Bucas, J. P. Sudreau, M. Hamon, C. Le Gall, and P. M. Sarradin, "CHEMINI: A new in situ CHEmical MINIatur-

ized analyzer," *Deep-Sea Research Part I - Oceanographic Research Papers*, vol. 56, pp. 1391–1399, AUG 2009.

[60] T. S. Moore, K. M. Mullaugh, R. R. Holyoke, A. S. Madison, M. Yucel, and G. W. Luther, III, "Marine Chemical Technology and Sensors for Marine Waters: Potentials and Limits," *Annual Review of Marine Science*, vol. 1, pp. 91–115, 2009.

[61] C.-C. Lin, J.-L. Hsu, and G.-B. Lee, "Sample preconcentration in microfluidic devices," *Microfluidics and nanofluidics*, vol. 10, pp. 481–511, MAR 2011.

[62] A. Milani, P. J. Statham, M. C. Mowlem, and D. P. Connelly, "Development and application of a microfluidic in-situ analyzer for dissolved Fe and Mn in natural waters," *Talanta*, vol. 136, pp. 15–22, MAY 1 2015.

[63] T. A. Franke and A. Wixforth, "Microfluidics for Miniaturized Laboratories on a Chip," *Chemphyschem*, vol. 9, pp. 2140–2156, OCT 24 2008.

[64] A. Gonzalez Crevillen, M. Hervas, M. Angel Lopez, M. Cristina Gonzalez, and A. Escarpa, "Real sample analysis on microfluidic devices," *Talanta*, vol. 74, pp. 342–357, DEC 15 2007.

[65] S.-E. Ong, S. Zhang, H. Du, and Y. Fu, "Fundamental principles and applications of microfluidic systems," *Frontiers in Bioscience-Landmark*, vol. 13, pp. 2757–2773, JAN 1 2008.

[66] R. D. Prien, "The future of chemical in situ sensors," *Marine Chemistry*, vol. 107, pp. 422–432, DEC 1 2007.

[67] D. Mark, S. Haeberle, G. Roth, F. von Stetten, and R. Zengerle, "Microfluidic lab-on-a-chip platforms: requirements, characteristics and applications," *Chemical Society Reviews*, vol. 39, no. 3, pp. 1153–1182, 2010.

[68] C. M. A. Brett, "Novel sensor devices and monitoring strategies for green and sustainable chemistry processes," *Pure and Applied Chemistry*, vol. 79, pp. 1969–1980, NOV 2007. 1st International IUPAC Conference on Green-Sustainable Chemistry, Dresden, GERMANY, SEP 10-15, 2006.

[69] C. Evenhuis, R. Guijt, M. Macka, and P. Haddad, "Determination of inorganic ions using microfluidic devices," *Electrophoresis*, vol. 25, pp. 3602–3624, NOV 2004.

[70] D. Janasek, J. Franzke, and A. Manz, "Scaling and the design of miniaturized chemical-analysis systems," *Nature*, vol. 442, pp. 374–380, JUL 27 2006.

[71] M. Brivio, W. Verboom, and D. Reinhoudt, "Miniaturized continuous flow reaction vessels: influence on chemical reactions," *Lab On A Chip*, vol. 6, pp. 329–344, MAR 2006.

[72] C. F. A. Floquet, V. J. Sieben, A. Milani, E. P. Joly, I. R. G. Ogilvie, H. Morgan, and M. C. Mowlem, "Nanomolar detection with high sensitivity microfluidic absorption cells manufactured in tinted PMMA for chemical analysis," *Talanta*, vol. 84, pp. 235–239, MAR 15 2011.

[73] L. Szabo, K. Herman, N. E. Mircescu, A. Falamas, L. F. Leopold, N. Leopold, C. Buzumurga, and V. Chis, "SERS and DFT investigation of 1-(2-pyridylazo)-2-naphthol and its metal complexes with Al(III), Mn(II), Fe(III), Cu(II), Zn(II) and Pb(II)," *Spectrochimica Acta Part A - Molecular and Biomolecular Spectroscopy*, vol. 93, pp. 266–273, JUL 2012.

[74] Z. Marczenko, M. Balcerzak, and E. Kloczko, *Separation, Preconcentration and Spectrophotometry in Inorganic analysis*. Elsevier, 2000.

[75] G. Supriyanto and J. Simon, "The chromatomembrane method used for sample preparations in the spectrophotometric determination of zinc and copper in pharmaceuticals," *Talanta*, vol. 68, pp. 318–322, DEC 15 2005.

[76] H. Watanabe, "Spectrophotometric determination of cobalt with 1-(2-pyridylazo)-2-naphthol and surfactants," *Talanta*, vol. 21, no. 4, pp. 295–302, 1974.

[77] R. Sturgeon, S. Berman, S. Willie, and J. Desaulniers, "Pre-concentration of trace-elements from sea-water with silica-immobilised 8-hydroxyquinoline," *Analytical Chemistry*, vol. 53, no. 14, pp. 2337–2340, 1981.

[78] M. Luhrmann, N. Stelter, and A. Kettrup, "Synthesis and properties of metal collecting phases with silica immobilised 8-hydroxyquinoline," *Fresenius Zeitschrift Fur Analytische Chemie*, vol. 322, no. 1, pp. 47–52, 1985.

[79] C. Lan, C and M. Yang, "Synthesis, properties and applications of silica-immobilised 8-quinolinol. Characterisation of silica-immobilised 8-quinolinol synthetised via Mannich reaction," *Analytica Chimica Acta*, vol. 287, pp. 101–109, MAR 10 1994.

[80] C. Measures, J. Yuan, and J. Resing, "Determination of Iron in seawater by flow injection-analysis using in-line preconcentration and spectrophotometric detection," *Marine Chemistry*, vol. 50, pp. 3–12, AUG 1995.

[81] A. Laes, R. Vuillemin, B. Leilde, G. Sarthou, C. Bournot-Marec, and S. Blain, "Impact of environmental factors on in situ determination of iron in seawater by flow injection analysis," *Marine Chemistry*, vol. 97, pp. 347–356, DEC 20 2005.

[82] M. C. Lohan, A. M. Aguilar-Islas, and K. W. Bruland, "Direct determination of iron in acidified (pH 1.7) seawater samples by flow injection analysis with catalytic spectrophotometric detection: Application and intercomparison," *Limnology and Oceanography-Methods*, vol. 4, pp. 164–171, JUN 2006.

[83] R. N. M. J. Pascoa, I. V. Toth, and A. O. S. Rangel, "A multi-syringe flow injection system for the spectrophotometric determination of trace levels of iron in waters using a liquid waveguide capillary cell and different chelating resins and reaction chemistries," *Microchemical Journal*, vol. 93, pp. 153–158, NOV 2009.

[84] N. Beck, R. Franks, and K. Bruland, "Analysis for Cd, Cu, Ni, Zn, and Mn in estuarine water by inductively coupled plasma mass spectrometry coupled with an automated flow injection system," *Analytica Chimica Acta*, vol. 455, pp. 11–22, MAR 18 2002.

[85] L. Kubota, J. Moreira, and Y. Gushikem, "Adsorption of metal-ions from ethanol on an iminosalicyl-modified silica-gel," *Analyst*, vol. 114, pp. 1385–1388, NOV 1989.

[86] M. Mahmoud and E. Soliman, "Silica-immobilized formylsalicylic acid as a selective phase for the extraction of iron(III)," *Talanta*, vol. 44, pp. 15–22, JAN 1997.

[87] S. Watanesk and A. Schilt, "Saparation of some transition-metal ions on silica-immobilised 2-pyridinecarboxaldehyde phenylhydrazone," *Talanta*, vol. 33, pp. 895–899, NOV 1986.

[88] N. Simonzadeh and A. Schilt, "Metal-ion chromatography on silica-immobilised 2-pyridinecarboxyaldehyde phenylhydrazone," *Talanta*, vol. 35, pp. 187–190, MAR 1988.

[89] M. Lohan, A. Aguilar-Islas, R. Franks, and K. Bruland, "Determination of iron and copper in seawater at pH 1.7 with a new commercially available chelating resin, NTA Superflow," *Analytica Chimica Acta*, vol. 530, pp. 121–129, FEB 7 2005.

[90] K. Hirayama and N. Unohara, "Spectrophotometric catalytical determination of an ultratrace amount of Iron(III) in water based on the oxidation of N,N-dimethyl-p-phenylenediamine by hydrogen-peroxide," *Analytical Chemistry*, vol. 60, pp. 2573–2577, DEC 1 1988.

[91] S. J. Ussher, A. Milne, W. M. Landing, K. Attiq-ur Rehman, M. J. M. Seguret, T. Holland, E. P. Achterberg, A. Nabi, and P. J. Worsfold, "Investigation of iron(III) reduction and trace metal interferences in the determination of dissolved iron in seawater using flow injection with luminol chemiluminescence detection," *Analytica Chimica Acta*, vol. 652, pp. 259–265, OCT 12 2009.

[92] S. Ussher, M. Yaqoob, E. Achterberg, A. Nabi, and P. Worsfold, "Effect of model ligands on iron redox speciation in natural waters using flow injection with luminol chemiluminescence detection," *Analytical Chemistry*, vol. 77, pp. 1971–1978, APR 1 2005.

[93] A. L. Annett, M. Skiba, S. F. Henley, H. J. Venables, M. P. Meredith, P. J. Statham, and R. S. Ganeshram, "Comparative roles of upwelling and glacial iron sources in ryder bay, coastal western antarctic peninsula," *Marine Chemistry*, vol. 176, pp. 21 – 33, 2015.

[94] C. Benito, A. Jaimez, C. Sanchez, and A. Navarro-Sabate, "Liquid and solid Scintillation: principles and applications," *Handbook of instrumental techniques from CCiTUB. Unitat de Proteccio Radiologica, Universitat de Barcelona*, 2012.

[95] W. Wang, "The Operational Characteristics of a Sodium Iodide Scintillation Counting System as a Single-Channel Analyzer," *Radiation Protection Management, Volume 20, No.5*, 2003.

[96] I. R. G. Ogilvie, V. J. Sieben, C. F. A. Floquet, R. Zmijan, M. C. Mowlem, and H. Morgan, "Reduction of surface roughness for optical quality microfluidic devices in PMMA and COC," *Journal of micromechanics and microengineering*, vol. 20, JUN 2010.

[97] A. Beaton, V. Sieben, C. Floquet, E. Waugh, S. Bey, I. Ogilvie, M. Mowlem, and H. Morgan, "An automated microfluidic colourimetric sensor applied in situ to determine nitrite concentration," *Sensors and Actuators B: Chemical, 156, (2), 1009-1014.*, 2011.

[98] A. Beaton, C. Cardwell, R. Thomas, V. Sieben, E. Legiret, FE; Waugh, P. Statham, M. Mowlem, and H. Morgan, "Lab-on-Chip Measurement of Nitrate and Nitrite for In Situ Analysis of Natural Waters," *Environmental Science & Technology, 46, (17), 9548-9556.*, 2012.

[99] V. Rerolle, C. Floquet, A. Harris, M. Mowlem, R. Bellerby, and E. Achterberg, "Development of a colorimetric microfluidic pH sensor for autonomus seawater measurements," *Analytica Chimica Acta*, 2013.

[100] S. Srijaranai, W. Autsawaputtanakul, Y. Santaladchaiyakit, T. Khameng, A. Siriraks, and R. L. Deming, "Use of 1-(2-pyridylazo)-2-naphthol as the post column reagent for ion exchange chromatography of heavy metals in environmental samples," *Microchemical Journal*, vol. 99, pp. 152–158, SEP 2011.

[101] K. Goto, S. Taguchi, Y. Fukue, K. Ohta, and H. Watanabe, "Spectrophotometric determination of manganese with 1-(2-pyridylazo)-2-naphthol and nonionic surfactant," *Talanta*, vol. 24, no. 12, pp. 752–753, 1977.

[102] F. Tadayon, M. Hanasaei, and M. Madadi, "Determination and preconcentration of manganese using ionic liquid based microextraction technique in biological samples," *SAVAP International*, vol. 58, no. 2, pp. 115–125, 2013.

[103] V. Caligur, "Detergent Properties and Applications," *BioFiles*, 2008.

[104] J. L. Manzoori, M. Amjadi, and T. Hallaj, "Preconcentration of trace cadmium and manganese using 1-(2-pyridylazo)-2-naphthol-modified TiO2 nanoparticles and their determination by flame atomic absorption spectrometry," *International Lournal Of Environmental Analytical Chemistry*, vol. 89, no. 8-12, pp. 749–758, 2009. 35th International Symposium of Environmental Analytical Chemistry, Gdansk, POLAND, JUN 22-26, 2008.

[105] H. Eskandari and A. Saghseloo, "Second and first-derivative spectrophotometry for efficient simultaneous and individual determination of palladium and cobalt using 1-(2-pyridylazo)-2-naphthol in sodium dodecylsulfate micellar media," *Analytical Sciences*, vol. 19, pp. 1513–1518, NOV 2003.

[106] H. Eskandari, "Highly selective derivative spectrophotometry for determination of nickel using 1-(2-pyridylazo)-2-naphthol in Tween 80 micellar solutions," *Bulletin Of The Korean Chemical Society*, vol. 25, pp. 1137–1142, AUG 20 2004.

[107] N. Agnihotri, V. Singh, and H. Singh, "Derivative spectrophotometric determination of copper(II) in non-ionic micellar medium," *Talanta*, vol. 45, pp. 331–341, DEC 19 1997.

[108] F. Xia and R. Cassidy, "Application of micelles in postcolumn reaction systems," *Analytical Chemistry*, vol. 63, pp. 2883–2887, DEC 15 1991.

[109] M. L. Salit*, , and G. C. Turk, "A drift correction procedure," *Analytical Chemistry*, vol. 70, no. 15, pp. 3184–3190, 1998. PMID: 21644656.

Acronyms

8-HQ 8-hydroxyquinoline 11

AUV autonomous underwater vehicle 17

CMC Critical micelle concentration 87

CPM counts per minute 40

DPD N,N-dimethyl-p-phenylenediamine dihydrochloride 29

HR-ICP-MS high resolution inductively coupled mass spectrometry 12

ICP-MS inductively coupled plasma-mass spectrometry 10

ICP-OES inductively coupled plasma optical emission spectrometry 10

IDA iminodiacetate 39

LED light-emitting diode 42

LOAC Lab on a Chip 10

LSC Liquid Scintillation Counting 40

Mn manganese . . . 2

N_2 dinitrogen . . . 2

NaI(Tl) Thallium-doped sodium iodide . . . 40

NTA nitrilotriacetic acid . . . 12

OEC oxygen evolving centre . . . 2

PAN 1-(2-pyridylazo)-2naphthol . . . 11

PMT photo-multiplier tube . . . 40

PSII Photosystem II . . . 2

RC reaction center . . . 2

REE rare earth elements . . . 3

SDS sodium dodecyl sulfate . . . 86

SPE Solid phase extraction . . . 9

SSC Solid Scintillation Counting . . . 40

Toyopearl Toyopearl AF-Chelate 650M . . . 11